Publicly Accessible Penn Dissertations

1-1-2014

T Cells Bearing a Chimeric Antigen Receptor Against the Tumor Vasculature Destroy the Tumor Endothelium and Result in Tumor Regression

Stephen Santoro
University of Pennsylvania, santoro.stephen@gmail.com

Recommended Citation

T Cells Bearing a Chimeric Antigen Receptor Against the Tumor Vasculature Destroy the Tumor Endothelium and Result in Tumor Regression

Abstract

Aberrant blood vessels enable tumor growth, provide a barrier to immune infiltration, and serve as a source of pro-tumorigenic signals. Targeting tumor blood vessels for destruction, or tumor vascular disruption therapy, can therefore provide significant therapeutic benefit. Here I describe the development of two chimeric antigen receptors (CAR)s against the tumor vasculature, targeting either tumor endothelial marker 1 (TEM1) or prostate-specific membrane antigen (PSMA). CAR T cells incorporating scFv78, an scFv isolated against TEM1, were able to recognize immobilized plate-bound TEM1 protein, but were unable to recognize TEM1 on the surface of endothelial cell targets. In contrast, anti-PSMA CAR T cells, which incorporate the J591 scFv, were able to recognize human PSMA (hPSMA) both in vitro and in vivo. To elucidate the role of intracellular signaling domains on endothelial cell killing, a panel of the J591-based CAR T cells was characterized, each harboring a different combination of the intracellular signaling domains, CD3 zeta (z), CD28 (28), and CD137/4-1BB (BB). I found that all anti-hPSMA CAR T cells were able to recognize and eliminate PSMA+ endothelial targets in vitro, regardless of signaling domain. Furthermore, T cells bearing the 3rd generation anti-hPSMA CAR, P28BBz, were able to recognize and kill primary human endothelial cells isolated from gynecological cancers. In addition, the P28BBz CAR T cells were able to mediate regression of hPSMA-expressing vascular neoplasms in mice. Finally, in murine ovarian cancers models populated by murine vessels expressing hPSMA, the P28BBz CAR T cells were able to ablate PSMA+ vessels, cause secondary depletion of tumor cells, and reduce tumor burden. Taken together, these results provide strong rationale for the use of CAR T cells as agents of tumor vascular disruption, specifically those targeting PSMA.

Degree Type
Dissertation

Degree Name
Doctor of Philosophy (PhD)

Graduate Group
Cell & Molecular Biology

First Advisor
George Coukos

Second Advisor
Sandra W. Ryeom

Keywords
Adoptive therapy, Chimeric antigen receptor, Endothelial cells, Prostate-specific membrane antigen, Vascular disruption

Subject Categories
Biology | Cell Biology | Oncology

T CELLS BEARING A CHIMERIC ANTIGEN RECEPTOR AGAINST THE TUMOR VASCULATURE DESTROY THE TUMOR ENDOTHELIUM AND RESULT IN TUMOR REGRESSION

Stephen Santoro

A DISSERTATION

in

Cell and Molecular Biology

Presented to the Faculties of the University of Pennsylvania

in

Partial Fulfillment of the Requirements for the

Degree of Doctor of Philosophy

2014

Supervisor of Dissertation

_____

George Coukos, M.D., Ph.D., Professor of Gynecologic Oncology

Graduate Group Chairperson

_____

Daniel S. Kessler, Ph.D., Associate Professor of Cell and Developmental Biology

Dissertation Committee:

Sandra W. Ryeom, Ph.D., Assistant Professor of Cancer Biology

Daniel J. Powell Jr., Ph.D., Associate Professor of Pathology and Laboratory Medicine

Carl H. June, M.D., Professor in Immunotherapy

Robert H. Vonderheide, M.D., Ph.D., Professor of Medicine

T CELLS BEARING A CHIMERIC ANTIGEN RECEPTOR AGAINST THE TUMOR VASCULATURE DESTROY THE TUMOR ENDOTHELIUM AND RESULT IN TUMOR REGRESSION

ACKNOWLEDGEMENTS

ABSTRACT

T CELLS BEARING A CHIMERIC ANTIGEN RECEPTOR AGAINST THE TUMOR VASCULATURE DESTROY THE TUMOR ENDOTHELIUM AND RESULT IN TUMOR REGRESSION

Stephen Santoro

George Coukos, M.D., Ph.D.

Aberrant blood vessels enable tumor growth, provide a barrier to immune infiltration, and serve as a source of pro-tumorigenic signals. Targeting tumor blood vessels for destruction, or tumor vascular disruption therapy, can therefore provide significant therapeutic benefit. Here I describe the development of two chimeric antigen receptors (CAR)s against the tumor vasculature, targeting either tumor endothelial marker 1 (TEM1) or prostate-specific membrane antigen (PSMA). CAR T cells incorporating scFv78, an scFv isolated against TEM1, were able to recognize immobilized plate-bound TEM1 protein, but were unable to recognize TEM1 on the surface of endothelial cell targets. In contrast, anti-PSMA CAR T cells, which incorporate the J591 scFv, were able to recognize human PSMA (hPSMA) both *in vitro* and *in vivo*. To elucidate the role of intracellular signaling domains on endothelial cell killing, a panel of the J591-based CAR T cells was characterized, each harboring a different combination of the intracellular signaling domains, CD3 zeta (ζ), CD28 (28), and CD137/4-1BB (BB). I found that all anti-hPSMA CAR T cells were able to recognize and eliminate PSMA$^+$ endothelial targets *in vitro*, regardless of signaling domain. Furthermore, T cells bearing the 3rd generation anti-hPSMA CAR, P28BBζ, were able to recognize and kill primary human

endothelial cells isolated from gynecological cancers. In addition, the P28BBζ CAR T cells were able to mediate regression of hPSMA-expressing vascular neoplasms in mice. Finally, in murine ovarian cancers models populated by murine vessels expressing hPSMA, the P28BBζ CAR T cells were able to ablate PSMA$^+$ vessels, cause secondary depletion of tumor cells, and reduce tumor burden. Taken together, these results provide strong rationale for the use of CAR T cells as agents of tumor vascular disruption, specifically those targeting PSMA.

TABLE OF CONTENTS

LIST OF TABLES AND FIGURES

TABLES

FIGURES

x

CHAPTER 1: INTRODUCTION

The deviant role of blood vessels in tumor development

The organs of the body depend upon the circulatory system for oxygen and nutrient exchange, waste removal, and the distribution of chemical signals as well as immune cells. Tumor development is also dependent upon the vasculature. In normal tissues, the distribution of blood vessels is well organized and structured, allowing for even perfusion and nutrient exchange to occur throughout vascularized organs. In stark contrast, tumor vasculature is torturous and unorganized, with microregions within the tumor often experiencing hypoxia and nutrient deprivation (**Figure 1a–d**). Nonetheless, tumors depend on these aberrant vessels for growth and remain dormant until the angiogenic switch occurs, a process necessary for tumors to enlarge beyond the diffusive limits of oxygen through tissue.[1] Physiological angiogenesis is tightly regulated and new vessels are only recruited into tissues when the equilibrium between pro-angiogenic and anti-angiogenic factors is perturbed, as in the case of wound healing. This process is known as the "angiogenic switch". The tumor and associated cells are able to manipulate this equilibrium, facilitating vessel formation, by producing pro-angiogenic factors.[2] During the angiogenic switch, normal regulation of vessel development is lost and abnormal tumor blood vessels are formed. The role of these vessels in tumor development is not restricted to oxygen and nutrient exchange, however, and the endothelial cells lining these vessels also play important and multifaceted roles in additional aspects of tumor progression.

Until recently, the crosstalk between the tumor and the endothelium was largely thought to be unidirectional. Tumor cells, as well as tumor associated cells, were known

to secrete pro-angiogenic factors, such as members of the vascular endothelial growth factor (VEGF) family, enabling tumor vascularization and facilitating nutrient exchange. Additional methods by which the endothelium could support tumor growth were considerably overlooked. A deeper understanding of tumor endothelial biology has begun to shift this paradigm, however, and the role for endothelial cell signaling in tumor development has gained appreciation. Work from the lab of Lee M. Ellis, for example, recently identified the tumor endothelium as a source of angiocrine factors that contribute to the stem-ness of nearby cancer cells, thereby promoting both disease severity and resistance to chemotherapy.[3] Tumor endothelial cells are also able to provide important growth signals to the tumor, such as interleukin (IL) 6,[4] which promote tumor cell proliferation. Taken together, these observations demonstrate that the tumor endothelium not only plays a supportive role in cancer progression, but also actively participates in tumor development.

In addition to directly facilitating tumor cell growth, tumor endothelial cells act as a barrier to immune infiltration. Work from our lab has shown that this may occur through at least two different mechanisms. Firstly, T cell homing and adhesion to vessels within the tumor can be interrupted by overexpression of genes related to vascular homeostasis and T cell adhesion, such as endothelin B receptor. The presence of endothelin B receptor, a G protein-coupled receptor that signals in response to the vasoactive peptides ET1, ET2, and ET3, abrogates the ability of T cells to infiltrate into the tumor through down regulation of intracellular adhesion molecule-1 on tumor endothelial cells.[5] Secondly, we have shown that tumor blood vessels up-regulate FasL

in response to prostaglandin, vascular endothelial growth factor A (VEGF-A), and IL-10. FasL expression by the tumor endothelium preferentially kills CD8$^+$ T cells while leaving T regulatory cells unharmed, thus creating an immunosuppressive tumor microenivornment.[6] These observations further underscore the importance of the tumor vasculature in tumor development and provide rationale for the development of therapies targeting these cells.

As multifaceted and essential contributors to the tumor microenvironment, tumor blood vessels are an ideal target for cancer therapy. Large numbers of tumor cells rely on a relatively small number of endothelial cells for oxygen and nutrient exchange, for example, and destruction of those endothelial cells can mediate a significant impact on the tumor burden.[7] In addition, the tumor endothelium is directly accessible to circulating lymphocytes, allowing them uninterrupted contact with tumor endothelial cells without requiring extravasation. Finally, tumor endothelial cells are generally believed to be more genetically stable than the tumor itself, making them less likely to escape therapy through mutation. Given these considerations, the design of anti-vascular therapies has focused on the identification of characteristics and proteins that distinguish between normal and aberrant blood vessels. Fortunately, the tumor vasculature is both morphologically and physiologically distinct (**Figure 1**), allowing for the development of novel therapeutic directed against these abnormal endothelial cells.

Anti-angiogenic therapy versus vascular disruption

Since Judah Folkman first proposed the notion of targeting the tumor vasculature as a means to treat cancer,[8] the idea has been approached using two distinct methods. Blood vessels are recruited to the tumor either through angiogenesis, vasculogenesis, or a combination of both processes. Angiogenesis involves the recruitment of endothelial cells from adjacent blood vessels, whereas endothelial progenitor cells give rise to *de novo* vessels through the process of vasculogenesis. Both processes involve the release of pro-angiogenic factors, such as basic fibroblast growth factor (bFGF) and VEGF, from the tumor microenvironment, thereby highlighting a potential avenue of therapeutic intervention. Therapies targeting either the soluble mediators of angiogenesis, or the receptors to which they bind, are referred to as anti-angiogenic therapies, and prevent the growth of new vessels. In contrast, vascular disruption therapy has been developed with the aim of specifically destroying the existing vasculature and eliciting catastrophic effects on the tumor (**Table 1, Figure 2**). Currently, anti-angiogenic agents have had the largest impact clinically.

Of the anti-angiogenic therapies developed, those targeting the VEGF family and its receptors are the most numerous. Inhibitors include VEGF aptamers, soluble VEGF receptors (VEGFRs), and tyrosine kinase inhibitors designed to impair VEGFR signaling.[9] The most notable of these agents, however, is a monoclonal neutralizing antibody (Ab) generated against VEGF-A and known as *bevacizumab,*. Although *bevacizumab* is available to patients, the addition of the antibody to existing treatment regimens has only resulted in a modest progression-free survival advantage for

individuals receiving the treatment.[10,11] This can likely be explained by a number of escape mechanisms employed by the tumor, and includes the use of compensatory pro-angiogenic signaling pathways, the recruitment of endothelial progenitor cells from the bone marrow, and the utilization of vasculogenic mimicry, where tumor cells act functionally as endothelial cells.[12,13,14] In addition to being resistant to anti-VEGF therapy, the tumor may become more aggressive in response to VEGF inhibition. Mouse models of pancreatic[15] and breast[16] cancer have demonstrated that inhibition of VEGF selects for tumor cells that are more metastatic and invasive. As such, there is room for improvement in the field of anti-angiogenic therapy. Vascular disruption represents a potential method by which many of these obstacles may be circumvented, and has therefore been investigated correspondingly.

Mechanisms of vascular disruption

In contrast to anti-angiogenic therapy, the intent of vascular disruption therapy is to actively destroy the existing tumor vasculature, with the aim of causing extensive necrosis at the center of established tumors. Currently, there are two primary classes of pharmacological vascular disruption agents (VDA)s: the tubulin-depolymerizing VDAs and the tubulin independent VDAs.[17] Representative agents from both classes, CA4P and ASA404, respectively, have demonstrated impressive anti-tumor effects in mouse models, but have failed to elicit similar efficacy in human trials.[18,19,20] After treatment with VDAs, a viable rim of tumor cells often remains at the periphery of the tumor, where oxygen and nutrient exchange can occur through neighboring tissues (**Figure 2**).

In part, this may explain why VDAs have been ineffective when used as a single agent in clinical trials. Synergy with other treatment modalities, including radiation, chemotherapy, and anti-angiogenic therapy, has been observed (reviewed by Siemann[17]). In addition to tumor cell viability at the tumor periphery, cancer persistence after vascular disruption therapy may also be sustained through the regrowth of new vessels derived from circulating endothelial progenitor cells recruited to the tumor following treatment.[21] In part to overcome this obstacle, our lab has focused on the development of T cell based vascular disruption therapies, as T cells have the potential to persist long term within the patient, and may be able to recognize and destroy new tumor endothelial cells as they form.

Wei et al. were the first to report tumor regression in response to an endothelial cell vaccination.[22] In this study, the authors found that xenogeneic transfer of primary human endothelial cells protected mice from subsequent tumor challenge. Auto-reactive antibodies were recovered from the serum of immunized mice and CD4 T cells were found to play a critical role in the anti-tumor response. In an effort to involve CD8 T cells in the anti-tumor vasculature response, work from our lab has focused on the development of a DNA vaccine against tumor endothelial marker 1 (TEM1). Both prophylactically and as a treatment, DNA vaccination against TEM1 was shown to induce an anti-TEM1 T cell response capable of preventing tumor growth and eliciting tumor regression.[23] Importantly, epitope spreading played a significant role in the anti-tumor response, and is a noteworthy advantage to using cell based vascular disruption techniques.

Anti-tumor vasculature T cells can either be created through vaccination or generated using an artificial T cell receptor (TCR) or chimeric antigen receptor (CAR). Engineered T cells have a number of significant advantages over T cells elicited in response to vaccination. Central and peripheral tolerance, for example, select against high affinity T cell clones that recognize self-antigens. This is detrimental to the anti-tumor response, as most tumor antigens are either closely related to normal proteins, or are over-expressed self-proteins. Engineered T cells can bypass this obstacle, as high-affinity receptors can be isolated and transduced into adoptively transferred T cells. In addition, *ex vivo* generated T cells can be expanded to large numbers before infusion, surpassing the expansion expected from a normal immune response, particularly one occurring within the immunosuppressive setting of the tumor microenvironment. Therefore, our lab has focused on the development of engineered T cells capable of recognizing the tumor vasculature.

CHAPTER 2: REDIRECTING T CELLS AGAINST THE

TUMOR VASCULATURE

Introduction

The process of tumor development is intricately linked to changes in the local tumor microenvironment. In addition to tumor cells, the microenvironment is comprised of immune cells, fibroblasts, and aberrant tumor blood vessels, as well as non-cellular components such as signaling molecules and the extracellular matrix. The relationship of the tumor with the microenvironment is dynamic, and cross talk between the two contributes to cancer progression.[6] Within the microenvironment, tumor blood vessels play a central role, providing both oxygen and nutrient exchange to the tumor.[1] In addition, endothelial cells lining the blood vessels (*i.e.* the endothelium) can provide growth signals, such as interleukin (IL) 6,[4] which promote tumor cell proliferation. The tumor endothelium can also provide a physical barrier to immune cell infiltration, actively protecting the tumor from immunosurveillance.[5,6] In addition, tumor endothelial cells are able to secrete angiocrine factors that contribute to the stemness of nearby cancer cells, promoting both disease severity and resistance to chemotherapy.[3] Together these findings emphasize the importance of the tumor vasculature in cancer progression and indicate that destruction of vessels may have an important impact on tumor development.

Adoptive transfer anti-vasculature T cells is an attractive therapeutic approach for vascular disruption, as engineered T cells have the potential to develop into memory T cell populations and can persist long-term in patients.[24] The persistence of these anti-vascular T cells will presumably impair the growth of the tumor by continually eliminating newly formed tumor vessels. In addition, tumor blood vessels are directly

10

accessible to circulating T lymphocytes. Furthermore, tumor endothelial cells are generally more genetically stable than tumor cells, and thus less able to develop immune escape variants. Finally, adoptively transferred T cells are able to induce epitope-spreading,[25] and possibly generate a *de novo* T cell response against the tumor and/or the tumor vasculature, thereby enhancing the potency of the anti-tumor response. As such, I sought to develop engineered T cells to target the tumor vasculature.

Engineering T cells to recognize the tumor vasculature

Adoptive cell-based therapy is defined as the *ex vivo* expansion and subsequent re-administration of autologous T cells into a tumor bearing patient. This can be performed through the expansion of tumor infiltrating lymphocytes (TIL), or by engineering T cells to express an exogenous receptor. The success of TIL therapy in the treatment of melanoma has, in large part, validated the use of T cells in cancer therapy. Data from three recent clinical trials performed at the NCI, for example, revealed objective responses in 52/93 patients treated with TIL therapy.[26] Impressively, nearly all of the complete responders remained disease free for over 64 months. Not all patients and cancers present with TIL, however, so emphasis has been placed on the generation of tumor antigen-specific T cell receptors (TCRs) that can be used to redirect patient T cells.[27]

The anti-tumor impact of TCR transduced T cells is also most evident in melanoma. T cells bearing high affinity TCRs against the tumor epitopes, MART-1 and gp-100, were able to elicit objective responses in 6/20 and 3/16 patients, respectively.[28]

These results are particularly impressive because the patients enrolled in these trials were heavily pretreated using conventional therapies prior to adoptive transfer and all showed signs of progressive disease. Although potent, there are significant disadvantages to TCR based ACT. The most notable of these is the restriction of a given TCR for a single MHC haplotype, which is further complicated by the fact that 40–90% of tumors are MHC class 1 deficient, as a result of immunoediting.[29] It is possible to avoid these obstacles, however, using a second class of engineered receptors, referred to as chimeric antigen receptors (CARs).

Chimeric antigen receptors

A CAR consists of an extracellular single chain variable fragment (scFv) fused to an intracellular signaling domain, most commonly the CD3ζ domain derived from the TCR complex (**Figure 3**). Early trials utilizing 1st generation CAR T cells (CD3ζ signaling only) failed to elicit significant anti-tumor responses. This was attributed to a lack of persistence of the CAR-bearing T cells.[30,31] Drawing on the knowledge of physiological T cell activation, it was predicted that the addition of costimulatory domains would increase the longevity and effort function of CAR-bearing T cells and thus second generation CARs were created utilizing costimulatory domains such as CD28 and 4-1BB. As anticipated, the 2nd generation CAR T cells were found to be superior to 1st generation CAR T cells in both effort function and persistence.[32,33] Finally, 3rd generation CARs were constructed using all three intracellular signaling domains (CD28,

4-1BB, and CD3ζ) and have been found to function as well as, if not better than 2nd generation CAR T cells when administered *in vivo*.[34,35]

The ability of these later generation CAR T cells to elicit profound anti-tumor effects in human patients was recently highlighted in the results of a small clinical trial for patients with chronic lymphocytic leukemia (CLL). Two of the three patients treated with CAR T cells directed against the B cell leukemia marker, CD19, experienced complete remission that remained durable for over two years, while the 3rd patient experienced a partial response.[24,36] In addition to being efficacious against blood-borne cancers, there is strong evidence to suggest that CAR T cells directed against the tumor vasculature can also elicit significant effects against solid tumors. For example, murine CARs directed against VEGFR-2[37] or VEGFR-1 and VEGFR-2[38] were effective in suppressing tumor growth in mice challenged with various tumors. However, these targets are also expressed by normal endothelial cells throughout the body, and therefore represent a risk for "on-target/off-tumor" toxicity. I therefore sought to develop CAR T cells capable of recognizing alternative tumor vascular antigens with more favorable expression profiles within normal tissues.

Identifying targetable tumor vascular antigens

The tumor vasculature is morphologically and physiologically distinct from the normal vasculature. Numerous surface proteins have been identified that are either upregulated or present exclusively on the vessels of the tumor.[39,40] Given their known role in angiogenesis, the VEGFRs were quickly identified as upregulated surface

receptors present more abundantly on the tumor vasculature than normal vessels.[41] VEGFR-1 and VEGFR-2 are also expressed by normal vessels throughout the body, however, making them suboptimal targets for vascular disruption therapy.[42] As such, the field has focused on the identification of unique tumor vascular antigens, which demonstrate a more restricted expression profile.

To identify novel tumor vascular targets, quantifiable gene expression assays, such as serial gene analysis (SAGE), have been used to detect genes that are present on the tumor endothelium but absent on the normal vasculature. By comparing the mRNA transcription profiles of endothelial cells isolated from colon tumors with that of normal colon endothelial cells, St. Croix et al. were able to identify 46 tumor endothelial markers expressed at least 10 fold higher by the tumor endothelium.[40] The transcript most abundantly expressed by the tumor endothelium was termed TEM1. Additional studies have confirmed TEM1 over-expression on the vasculature of a variety of human cancers,[43,44] including ovarian carcinoma.[39,44] In contrast, TEM1 expression appears to be restricted on normal adult tissues.[45,46] Although a functional role for TEM1 has not been completely elucidated, over-expression of the protein has been shown to correlate with disease severity and recurrence in breast cancer.[43] This is further supported by the observation that TEM1 knock out (TEM1$^{-/-}$) mice show resistance to tumor development.[47] Importantly, the TEM1$^{-/-}$ mice are otherwise healthy and do not display complications in wound healing or angiogenesis, suggesting that therapies directed against TEM1 will elicit significant anti-tumor effects with minimal toxicity. This assertion is further supported by the recent work of Facciponte et al, who showed that

vaccination against TEM1 was able to elicit a strong anti-tumor response, without observable toxicity or impairment in either wound healing or reproductive health.[23] Taken together, these data suggest that TEM1 would be an ideal target for CAR based vascular disruption therapy due to its favorable expression profile and implication in tumorigenesis.

Alternative tumor vascular antigens have also been identified. One such example is prostate-specific membrane antigen (PSMA), a type II membrane protein of the M28 peptidase family that is also known as glutamate carboxypeptidase II (GCPII) or folate hydrolase 1 (FOLH1). While validating an antibody against the extracellular region of PSMA, Liu et al. identified expression of the protein on the vasculature of a panel of solid tumors.[48] This observation was confirmed by others, and expanded to include a wide variety of solid tumors (summarized in **Table 2**).[49,50,51] While PSMA is absent on the normal endothelium, it has been detected on a subset of normal adult tissues.[52] Antibody therapies directed against PSMA have been largely free of toxicity,[53] however, suggesting that T cell based therapies targeting PSMA will also have a favorable safety profile (reviewed in **Chapter 3** and discussed in **Chapter 4**). Thus, there is also strong rationale for the development of anti-vascular CAR T cells directed against PSMA.

Tumor endothelial marker 1

TEM1 (CD248 or endosialin) is a 757 amino acid type I membrane bound protein, which consists of a large extracellular domain C-type lectin domain, a Sushi/CCP/scr

domain, and 3 EGF repeats.[54] Initially identified by immunohistochemical staining of tumors sections stained with a mouse monoclonal antibody (m)Ab isolated from mice inoculated with human fetal fibroblasts, TEM1 was observed on the tumor vasculature.[55] In mice, TEM1 is expressed during embryonic development, but has a limited expression profile in adult animals, making it an attractive target for vascular disruption therapy.[56] Furthermore, TEM1 has been implicated in tumor progression, as TEM1$^{-/-}$ mice demonstrate impaired tumor growth, but are otherwise developmentally normal.[47] Given these characteristics, I sought to develop CAR T cells that would recognize TEM1.

Development of a CAR to target TEM1

Utilizing a yeast display library generated from a patient with thrombotic thrombocytopenic purpura, Zhao et al. isolated 5 scFv fragments capable of recognizing the extracellular portion of TEM1.[57] The binding potential of these scFvs varied, with scfv78 exhibiting the highest affinity (**Table 3**). I cloned each of the five scFvs (78, 131, 132, 133, and 137) into a series of self-inactivating lentiviral cassettes (**Figure 4a**), which utilize 3rd generation safety features.[58] From these vectors, CAR expression was driven by the EF-1α promoter. All constructs contained an eGFP reporter and the CD3ζ intracellular signaling domain. Primary human T cells were transduced with lentivirus generated from these constructs, and transduction efficiency was monitored by eGFP, which was detected by flow cytometry (**Figure 4b**). To test whether the eGFP reporter accurately reflected CAR surface expression in transduced T cells, I stained scFv78 CAR

T cells with a goat anti-rabbit F(ab)$_2$ fragment. Surface expression correlated highly with eGFP expression, validating the use of the eGFP reporter in these cells (**Figure 4c**).

Next, I sought to evaluate the ability of the anti-TEM1 T cells to recognize immobilized TEM1 protein. The anti-TEM1 CAR T cells were cultured in wells coated with either recombinant human TEM1 (hTEM1) protein or BSA as an irrelevant protein control. An IFN-γ ELISA was performed on the supernatants collected from the wells after overnight co-culture and I found that T cells bearing the scFv78 CAR were able to recognize the plate-bound hTEM1 protein (**Figure 5a**). In contrast, T cells harboring any of the lower affinity CARs were unable to recognize the plate bound protein, suggesting that the affinity of these scFvs may not be sufficient to confer recognition and activation to the CAR T cells (**Table 3**). scFv78 is capable of recognizing both human and murine TEM1 (mTEM1).[57] To test whether the 78ζ CAR T cells could recognize mouse and/or human TEM1 on the surface of endothelial cells, I performed overnight co-cultures of the 78ζ CAR T cells with either the 2H11 cell line, which has been shown to express murine TEM1,[57] or the MS1^{TEM1} cell line which I had previously engineered to express human TEM1 (**Figure 5b**). Surprisingly, I found that the 78ζ CAR T cells were unable to recognize either murine or human TEM1 when expressed on the surface of endothelial cells (**Figure 5c**). T cells bearing a CAR against mesothelin (P4ζ) were used as a specificity control in this experiment, and reacted exclusively against the ovarian cancer cell line A1847, which is known to express mesothelin.[59]

One potential explanation as to why the 78ζ CAR T cells could recognize immobilized TEM1 protein, but not TEM1 expressed on the cell surface, is that the hinge

17

domain connecting scFv78 to the transmembrane region of the CAR may not extend sufficiently from the T cell surface to allow epitope recognition. This is supported by the observation that the soluble form of scFv78 could be used to detect TEM1 on endothelial cells (see **Figure 5b**). Furthermore, others have shown that the extension of an scFv from the surface of a CAR T cell can influence the T cell's ability to recognize its target antigen.[60] Therefore, I cloned scFv78 into a CAR construct containing the IgG4 hinge, rather than the CD8α hinge. The CD8α hinge domain, isolated from the TCR complex, is 45 amino acids in length. In contrast, the IgG4 hinge is 231 amino acids (**Figure 6a**), and extends further from the T cell surface than the CD8α hinge domain (**Figure 6b**). CAR T cells bearing one of the two hinge domains were cultured with endothelial targets expressing hTEM1, and IFN-γ was measured in supernatants collected after overnight co-culture. I did not detect IFN-γ production from either set of anti-TEM1 CAR-bearing T cells, regardless of hinge domain, nor did I detect killing of the target cell lines, as measured by luciferase killing assay (**Figure 6c,d**). T cells bearing a CAR against human folate receptor α (FR), were used as a specificity control throughout these experiments, and were found to react solely against targets engineered to express folate receptor. These data suggest that the epitope recognized by scFv78 may be deeply hidden within the proteins of the surface membrane and also demonstrate that extension of the hinge domain of the scFv78 CAR, using the IgG4 hinge, will not overcome this obstacle.

Recent work from the Powell lab has demonstrated that T cells bearing a biotin-binding immune receptor (BBIR) can react against targets labeled with biotinylated antibody (**Figure 7a**).[61] Since I observed that the soluble form of scFv78 was able to

label TEM1$^+$ cells (**Figure 5b**), I hypothesized that BBIR T cells may be able to recognize TEM1$^+$ endothelial labeled with biotinylated scFv78. To begin, I biotinylated scFv78, as well as two additional antibodies known to bind TEM1 (K16 and MORAb004), using a commercially available biotinylation kit. To confirm successful biotinylation, the MS1 and MS1^{TEM1} endothelial cells were stained using the biotinylated anti-TEM1 antibodies (**Figure 7b**). Surprisingly, co-culture of the BBIR T cells with the labeled target cells did not result in recognition of the MS1^{TEM1} endothelial cells, regardless of the antibody or scFv used (**Figure 7c**). Taken together, these results further suggest that developing CAR T cells capable of recognizing TEM1 may be difficult using the currently available antibodies and scFvs.

Prostate-specific membrane antigen

Prostate-specific membrane antigen (PSMA) is a 750 amino acid type II membrane bound protein. Contrary to its name, PSMA is also expressed in the neovasculature of a wide variety of solid tumors (see **Table 2**), making it a potential target for CAR mediated endothelial cell killing. The *PSMA* locus encodes a number of splice variants, including multiple membrane-bound and cytosolic isoforms of the protein,[62,63] and the ratio of membrane to cytosolic PSMA was shown to be higher in prostate cancer cells when compared to the normal prostate.[64] Recent studies have demonstrated that the surface expression of PSMA confers a proliferative advantage to tumor cells through its function as a hydrolase of poly- and gamma-glutamated folate.[65] In addition, PSMA is known to function as a *N*-acetylated α-linked acidic dipeptidase

19

(NAALADase) of the neuropeptide NAAG in the brain.[66] As such, it is presumed that PSMA plays a metabolic role on the activated tumor endothelium. However, additional functions have also been ascribed to PSMA. PSMA was shown to be important in endothelial cell invasion, for example, and mice lacking PSMA exhibit impaired angiogenesis.[67] Furthermore, expression of PSMA by the LNCaP prostate cancer cell line has been shown to induce the expression and secretion of interleukin (IL) 6, which increases the proliferative potential of the tumor cells.[68] Since the tumor endothelium has also been shown to be an important source of IL-6,[4] it is conceivable that PSMA signaling is also involved in the production of IL-6 from these cells as well. Taken together, these data describe PSMA as a tumor endothelial marker, and also implicate the protein in tumor progression. As such, there is strong rationale to pursue the development of CAR T cells to target the endothelial cells that express PSMA.

The design and characterization of a CAR against PSMA

Research from the laboratory of Michel Sadelain has shown that CAR T cells targeted against hPSMA (hereafter referred to as PSMA) are able to eliminate prostate cancer cells *in vitro* as well as *in vivo*.[35] The scFv utilized in these constructs was derived from the mouse mAb J591, which was also used to identify PSMA on blood vessels within a number of solid tumors.[48,49,50] I therefore utilized the J591 scFv in the design of my CAR constructs, which I referred to as Pζ, P28ζ, PBBζ, and P28BBζ based upon the intracellular signaling domain incorporated into their design. In addition, I also utilized a specificity control CAR, FR28BBζ, which recognized the non-vascular antigen, human

folate receptor alpha (FRα).[69] Each CAR was subcloned downstream of an eGFP reporter within the pELNS lentiviral cassette (**Figure 8a,b**). Transduction efficiencies ranged from 50–90% in primary human T cells (**Figure 8c**). To confirm CAR surface expression, the P28BBζ T cells were stained with a goat anti-mouse $F(ab)_2$ fragment. eGFP expression and CAR surface detection were strongly correlated, validating the use of the eGFP reporter as a proxy for CAR expression (**Figure 9**).

The effector function and persistence of CAR-bearing T cells is dependent upon the signaling domains incorporated in their design. Co-stimulation through CD28 and/or 4-1BB augments CAR T cell function, generating a more potent anti-tumor response.[34,35] Although this has been described in the context of tumor cell killing, there is a paucity of data defining the role of co-stimulation in endothelial cell destruction. Therefore, I compared the ability of my anti-PSMA CAR T cells, containing the ζ, 28ζ, BBζ, or 28BBζ signaling domains, to function against endothelial targets *in vitro*.

Although PSMA is present on the tumor endothelium *in vivo*, it has not been described on endothelial cells in culture. To ascertain whether cultured human endothelial cells express PSMA, I stained both the immortalized HMEC-1 cell line[70] as well as primary human umbilical vein endothelial cells (HUVEC), using the J591 mAb. I was unable to detect PSMA on either the HMEC-1 (see **Figure 11a**, top row) or the HUVEC (not shown). I therefore engineered the HMEC-1 to express PSMA isoform 1, using lentivirus (see **Figure 11a**, bottom row). To compare the ability of the different CARs to redirect T cells towards endothelial PSMA, I first measured the proliferative capacity of the CAR bearing T cells in response to the HMEC-1^{PSMA} cell line. All CAR

T cells, regardless of their signaling domain, proliferated in response to the HMEC-1^{PSMA} (**Figure 8d,e**), but did not proliferate in response to the antigen negative HMEC-1 (not shown). There were no statistical differences between the groups. Control FR28BBζ CAR T cells did not show any significant proliferation in response to the HMEC-1^{PSMA} when compared to untransduced T cells (**Figure 8e**). Similarly, I observed that all the anti-PSMA CAR T cells were able to specifically kill the HMEC-1^{PSMA} during overnight co-culture, with no significant differences detected between the anti-PSMA T cells, regardless of signaling domain (**Figure 8f**). Finally, I compared the ability of each CAR to confer resistance to apoptosis by measuring the anti-apoptotic factor, Bcl-xL, after activation. After co-culture with the HMEC-1^{PSMA}, the P28BBζ T cells induced the highest levels of Bcl-xL expression, although this observation did not reach statistical significance (**Figure 10**). Interestingly, in the context of tumor cell targeting, the impact of the different CAR signaling domains was found to be less evident *in vitro* and more pronounced *in vivo*.[34] In this setting, third generation CAR T cells (28BBζ) were found to be equivalent or superior to either 1st (ζ) or 2nd (28ζ or BBζ) generation CAR T cells.[34,35] Thus, I selected the P28BBζ T cells for further experimentation (**Chapter 3**).

Conclusions

TEM1, although an attractive tumor vascular marker, has been difficult to target using currently available CAR T cells. Of the 5 anti-TEM1 scFvs isolated by Zhao et al.,[57] only T cells bearing the scFv78-based CAR were able to recognize immobilized plate bound TEM1 protein. Unfortunately, this recognition did not correspond to a

commensurate recognition of TEM1 on the surface of endothelial cell lines (**Figure 5**). I hypothesized that the binding epitope for scFv78 may be embedded within the proteins of the endothelial cell surface, and that hinge extension could liberate the scFv sufficiently to allow recognition and T cell activation. Co-culture of T cells bearing an extended hinge domain, however, failed to recognize TEM1 when expressed on the surface of targeted cell lines (**Figure 6**). Finally, I utilized a "universal" CAR T cell approach, where TEM1$^+$ targets were labeled with biotinylated scFv78 and co-cultured with T cells bearing a streptavidin-based BBIR. Although staining with scFv78 was confirmed by flow cytometry, the BBIR T cells failed to recognize the labeled targets (**Figure 7**). Taken together, these data suggest that the binding epitope for scFv78 is masked in such a way that given these current CAR designs, it cannot be recognized. Further study should be directed towards the development of CAR T cells with more flexible hinge domains and also the isolation of novel anti-TEM1 scFvs that may bind a more accessible region of the TEM1 protein.

In contrast, I also demonstrated that T cells bearing J591-based CARs were able to successfully recognize and eliminate human endothelial cells engineered to express PSMA. *In vitro,* I noted that anti-PSMA CAR T cells were able to proliferate in response to antigen, and successfully eliminate PSMA$^+$ targets, regardless of the signaling domains incorporated into their design. Further study would be needed to extend these observations *in vivo*, but I expect that the differences between the signaling domains will become more apparent, as has been demonstrated for tumor targeting CAR T cells.[34,35] Importantly, this work establishes that T cells bearing J591-based CARs can recognize

PSMA on the surface of endothelial cells, and activate in response to the antigen. The anti-PSMA CAR T cells identified in this work were subsequently used to interrogate the effects of T cell-mediated vascular disruption, which is described in **Chapter 3**.

CHAPTER 3: T CELLS BEARING A CHIMERIC ANTIGEN RECEPTOR AGAINST PSMA MEDIATE VASCULAR DISRUPTION AND RESULT IN TUMOR REGRESSION

Introduction

Vascular disruption has the potential to mediate profound anti-tumor effects, as evidenced by murine tumor models (**Figure 2**).[18,20] The impact of utilizing T cells to elicit vascular disruption, however, is less well established. Recent work targeting VEGFR2 has demonstrated that CAR T cells can destroy the tumor endothelium and that vascular disruption impairs tumor growth.[37] I aimed to build upon this observation and demonstrate that targeting the tumor vasculature with CAR T cells against PSMA can cause tumor cell death and subsequent tumor regression.

Here, I demonstrate that 3rd generation CAR T cells, containing the 28BBζ signaling domain, efficiently and specifically target human and mouse endothelial cells expressing the PSMA *in vitro*, as well as eliminate murine hemangioma and hemangiosarcoma tumors expressing PSMA *in vivo*. I also demonstrate the P28BBζ T cells can ablate PSMA$^+$ tumor vessels within two ovarian tumor models populated with murine endothelial cells transduced to express PSMA, and that elimination of these vessels results in secondary depletion of tumor cells and reduced tumor burden. Overall this work demonstrates for the first time that PSMA is a valid target for CAR T cell-mediated tumor blood vessel destruction, and highlights the viability of the approach as an effective anti-cancer therapy.

P28BBζ T cells recognize and eliminate PSMA-positive endothelial cells *in vitro*

To begin, I engineered human PSMA expression on the surface of the immortalized human endothelial cell line, HMEC-1, as well as the surface of two mouse endothelial cell lines, the immortalized MS1 line as well as the H5V angiosarcoma line (**Figure 11a**). To assess the specificity and ability of the P28BBζ T cells to react against these endothelial targets, I performed IFN-γ ELISA on supernatants collected after overnight co-culture of the CAR T cells with the PSMA-negative human (HMEC-1) or mouse (MS1, H5V) endothelial cell lines and their PSMA-transduced counterparts (HMEC-1^{PSMA}, MS1^{PSMA}, H5V^{PSMA}). I found that IFN-γ production by the P28BBζ CAR T cells was limited to the cultures containing the PSMA^{+} endothelial cells (**Figure 11b**). Next, I asked whether the P28BBζ CAR T cells would be able to specifically kill the PSMA^{+} endothelial cells. Using a chromium release assay, I found that the P28BBζ CAR T cells eliminated the majority of the PSMA^{+} endothelial cells within 18 h of co-culture, while the PSMA^{-} cell lines were largely unaffected (**Figure 11c**).

PSMA is expressed on the vasculature of primary and metastatic cancer

PSMA has been detected on tumor blood vessels in a variety of cancers, including ovarian[51] (summarized in **Table 2).** To confirm this observation I performed immunohistochemistry on a tissue microarray (TMA) comprised of 13 primary ovarian cancer specimens and 15 matched metastases (**Figure 12a,** top row). I observed PSMA

expression on vessel-like structures within the majority of tumors, with 12/13 (85%) of the subjects expressing PSMA within their primary ovarian lesion(s), and 14/15 (93%) expressing PSMA on one or more of their metastases (**Figure 12b**). I did not identify PSMA on any of the 16 normal ovary cores analyzed. Endothelial expression of PSMA was confirmed by co-staining of the TMA using a CD34 antibody in addition to the anti-PSMA antibody (**Figure 12a**, bottom row). Here I noticed the presence of CD34$^+$PSMA$^-$ vessels in some of the cores analyzed (**Figure 12c**), corroborating observations made in other cancer types where PSMA expression was noted to be heterogeneous on vessels within the tumor (**Table 4**). To define the percentage of endothelial cells expressing PSMA within the tumor, I examined freshly dissociated cancer samples by flow cytometry. In support of my observations by IHC, I found PSMA expression on approximately 40–60% of the CD45$^-$CD31$^+$ endothelial cells (**Figure 12d**).

Next I asked whether the P28BBζ CAR T cells were capable of recognizing and killing tumor endothelial cells isolated from individuals with cancer. Tumor endothelial cells were enriched from freshly dissociated tumor samples first by negative selection of CD45$^+$ leukocytes and then by positive selection of CD31$^+$ endothelial cells using magnetic bead sorting. CD31-enriched and CD31-depleted tumor-derived cells were then incubated with P28BBζ CAR T cells for 18 h. I found that the P28BBζ CAR T cells substantially reduced the percentage of PSMA$^+$ endothelial (CD45$^-$CD31$^+$) cells in the primary tumor-derived cells. The control FR28BBζ CAR T cells had no impact on the percentage of PSMA$^+$ cells remaining in the culture (**Figure 12e**). To confirm the activation of the P28BBζ CAR T cells in these cultures, I performed IFN-γ ELISA on the

supernatants collected from the overnight co-cultures of the P28BBζ CAR T cells with either the CD31-enriched or the CD31-depleted populations. IFN-γ was produced in all instances where the P28BBζ T cells were co-cultured with the CD31-enriched endothelial cells (**Figure 12f**). Interestingly, I also observed IFN-γ production in one of the CD31-depleted co-cultures (**Figure 12f**, #1913). To determine whether expression of PSMA by the tumor cells could explain this observation, I stained the CD45⁻CD31⁻ population for PSMA as well as FRα, a tumor-specific antigen in ovarian cancer.[71] For subject #1913, I found that a substantial portion of the FRα⁺ cells stained positive for PSMA (**Figure 13a**). Because the main cell populations in the CD45⁻CD31⁻ fraction are tumor cells and stroma fibroblasts, and because the stroma of gynecologic cancers does not express the FRα,[72,73] these findings suggest that tumor cells for some individuals with ovarian cancer may also express PSMA, which has been noted for other cancers.[52] Collectively, this data, along with numerous published reports (**Table 2),** demonstrate that PSMA is widely expressed in the tumor vasculature and provide rationale for the development of CAR T cell therapy against this antigen.

P28BBζ CAR T cells target human tumor vasculature expressing PSMA

To simulate the interactions of P28BBζ CAR T cells with human tumor blood vessels *in vitro*, I plated HMEC-1 or HMEC-1^PSMA endothelial cells on Matrigel basement membranes and allowed the cells to self-assemble into microvessels (8 h). Upon assembly, T cells were added, and the cultures were monitored for 48 h by

fluorescence microscopy (**Figure 14a**). As early as 24 h after addition of the T cells to the microvessels, I observed specific localization of the P28BBζ CAR T cells with the HMEC-1^{PSMA} microvessels. Within 48 h, the HMEC-1^{PSMA} vessels were destroyed (**Figure 14b**). In contrast, the antigen-negative microvessels persisted throughout the duration of the co-culture with the P28BBζ CAR T cells. As expected, the control FR28BBζ CAR T cells, directed against the FRα, did not impact the persistence of either the HMEC-1 or HMEC-1^{PSMA} microvessels. These data indicate that the P28BBζ CAR T cells were able to specifically recognize PSMA$^+$ vessels, but not the normal (PSMA$^-$) vascular structures, *in vitro*.

I next assessed the ability of the P28BBζ CAR T cells to recognize human endothelial cells expressing PSMA *in vivo*. I transplanted Matrigel plugs containing either HMEC-1 (left flank) or HMEC-1^{PSMA} (right flank) into severely immunodeficient NSG mice (**Figure 15a**). Immediately after transplantation of the Matrigel plugs, mice were given an intravenous (i.v.) injection of either P28BBζ CAR T cells or control FR28BBζ CAR T cells. The plugs and spleens were harvested 11 days after inoculation and analyzed for the presence of CAR-positive T cells via flow cytometry. In mice receiving the P28BBζ T cells, I found large numbers of CAR T cells in the plugs containing the HMEC-1^{PSMA} cells, whereas the plugs containing control HMEC-1 cells were largely devoid of T cells (**Figure 15b,c**). Similarly, very few FR28BBζ control T cells were found in the plugs containing either the PSMA positive or negative endothelial cell lines. Finally, I measured the percentage of CAR T cells found in the spleens of the treated mice and found substantially more P28BBζ CAR T cells compared to mice that

received the FR28BBζ control T cells (**Figure 15d**). Together, these data demonstrate that the P28BBζ CAR T cells are able to recognize and accumulate on PSMA$^+$ endothelial cells, and that they are able to persist *in vivo* in the presence of the antigen.

P28BBζ T cells eliminate PSMA$^+$ vascular neoplasms

Because the HMEC-1 model did not reproducibly form vascular structures *in vivo*, I used two well-established murine endothelial models, the MS1 hemangioma[74] model and the H5V hemangiosarcoma[75] model, to test the therapeutic efficacy of the P28BBζ CAR T cells. First, NSG mice were injected subcutaneously (s.c.) with MS1 cells (left flank) and MS1^{PSMA} cells (right flank), both of which had been previously engineered to express firefly luciferase to allow for non-invasive, real time tumor measurement throughout tumor progression and treatment. Mice were treated with a single i.v. administration of 5.0×10^6 CAR T cells 24 days after tumor inoculation (**Figure 16a**). In mice receiving the P28BBζ CAR T cells, I observed rapid regression of the MS1^{PSMA} hemangiomas, whereas the antigen-negative MS1 flank was unaffected (**Figure 16b**). Macroscopic examination of the hemangiomas upon sacrifice revealed that injection of the P28BBζ CAR T cells led to complete regression of the PSMA$^+$ tumors (**Figure 16c**). The control FR28BBζ CAR T cells had no impact on either of the hemangiomas. I also tested the P28BBζ T cells against larger, more developed MS1 and MS1^{PSMA} hemangiomas (**Figure 17a**). Here too, I observed rapid regression of the MS1^{PSMA} tumors after administration of the P28BBζ CAR T cells, as measured by both luciferase luminescence and caliper measurement (**Figure 17b**), which I confirmed

31

visually upon sacrifice of the mice (**Figure 17c**). Importantly, in both treatment models the P28BBζ CAR T cells demonstrated specificity and reactivity exclusively against the PSMA$^+$ tumors.

Finally, I assessed the ability of the P28BBζ CAR T cells to treat murine H5V hemangiosarcoma, an aggressive vascular target that metastasizes to the lung. Twenty-one days following i.v. inoculation with H5V^{PSMA} endothelial cells, NSG mice were given three i.v. injections of $5.0×10^6$ CAR T cells 72 h apart (**Figure 18a**). I monitored the progression and response of the tumors to treatment by luciferase luminescence, and mice were sacrificed upon losing 10% of their initial body mass. By the third injection of CAR T cells, the H5V^{PSMA} cells were nearly undetectable in the P28BBζ CAR treatment group, whereas no effect was seen in the FR28BBζ CAR treatment group (**Figure 18b,c**). Furthermore, mice treated with the P28BBζ CAR T cells lived significantly longer than those treated with PBS or FR28BBζ T cells (**Figure 18d**). Collectively, these models demonstrate that the P28BBζ CAR T cells are able to traffic to and eliminate aberrant PSMA$^+$ tumor vessels *in vivo*, and that PSMA-targeting CAR T cells are potent mediators of tumor vascular disruption

CAR T cells ablate PSMA$^+$ vasculature in solid tumors

Elimination of tumor vessels by vascular disrupting agents can result in the regression of solid tumors.[76] To test whether P28BBζ CAR T cells could elicit a similar effect, I developed a syngeneic vasculature/tumor chimeric transplant model. Briefly, MS1 (or MS1^{PSMA}) murine endothelial cells were co-injected with either murine ID8

ovarian tumor cells or ID8^{VEGF} ovarian tumor cells, which were engineered to overexpress mouse VEGF$_{164}$.[77] The endothelial and tumor cells were combined at an optimal ratio such that the majority of tumor blood vessels would be derived from the MS1/MS1^{PSMA} endothelial cells.[78,79,80] **Figure 19a** illustrates a representative experiment where mice were inoculated with ID8^{VEGF}, MS1/ID8^{VEGF}, or MS1^{PSMA}/ID8^{VEGF} tumors. By day 41, the majority of the CD31^{+} endothelial cells taken from the ID8^{VEGF}/MS1^{PSMA} tumors were found to express PSMA by immunofluorescence microscopy, confirming that the exogenous MS1 endothelial cells were substantially contributing to the tumor vasculature in this model (**Figure 19b**). These results were verified by flow cytometry analysis, which showed that upwards of 65% of CD31^{+} endothelial cells purified from tumors were PSMA^{+} (**Figure 19c**). Importantly, the CD31^{+} endothelial cells contributed less than 2% to the total cells isolated from the chimeric tumors, which was similar to what was observed for the more ID8^{VEGF}-only tumors, in which the vasculature was derived from endogenous endothelial cells. As such, I concluded that majority of the tumor was derived form the ID8^{VEGF} cells or stromal cells and not the co-injected MS1 endothelial cells (**Figure 19d**). In addition, we noted no difference in the tumor growth kinetic between the ID8^{VEGF} and ID8^{VEGF} tumors enriched with MS1 or MS1^{PSMA} cells (**Figure 19e**), further demonstrating that the chimeric tumors reproduced a "normal" tumor growth condition, and also confirming that the addition of the MS1 or MS1^{PSMA} cells did not substantially contribute to the volume of these tumors.

I next asked whether the proportion of MS1-derived vessels was consistent throughout tumor development. For these experiments I used MS1 and MS1^{PSMA} cells

engineered to express firefly luciferase and ID8^{VEGF} tumor cells engineered to express eGFP. In mice injected with either MS1/ID8^{VEGF} or MS1^{PSMA}/ID8^{VEGF} tumors, I compared seven longitudinal luciferase luminescence measurements, obtained between day 17 and 41, to seven longitudinal eGFP radiant efficiency measurements obtained at the same time points (**Figure 20a–e**). I performed linear regression analyses on the values obtained and found that endothelial luminescence was strongly correlated with tumor fluorescent radiant efficiency (**Figure 20a–e**), indicating that the exogenous endothelial cells expanded proportionally to the tumor cells. Thus, I concluded that within this tumor model the exogenous endothelial cells provided the main source of tumor endothelial cells required for neovascular formation. This data taken together indicates that the presence of the MS1 or MS1^{PSMA} vessels largely obviated the need for endogenous endothelial cell recruitment, and also shows that the MS1 endothelial cells do not constitute a significant portion of the cells within the tumor, supporting the assertion that the MS1 cells are predominantly forming tumor blood vessels and not contributing substantially to the overall tumor mass. Finally, I observed that the MS1 and MS1^{PSMA} endothelial cells could be followed non-invasively during tumor growth within this model, allowing for their persistence or elimination to be monitored after treatment with CAR T cells.

To test the ability of the P28BBζ CAR T cells to ablate the tumor vasculature *in vivo*, I first utilized the MS1/ID8 tumor model. NSG mice were injected with MS1/ID8 (left flank) and MS1^{PSMA}/ID8 (right flank) tumors, which were allowed to develop for 81 days before treatment with a single injection of 1.0×10^7 CAR T cells (**Figure 21a**). I

found that the P28BBζ CAR T cells were able to quickly eliminate the MS1$^{\text{PSMA}}$ endothelial cells, as indicated by luciferase luminescence measurements (**Figure 21b**, lower panel). In contrast, vessels within the MS1/ID8 tumors were unaffected by the P28BBζ CAR T cells (**Figure 21b**, upper panel). Administration of the FR28BBζ CAR T cells had no impact on the tumor blood vessels, confirming the specificity of the P28BBζ T cells.

Since VEGF plays an important role in the development and stabilization of new tumor vessels, and has been implicated in tumor resistance to VDAs,[81] I next sought to evaluate the *in vivo* impact of the P28BBζ CAR T cells on the vasculature of solid tumors expressing high levels of VEGF-A using the ID8$^{\text{VEGF}}$ model.[77] The MS1/ID8$^{\text{VEGF}}$ tumors grew more rapidly than the MS1/ID8 tumors, necessitating that the mice be sacrificed within approximately 40 days to avoid ulceration. Mice were therefore treated earlier and with three injections of 5.0×10^6 CAR T cells, beginning 25 days after tumor inoculation (**Figure 22a**). P28BBζ CAR T cells induced rapid regression of the PSMA$^+$ MS1 endothelial cell mass but had no effect on control MS1 cells (**Figure 22b**). In addition, the control FR28BBζ CAR T cells had no impact on the blood vessels of either tumor. Upon sacrifice I collected and enzymatically dissociated all tumors, which were subsequently stained using antibodies for CD31 and PSMA and analyzed via flow cytometry. No CD31$^+$PSMA$^+$ endothelial cells were found within the tumors of the P28BBζ-treated mice. In control treated mice, between 6080% of the CD31$^+$ endothelial cells were PSMA$^+$ within the MS1$^{\text{PSMA}}$/ID8$^{\text{VEGF}}$ tumors (**Figure 22c**). These findings

indicate that, like VDAs, CAR T cells can trigger regression of established tumor vasculature.

CAR T cells induce secondary loss of tumor cells and regression of solid tumors

To assess whether vascular disruption was causing the secondary loss of tumor cells, I examined the effects of P28BBζ CAR T cells on tumor growth in the experiments described above. In the MS1/ID8 model (experiment outlined in **Figure 21a**), treatment with P28BBζ CAR T cells led to a significant decrease in the overall size of the MS1^{PSMA}/ID8 tumors,, but not of the antigen-negative MS1/ID8 tumors (**Figure 23a**). In addition, growth of MS1^{PSMA}/ID8^{VEGF} tumors was significantly impaired in P28BBζ treated mice (**Figure 24a,b**). This response was noted to be dose-sensitive, as mice treated with a single injection of 1×10^{7} CAR T cells did not eliminate PSMA^{+} endothelial cells as rapidly and did not inhibit the growth of ID8^{VEGF} tumors as effectively as mice treated with three injections of 5×10^{7} CAR T cells. These data demonstrate that even in the context of VEGF overexpression, elimination of the antigen-positive vasculature by CAR T cells can lead to significant tumor regression.

Given that endothelial cells account for less than 2% of the cells found within the MS1/ID8^{VEGF} and MS1^{PSMA}/ID8^{VEGF} tumors (see **Figure 20d**), I hypothesized that the regression I observed in the P28BBζ-treated mice was not merely reflecting the loss of the MS1^{PSMA} cells from the ID8^{VEGF} tumors, but rather indicating a significant loss of

tumor cells in response to T cell mediated vascular disruption. To ascertain whether this was true, I developed an ID8^{VEGF} model in which the tumor cells expressed firefly luciferase, while MS1 cells did not. As before, NSG mice were inoculated with MS1/ID8^{VEGF} (left flank) and MS1^{PSMA}/ID8^{VEGF} (right flank) tumors. Three administrations of 5.0×10^7 CAR T cells were given, beginning on day 22 (**Figure 25a**). Both luciferase luminescence, as well as tumor volume measurements revealed that treatment with the P28BBζ T cells impaired tumor growth (**Figure 25b**). To determine if the P28BBζ T cells were mediating tumor cell destruction, I compared the fold change in tumor cell luminescence in mice receiving the P28BBζ T cells. I observed a significant decrease in tumor luminescence from the MS1^{PSMA}/ID8^{VEGF} tumors after the second injection of P28BBζ T cells, between days 24 and 28 (**Figure 25c**). In contrast, I observed a significant increase in signal from the antigen negative MS1/ID8^{VEGF} tumors during that same period (**Figure 25c**). Upon sacrifice of the animals, I confirmed elimination of the MS1^{PSMA} endothelial cells via flow cytometry (not shown). Together, these data demonstrate that destruction of the vasculature does indeed result in tumor cell loss.

Finally, I sought to determine whether bystander killing of adjacent ID8^{VEGF} tumor cells could explain the reduction in tumor signal I observed in this model. I performed an *in vitro* killing assay where I co-cultured MS1^{PSMA} endothelial cells overnight at increasing ratios with ID8^{VEGF} tumor cells and T cells. MS1^{PSMA} cells were eliminated by the P28BBζ CAR T cells, but the ID8^{VEGF} cells were unaffected by the T cells (**Figure 25d**). These data suggest that tumor regression *in vivo* occurred through

37

indirect loss of tumor cells, related to the disruption of the vasculature, rather than a direct bystander effect.

The distribution of membrane-bound PSMA isoforms in normal tissue

One possible concern in targeting PSMA with CAR-bearing T cells is the potential for on target/off organ toxicity. PSMA has been detected by immunohistochemistry in a number of organs,[50,52] (summarized in **Table 5)** and was confirmed by us using the 3E6 antibody (**Table 5, Figure 26**). The interpretation of this data, however, is complicated by a number of factors. I observed apical expression of PSMA in the ducts of the prostate, the kidney tubules, and the intestines (**Figure 26**), which others have suggested may provide a degree of immune privilege to these sites, as the apical surfaces of these cells are separated from circulation by tight junctions.[82] This may explain why clinical trials performed with radiolabeled J591 antibody did not show localization of the antibody to either the intestine or kidney.[53] Additionally, the presence of multiple PSMA splice variants has further complicated the direct interpretation of the existing immunohistochemistry data (**Figure 27**). Of the known membrane-bound isoforms of PSMA, only isoforms 1 and 2 have confirmed physiological relevance.[83] Isoform 1 is more abundant than isoform 2, but the relative distribution of each is unclear. Isoform 2 is nearly identical to full-length PSMA, but is missing exon 18. Prior to this study, the J591 scFv was known to bind an extracellular epitope of PSMA, but it was unknown whether the antibody could distinguish between the two isoforms.

Therefore, I first sought to determine whether the J591-based CAR T cells could distinguish between PSMA isoform 1 and isoform 2.

Immortalized human microvascular endothelial cells (HMEC-1) were engineered to express either PSMA isoform 1 or 2 using lentiviral transduction. Primary human T cells were then transduced to express the Pζ CAR and monitored for CAR expression (See **Figure 8c**). Analysis of INF-γ after co-culture revealed specific activation of the CAR bearing T cells exclusively by the isoform 1-bearing HMEC (**Figure 28**). Importantly, this shows that the Pζ CAR T cells can distinguish between the two PSMA isoforms and identifies a previously unappreciated specificity for the J591 scFv. This also suggested that the binding epitope for J591 lies within exon 18, as this is the only region missing between the two isoforms. This observation, however, also raised questions concerning the distribution of the two isoforms, particularly whether differential expression of either isoform may occur in either normal or neoplastic tissue. Reliance on standard antibody-based assays to distinguish the two isoforms was unlikely to succeed, as extensive homology between the two isoforms exists. I therefore utilized RT-PCR to distinguish between the two isoforms in a panel of normal tissues.

To avoid amplification of non-membrane bound variants of PSMA, I designed PCR primers to sit within the transmembrane region and exon 19, which are shared between PSMA isoform 1 and PSMA isoform 2. Using these primers, PCR products of 2016 bp and 1922 bp were expected from PSMA isoform 1 and 2, respectively (**Figure 29a**). To confirm the specificity of these primers, I performed a PCR on cDNA collected from the transduced HMEC-1 cells, which were engineered to express either isoform 1 or

2, and the LNCaP prostate cancer cell line, which was previously identified to express both isoforms.[84] Polyacrylamide gel electrophoresis revealed the expected result, and demonstrated that PSMA isoform 1 and 2 could be resolved using this methodology (**Figure 29b**).

cDNA was then collected from a panel of 20 normal tissues, and PCR for ribosomal RNA 18s, was performed as a loading control for each of the samples (**Figure 30**). PCR analysis of the isoforms revealed expression of both in the brain, colon, kidney and prostate, and to a lesser extent, the spleen, liver, lung, ovary, and placenta (**Figure 31**). Importantly, few differences in the expression of each isoforms were noted, indicating that the preference of the J591 scFv for isoform 1 would not likely yield a therapeutic advantage. However, this study has identified a list of normal organs that should be monitored carefully during the administration of anti-PSMA CAR-bearing T cells, and underscores the importance of developing safety features for CAR therapy (discussed in detail within **Chapter 4**). In addition, this study confirms the presence of PSMA isoform 2 in a number of tissues, and highlights the need for further study of this isoform in normal physiology.

Conclusions

Although numerous studies have demonstrated the anti-tumor effect of CAR T cells, only a small selection of these have focused on the ability of engineered T cells to disrupt the vasculature. Here, I have shown that T cells bearing a CAR against PSMA can mediate vascular disruption, which leads to tumor regression. *In vitro*, the P28BBζ T cells were capable of recognizing and eliminating endothelial targets (**Figure 11**), as well as microvessels formed from these cells (**Figure 14**). In addition, the P28BBζ CAR T cells were able to eliminate hemangiomas as well as hemangiosarcomas *in vivo* (**Figure 16–18**). Lastly, in two solid ovarian tumor models, I found that administration of the P28BBζ T cells was able to eliminate PSMA$^+$ tumor vasculature, and result in the loss of tumor cells as well as elicit tumor regression (**Figure 21–25**). Taken together, these data support the observation that CAR T cells can effectively disrupt the tumor vasculature, and that elimination of the vasculature by antigen specific T cells can result in tumor regression. Complete eradication of solid tumor was not observed in these models, however, and future studies should aim to address this shortcoming through combinatorial approaches. Conventional VDAs have demonstrated synergy with radiation, chemotherapy, and anti-angiogenic therapies, suggesting a role for such combinations in CAR mediated vascular disruption.[85] Even so, it should be noted that this is the first study to demonstrate that CAR bearing T cells are able to eliminate PSMA$^+$ vasculature within the tumor, and that elimination of these cells can have profound effects on tumor progression. As such, this work supports the further development of anti-PSMA CAR T cells for use in vascular disruption therapy.

CHAPTER 4: DISCUSSION AND FUTURE DIRECTIONS

Recent clinical trials have demonstrated the power of CAR T cell-based immunotherapy for individuals with advanced cancer. Remarkable responses have been reported, for example, in patients receiving CD19-specific CAR T cell therapy for the treatment of acute lymphocytic leukemia.[24,36,86] In addition, active remission has been reported in patients with neuroblastoma after treatment with CAR T cells directed against the ganglioside, GD2.[87] A critical component to the clinical success of adoptive CAR T cell treatment is the choice of target antigen. Ideally the target is immunogenic, related to oncogenesis, and is stably, selectively, and abundantly expressed in tumor tissue. Recently, we and others have shifted focus towards targeting the tumor vasculature, as opposed to the tumor itself, since these cells represent a more 'universal' and genetically stable target.[23,88] Not only would this strategy cut off oxygen and nutrient exchange to the tumor, as well as important growth factors, but it would also breakdown a physical barrier against immune cell infiltration.[89] One tumor endothelial-specific target is TEM1. The potency of generating a T cell response against this antigen is evident through studies using DNA vaccines.[23] The development of CAR T cells against this antigen, however, has been difficult. I was able to generate a T cell response against plate-bound recombinant TEM1 protein using the scFv78 CAR, but was unable to demonstrate reactivity against TEM1 expressed on the surface of endothelial cells. This suggests that the epitope targeted by scFv78 may be "masked" by the milieu of surface proteins on the target cells or that it may be too distal from the CAR receptor to properly engage, as soluble scFv78 was able to label TEM1 on the surface of these cells. These data underscore a largely underappreciated aspect of CAR development and stress the

importance of epitope accessibility when choosing a scFv for use in CAR. Finally, I have also shown that T cells bearing a CAR against PSMA, an antigen upregulated on the tumor endothelium in many types of cancer, can destroy the tumor vasculature and elicit tumor regression. Together, the wide expression of PSMA across many solid tumor types, and the ability of the P28BBζ T cells to elicit tumor regression through vascular disruption, justifies the pursuit of this therapeutic approach.

One major advantage of using CAR T cells to disrupt the tumor vasculature, as opposed to conventional VDAs, is their ability to self-replicate and to persist long-term in patients.[24] In addition, CAR T cells can trigger epitope spreading and help to reprogram the tumor microenvironment.[25] Given the persistence and power of CAR T cells, a second critical component to the clinical success of CAR T cell therapy is safety. This cannot be overstated, as unexpected CAR cross-reactivity with healthy tissues has, unfortunately, resulted in patient deaths.[87] Prior to this study, tumor blood vessels destruction had been successfully demonstrated using CAR T cells engineered to recognize VEGFR-1 and VEGFR-2[38] or VEGFR-2 alone.[37] Although encouraging, VEGF receptors are also expressed by normal endothelial cells throughout the body and thus represent a significant risk for "on-target/off-tumor" toxicity. In contrast, PSMA has not been found on normal blood vessels. Nevertheless, it has been detected by IHC in the prostate, kidney, liver, intestine, and colon, as well as on the astrocytes of the brain.[52,90,91] Discrepancies exist between these studies, however, and interpretation of the data is complicated by the existence of splice variants,[62,63] the localization of the protein on the cell surface (apical *versus* basal), the process of tissue collection, the method of fixation,

and the antibodies used to detect PSMA. Recognition of PSMA by the CAR T cells described here is mediated through the well-characterized scFv, J591. Encouragingly, imaging studies performed with radiolabeled J591 did not show accumulation of the mAb in either the kidneys or the small intestine.[53] Furthermore, a phase 1 clinical trial with the J591 mAb demonstrated positive localization of the antibody to tumors with PSMA$^+$ vasculature.[92] Overall, this evidence suggests that J591-based CAR T cells will have a favorable safety profile in patients.

Additional approaches exist, however, that could increase the safety of CAR bearing T cells against both the tumor and/or the tumor vasculature. In mice, CAR T cells generated through RNA transfection were seen to approach the efficacy of lentivirally transduced T cells when given in multiple administrations after lymphodepleting chemotherapy.[93] These T cells have the advantage of losing CAR expression over time, through cellular division and mRNA degradation, and offer a potential solution to the "on-target/off-tumor" reactivity of persistent T cells after tumor elimination. Another approach to eliminate these cells would be to include a "suicide switch", such that the CAR-bearing T cells could be selectively eliminated through the administration of a drug or pro-drug. Herpes simplex thymidine kinase (HSV-tk) was the first robustly tested inducible suicide gene, and administration of the drug ganciclovir was shown to result in the death of cells harboring HSV-tk. However, further study demonstrated that HSV-tk can be immunogenic,[94] and that silencing of the gene can result in ganciclovir-resistance,[95] ultimately leading to the search for additional genes. More recently, inducible activation of caspase 9 (iC9) has gained favor. In patients, it

was demonstrated that T cells carrying the iC9 gene could be selectively eliminated from those experiencing graft versus host disease (GVHD) by treatment with the dimerizing drug, AP1903.[96] In these patients, symptoms of GVHD resolved with the destruction of the transduced T cells. In a mouse model of non-Hodgkins lymphoma, 3rd generation CAR T cells, like the P28BBζ T cells used here, were also found to be susceptible to inducible apoptosis by the iC9 suicide gene,[97] Finally, CAR T cells could be engineered to contain split-signaling CARs where signal 1 (CD3ζ) would be linked to a scFv recognizing one target while signal 2 (such as CD28 and/or 4-1BB) would be linked to a second scFv recognizing another target. This has been demonstrated by Lanitis *et. al.,*[59] and could be applicable for vascular targeting, for example, using CAR T cells engineered to recognize PSMA (signal 1) and a second tumor endothelial target, thus providing increased therapeutic safety. Additional tumor endothelial targets have been identified in ovarian cancer[5,98] and other tumors,[40] enabling these combinatorial designs.

The heterogeneous expression of PSMA on the tumor vasculature may represent a significant obstacle for PSMA-directed anti-vascular therapy. Here I found that over 85% of women with ovarian cancer expressed PSMA on their tumor vasculature, but also that only 40–60% of the $CD31^+$ endothelial cells isolated from their gynecological tumors expressed PSMA. The biology of this heterogeneity has not yet been investigated. It is possible that upregulation of PSMA reflects a state of metabolic activation of tumor endothelial cells, requiring increased folate uptake. In fact, PSMA exhibits hydrolase activity, which hydrolyzes the gamma-glutamyl tail of folate polyglutamates, resulting in folates that can be readily taken up by cells. At physiological folate concentrations,

overexpression of PSMA was found to confer growth advantage to tumor cells and enhance their invasive activity.[65] Importantly, angiogenesis is severely impaired in PSMA-null mice and the enzymatic activity of PSMA is required for endothelial cell invasion *in vitro* through regulation of integrin signaling.[67] Therefore, PSMA-expressing endothelial cells may be critical for neovascular formation, and their persistent immune-mediated elimination could not only disrupt the existing vasculature but also prevent new blood vessel formation. This hypothesis has not yet been fully tested, and it remains to be seen whether anti-PSMA CAR T cells could influence the re-generation of tumor blood vessels through this mechanism. It is worth noting, however, that in my adoptive CAR T cell transfer studies the P28BBζ T cells were able to persistently suppress almost the entire PSMA-expressing fraction of tumor endothelial cells.

Unfortunately, elimination of the PSMA$^+$ vessels from the MS1^{PSMA}/ID8^{VEGF} tumor model did not result in complete tumor regression. This could be due to the fact that only a fraction of the tumor endothelial cells expressed PSMA within this model, as was the case for the human tumor specimens I analyzed. One method to overcome this obstacle would be to combine the anti-PSMA CAR T cells with additional treatment modalities. Conventional VDAs have been combined with both radiation and chemotherapy for improved tumor control,[85] suggesting that a similar approach could also augment the efficacy T cell mediated vascular disruption. In addition, VDAs have also been successfully administered with anti-angiogenic agents as a means to target the existing tumor blood vessels, as well as impair the growth of new vessels.[99] In fact, anti-angiogenic therapy has already been shown to synergize with CAR T cell therapy (1st

generation) directed against the VEGF receptors.[38] Another approach to increase the efficacy of the anti-PSMA CAR T cells would be to combine them with CAR T cells or TCR-engineered T cells that recognize a second tumor endothelial antigen or the tumor itself. The group of Steven Rosenberg illustrated this approach by showing that B16 tumors could be successfully eradicated in mice when anti-VEGFR-2 CAR T cells were combined with tumor-targeting T cells, but not when the mice were treated with the anti-vascular CAR T cells alone.[100] Building on this observation, I also posit that patients whose tumor expresses PSMA on both the endothelium and tumor, as was observed here for one subject with ovarian cancer and has been noted in a number of cancers,[52] may respond more successfully to treatment with anti-PSMA T cells. The answer to this question continues to be pursued within our lab.

In conclusion, I have demonstrated that 3rd generation CAR T cells can target and eliminate PSMA-expressing endothelial cells of the tumor vasculature both *in vitro* and *in vivo*, and that elimination of these cells can result in tumor regression. I propose that split-signaling may enhance their safety profile, and that, in combination with other treatments such as chemotherapy, radiation, and/or tumor cell targeting T cells, they will provide important clinical benefit to patients.

CHAPTER 5: MATERIAL AND METHODS

CAR construction

The J591 [35] and MOv19 [69] scFvs were gifts from M. Sadelain and D. Powell, respectively. The pELNS lentiviral vector and the genes encoding the CAR signaling domains ζ, 28ζ, BBζ, and 28BBζ were gifts from C. June.[34] pELNS is a third generation self-inactivating lentiviral expression cassette based on pRRL-SIN-CMV-eGFP-WPRE;[58] with transgene expression driven by the EF-1α promoter. The constructs were engineered to express an upstream eGFP reporter separated from the CAR by a T2A sequence. The J591 and MOv19 scFvs were amplified via PCR and subcloned into an intermediary vector (pCLPS) using 5' BamHI and 3' NheI restriction enzyme cut sites. 5' primer, J591F = ATCGggatccGTGCAGCTGCAGCAGTCAGG and 3' primer, J591R = GCTAgctagcCCGTTTCAGGTCCAGCATGG. BamHI and NheI cut sites are underlined, respectively. The resulting constructs contained the full-length CAR construct, including signaling domain(s). The full-length sequence for each CAR was then isolated from the pCLPS vectors using 5' AvrII and 3' SalI restriction enzyme cut sites. Finally, the CAR constructs were ligated into the pELNS vector backbone, which was gel-purified after digestion with XbaI (compatible with AvrII) and SalI restriction enzymes. The anti-TEM1[57] and anti-mesothelin (P4)[59] CARs were constructed in a similar manner using primers directed against their respective scFvs.

Lentiviral production

Lentivirus was generated as previously described.[59] Briefly, 2.0×10^6 293T cells were plated in T-150 tissue culture flask 18 h before transfection with transgene (15 μg,

pELNS) and packaging plasmids (7 µg pVSV-G, 18 µg pRSV-REV, and 18 µg pMDLg/p.RRE). Supernatants were collected at 24 and 48 h and were then combined and concentrated via ultracentifugation at 28,000 RPM for 3 h. Virus was re-suspended in 2 mL RPMI (10% FBS, 100 IU mL^{-1} penicillin, and 100 µg mL^{-1} streptomycin sulfate), flash frozen, and stored at −80° until needed.

Human T cell Transduction

T cells were isolated from healthy donors by the Human Immunology Core at the University of Pennsylvania under a protocol approved by the University Institutional Review Board. With minor modifications, T cells were transduced as previously described.[59] Briefly, T cells were cultured in RPMI supplemented with 10% FBS, 100 IU mL^{-1} penicillin, and 100 µg mL^{-1} streptomycin sulfate. 20 h prior to transduction, 5.0×10^5 T cells were activated using anti-CD3/anti-CD28 coated beads (Invitrogen, Carlsbad, CA) at a 2:1 bead to T cell ratio in RPMI supplemented with 50 IU mL^{-1} recombinant human IL-2 (Peprotech, Rocky Hill, NJ). Activated T cells were spinoculated at 1000 g for 90 min with lentivirus (MOI of 10) and polybrene (8 µg mL^{-1}; Sigma-Aldrich, St. Louis, MO) in a total volume of 1 mL. 24 h after spinoculation, half the media was removed (0.5 mL) and cells were given 1.5 mL of fresh RPMI with 50 IU mL^{-1} recombinant human IL-2. The media was replenished every other day with fresh RPMI and IL-2 (50 IU mL^{-1}) so that T cell density did not exceed $\sim 1.0 \times 10^6$ mL^{-1}. The T cells were used between 14–28 d after transduction.

Cell lines

Low-passage (P16) 293T cells purchased from the American Type Culture Collection (ATCC, Manassas, VA) were used for the production of lentivirus particles. The MS1 (mouse pancreatic islet) endothelial cell line was also purchased from the ATCC. Immortalized H5V (mouse heart endothelial cells) were previously acquired.[75] 293T, MS1, and H5V cell lines were grown in RPMI supplemented with 10% FBS, 100 IU mL^{-1} penicillin, and 100 μg mL^{-1} streptomycin sulfate. HMEC-1 cells, an SV40 transformed human microvascular endothelial cell line,[70] were obtained from the Centers for Disease Control and Prevention (Atlanta, GA) and grown in MCDB 131 media (Invitrogen, Carlsbad, CA) containing mouse EGF (BD, Franklin Lakes, NJ), hydrocortisone (Sigma-Aldrich, St. Louis, MO), 10% FBS, 100 IU mL^{-1} penicillin, and 100 μg mL^{-1} streptomycin sulfate and 1x GlutaMax (Invitrogen, Carlsbad, CA).

Flow Cytometry

CAR T cells were identified primarily through detection of their eGFP reporter. For surface detection, T cells were stained with an APC-conjugated goat anti-mouse F(ab$_2$) fragment (Jackson, West Grove, PA; #115-136-072). Bcl-xL expression was detected using a mouse anti-human Bcl-xL Ab (SouthernBiotech, Birmingham, AL; clone 7B2.5) after fixation and permeabilization with an intracellular staining kit (eBioscience, San Diego, CA). PSMA was detected using a humanized J591 mAb (gift from N. Bander) and an APC-conjugated anti-human secondary Ab (Jackson, West Grove, PA; #109-136-098). Positive staining was assessed by comparison with a human

IgG isotype control Ab (Enzo, Farmingdale, NY; #ALX-804-133-C100). In addition to the J591 mAb, human tumor digests were stained with APC-Cy7-conjugated anti-human CD45 (BD, Franklin Lakes, NJ; clone 2D1), Pacific-Blue-conjugated anti-human CD31 (BioLegend, San Diego, CA; clone WM59), and PE-conjugated anti-folate receptor (R&D, Minneapolis, MN; clone 548908) Abs prior to analysis. Harvested mouse tumors were also stained with the J591 mAb, as well as APC-Cy7-conjugated anti-human CD45 (BD, Franklin Lakes, NJ; clone 2D1) and Pacific-Blue-conjugated anti-mouse CD31 (BioLegend, San Diego, CA; clone 390) Abs. All samples were stained with the fixable viability dye eFlour 506 prior to analysis (eBioscience, San Diego, CA).

T cell proliferation studies

Prior to co-culture with target cell lines, T cells were labeled with CellVue® Claret as described in the kit's technical bulletin (Sigma-Aldrich, St. Louis, MO). Labeling was confirmed by flow cytometry prior to co-culture. 1.0×10^5 CAR T cells were then cultured with 5.0×10^4 HMEC-1 or HMEC-1^{PSMA} (E:T = 2:1) for 5 days in 48-well flat-bottom plates. Flow cytometry was used to analyze the intensity of CellVue® staining after co-culture. CAR$^+$ T cells were identified by eGFP expression. To quantify the membrane staining between the T cells cultured with the HMEC-1 versus HMEC-1^{PSMA}, the geometric mean fluorescence intensity (MFI) of Cellvue® Claret staining was measured for the CAR-positive T cells. To normalize across multiple donors, the MFI of CellVue® staining on CAR$^+$ T cells after co-culture with HMEC-1^{PSMA} was divided by the MFI of the CAR$^+$ T cells after co-culture with the HMEC-1.

Cytokine Release Assays

IFN-γ ELISAs were performed as directed in the Human IFN-γ ELISA MAX technical manual (BioLegend, San Diego, CA). For co-culture of CAR T cells with immobilized protein, recombinant TEM1 or BSA was coated onto an adsorbent nunc plates at 2.5 μg mL^{-1} overnight using carbonate/bicarbonate buffer. 1.25×10^5 T cells were added to each well and cultured overnight (18 h) before supernatants were collected and analyzed by IFN-γ ELISA. For cell line assays, 7.5×10^4 CAR T cells were cultured overnight with 2.5×10^4 endothelial targets (E:T = 3:1), unless otherwise noted in the figure legends. Triplicate cultures were performed in 96-well flat-bottom plates. Supernatants were collected from each well after 18 h. For assays utilizing primary human tumor samples, 9.0×10^4 CAR T cells were cultured overnight with 3.0×10^4 enriched endothelial targets (E:T = 3:1). Cultures were performed in 96-well flat-bottom plates and supernatants were collected after 18 h.

Biotin Binding Immune Receptor Assays

Lentivirus was for the BBIR was generously given donated by the laboratory of Daniel Powell. T cells harboring the BBIR were plated with labeled targets at ratios described in the figure legends. Prior to co-culture, cells were detached from tissue culture plates using 2mM EDTA and labeled using biotinylated anti-TEM1 antibodies at a concentration of 2.5 μg mL^{-1}. Half the labeled cells were used for flow cytometry to

confirm binding, whereas the other half of the cells was utilized in co-culture. Co-cultures were performed overnight (18 h), at which point supernatants were collected for analysis for IFN-γ by ELISA.

Cytotoxicity assays

^{51}Cr release assays were performed as previously described [59]. CAR T cells were cultured for 18 h with endothelial targets at E:T ratios of 10:1, 3:1, and 1:1. Specific lysis was calculated as (experimental − spontaneous lysis / maximal − spontaneous lysis) × 100. Luciferase based assays were performed similarly; CAR T cells were co-cultured for 18 h with endothelial targets engineered to express firefly luciferase at the ratios indicated in the figure legend(s). Co-cultures were performed in triplicate using opaque 96-well flat-bottom plates in phenol-free RPMI. Firefly luminescence measurements were taken according to Luc-Screen® technical manual (Life Technologies, Grand Island, NY). The percentage of specific lysis was calculated as 100 − (luciferase signal treated / luciferase signal untreated × 100).

Time-lapse microscopy

24-well flat-bottom plates were coated with a thin layer (300 μL per well) of Matrigel (BD, Franklin Lakes, NJ) and allowed to solidify at 37° C for 30 min. Next, either 1.0×10^5 HMEC-1 or 1.0×10^5 HMEC-1^{PSMA} endothelial cells were seeded into the wells. Microvessels were given 8 h to form prior to addition of the CAR T cells. After 8

h, 3.0×10^5 CAR T cells were added to each well and images were taken at 0, 24, and 48 h after initiation of the co-culture (E:T = 3:1). Cells were kept in an environmentally controlled chamber at 37° C with 5% CO_2 throughout the experiment. X-Y coordinates were saved for each well so that the identical field of view could be captured at each time point. Pictures were taken using a fluorescence microscope (ECLIPSE Ti; Nikon Corporation, Tokyo, Japan) equipped with a charge-coupled device camera (Photometrics CoolSnap HQ2; Roper Industries, Inc, Sarasota, FL, USA) and NIS-Elements AR software (v 3.2; Nikon Corporation). Original magnification shown, 40× or 100×, as described in the figure legends.

Immunohistochemistry

For human TMA and normal organ slide staining, paraffin-embedded tissues were baked at 60 ˚C for 1 h, deparrafinized in xylenes, rehydrated in sequential gradations of alcohol, and washed in water. Depending on the Ab, antigen retrieval was performed using either citrate or EDTA buffer. Endogenous peroxidase was inactivated with Dual Endogenous Enzyme block (Dako, Carpnteria, CA). Following Ab staining, TMAs were visualized with diaminobenzidine tetrahydrochloride (Dako, Carpnteria, CA) or an alkaline phosphatase red substrate kit (dual stains). Sections were then counterstained with hematoxylin. Sections were stained with an anti-human PSMA Ab (Dako, Carpnteria, CA; clone 3E6) alone, or in combination with anti-human CD34 Ab (Thermo Scientific, Waltham, MA; rabbit polyclonal). The TMAs and slides were then scanned and analyzed using ImageScope software. For TMAs that included multiple cores from

56

the same subject, individuals were considered PSMA$^+$ if staining could be confirmed on any of the cores from that subject. Damaged or absent cores were excluded from analysis.

Enrichment of human CD31$^+$ endothelial cells

Human tumor specimens were gathered with approval from the UPENN institutional review board in compliance with the US Health Insurance Portability and Accountability Act (HIPAA). Briefly, tumors were mechanically or enzymatically digested to yield a single cell suspensions that were subsequently frozen and stored at –150° C until needed. Samples were rapidly thawed in a 37° C water bath. Viable cells were counted using Trypan Blue. Tumor digests were first depleted for CD45 using Miltenyi anti-human CD45 beads, as per manufacturers instructions (Miltenyi, San Diego, CA). The CD45$^-$ fraction was then enriched for human CD31 endothelial cells using Miltenyi anti-human CD31 beads (Miltenyi, San Diego, CA). Both the CD45$^-$ CD31$^-$ and CD45$^-$CD31$^+$ population were retrieved and analyzed by flow cytometry and/or used in functional assays.

RT-PCR of PSMA isoforms in normal tissues

A panel of normal tissue human RNA was obtained through Ambion/Life Technologies (FirstChoice® Human Total RNA Survey Panel, Grand Island, NY). Each RNA sample was pooled from at least three distinct donors. cDNA was synthesized

using the SuperScript® First Strand Synthesis kit (Life Technologies, Grand Island, NY). PCR for the internal control reference gene, ribosomal RNA 18s, was performed to confirm equivalent starting concentrations of cDNA. (18s Forward: 5'-CAGCCACCCGAGATTGAGCA-3', 18s Reverse: 5'-TAGTAGCGACGGGCGGTGTG-3')(25 cycles at: denaturation: 94°, annealing: 52°, elongation 72°). PCR for PSMA isoforms 1 and 2 were performed using primers specific to the transmembrane and exon 19 regions shared between the two isoforms. (PSMA TMF: 5'-CTGGTGCTGGCGGGTGGCTTC-3', PSMA 19R: 5'-GTGGCTGCTTGGAGCATAGATG-3')(38 cycles at: denaturation: 92°, annealing/elongation 68°). Samples were run on a 5% polyacrylamide gel using gel electrophoresis and visualized using a gel imaging station.

Mice

All protocols were reviewed and approved by the Institutional Animal Care and Use Committee at the University of Pennsylvania. All experiments were done using female NOD.Cg-*Prkdc^{scid} Il2rg^{tm1Wjl}*/SzJ (NSG) mice (aged 8-10 weeks) purchased from and housed at the Stem Cell Xenograft Core (SCXC), a germ-free facility at University of Pennsylvania.

In vivo assays with HMEC-1 cells

Matrigel plugs containing HMEC-1 (left flank) and HMEC-1^{PSMA} (right flank) endothelial cells were injected s.c. on the flanks of mice. CAR-positive T cells were administered via tail vein injection immediately following implantation of the plugs. The number of cells inoculated/injected is notated in the figure legend(s). Mice were sacrificed after 11 days and the Matrigel plugs retrieved and digested with 3U mL^{-1} dispase (Sigma-Aldrich, St. Louis, MO) and 25 μg mL^{-1} DNase to yield a single cell suspension. The cells collected from the plugs, as well as splenocytes collected from the spleens of the sacrificed animals, were then stained and analyzed by flow cytometry.

In vivo assays with MS1 cells

Mice were injected s.c. on each flank with MS1 (left flank) and MS1^{PSMA} (right flank) endothelial cells and CAR-bearing T cells were administered as noted in the figure legend(s). Hemangioma development and response to treatment was monitored twice a week by measuring luciferase luminescence. Mice were injected intraperitoneally with 100 μL of D-Luciferin stock solution (30 mg mL^{-1}, GoldBio, St. Louis, MO), anesthetized using isofluorane, and imaged 20 min after luciferin injection. To avoid bias, the PSMA^{+} tumor (right flank) was measured first. Mice were then flipped, and the antigen negative tumor (left flank) was analyzed, typically 1-2 minutes after the right flank. Data were gathered using a Xenogen IVIS imaging system, and analyzed using Living Image software (PerkinElmer, Waltham, MA). When palpable, tumors were

measured with Vernier calipers and volumes were calculated using the equation $V = \frac{1}{2}$ (L $\times W^2$).

In vivo assays with H5V cells

Mice were injected i.v. with H5V^{PSMA} endothelial cells and CAR T cells were administered as noted in the figure legend(s). Tumor development and response to treatment was monitored twice a week by measuring luciferase luminescence. Mice were injected with luciferin as described above. Luciferin was injected as described above and 20 min after injection the ventral surface of the animals was imaged. Mice were weighed twice per week and sacrificed if/when they lost more than 10% of their initial body mass.

In vivo assays with MS1/ID8 cells

Mice were injected s.c. on each flank with MS1/ID8 (left flank) and MS1^{PSMA}/ID8 (right flank) cells and CAR T cells were administered as noted in the figure legend(s). Luciferase luminescence and tumor volume were measured as described for the MS1 tumors. After termination of the MS1/ID8^{VEGF} experiment, the remaining tumors were excised and split for analysis. Half the tumor was embedded and frozen in Tissue-Tek® O.C.T. medium (VWR, Philadelphia, PA), while the other half was digested overnight in serum free RPMI containing collagenase (175 CDU mL^{-1}) and DNAse (20 Kunitz units mL^{-1}). After digestion, tumors were filtered through a 70 μm mesh filter and treated with ACK buffer to lyse red blood cells. Digests were then

60

analyzed by flow cytometry. Tumors not large enough to be split were embedded in O.C.T. and frozen. For the ID8^{VEGF}, MS1/ID8^{VEGF}, MS1^{PSMA}/ID8^{VEGF} control mice eGFP radiance was also measured. The ID8^{VEGF} tumor cells brightly express an eGFP reporter (data not shown). Spectral unmixing for eGFP was performed using the Living Image software, and the results were plotted against luciferase luminescence values taken concurrently. Finally, ID8^{VEGF} cells were also transduced to express firefly luciferase. For experiments utilizing these tumor cells, non-luciferase bearing MS1 cells were co-injected with the ID8^{VEGF} so that the signal from the tumor could be visualized independently without reflecting the contribution of the MS1 derived vasculature.

Statistical Analysis

Values are expressed as the mean ± either SD or SEM, as indicated in the figure legends. Statistical differences were determined to be significant *at P < 0.05*. Specific tests used are described in the figure legends. All analyses were performed using Graphpad Prism Software.

CHAPTER 6: REFERENCES

References

1.   Bergers, G, and Benjamin, LE (2003). Tumorigenesis and the angiogenic switch. *Nature reviews Cancer* **3**: 401-410.

2.   Baeriswyl, V, and Christofori, G (2009). The angiogenic switch in carcinogenesis. *Seminars in cancer biology* **19**: 329-337.

3.   Lu, J, Ye, X, Fan, F, Xia, L, Bhattacharya, R, Bellister, S*, et al.* (2013). Endothelial cells promote the colorectal cancer stem cell phenotype through a soluble form of Jagged-1. *Cancer cell* **23**: 171-185.

4.   Neiva, KG, Warner, KA, Campos, MS, Zhang, Z, Moren, J, Danciu, TE*, et al.* (2014). Endothelial cell-derived interleukin-6 regulates tumor growth. *BMC cancer* **14**: 99.

5.   Buckanovich, RJ, Facciabene, A, Kim, S, Benencia, F, Sasaroli, D, Balint, K*, et al.* (2008). Endothelin B receptor mediates the endothelial barrier to T cell homing to tumors and disables immune therapy. *Nature medicine* **14**: 28-36.

6.   Motz, GT, Santoro, SP, Wang, LP, Garrabrant, T, Lastra, RR, Hagemann, IS*, et al.* (2014). Tumor endothelium FasL establishes a selective immune barrier promoting tolerance in tumors. *Nature medicine*.

7.   McKeage, MJ, and Baguley, BC (2010). Disrupting established tumor blood vessels: an emerging therapeutic strategy for cancer. *Cancer* **116**: 1859-1871.

8.   Folkman, J (1971). Tumor angiogenesis: therapeutic implications. *The New England journal of medicine* **285**: 1182-1186.

9.   Niu, G, and Chen, X (2010). Vascular endothelial growth factor as an anti-angiogenic target for cancer therapy. *Current drug targets* **11**: 1000-1017.

10.   Hurwitz, H, Fehrenbacher, L, Novotny, W, Cartwright, T, Hainsworth, J, Heim, W*, et al.* (2004). Bevacizumab plus irinotecan, fluorouracil, and leucovorin for metastatic colorectal cancer. *The New England journal of medicine* **350**: 2335-2342.

11.   Aghajanian, C, Blank, SV, Goff, BA, Judson, PL, Teneriello, MG, Husain, A*, et al.* (2012). OCEANS: a randomized, double-blind, placebo-controlled phase III trial of chemotherapy with or without bevacizumab in patients with platinum-sensitive recurrent epithelial ovarian, primary peritoneal, or fallopian tube cancer.

Journal of clinical oncology : official journal of the American Society of Clinical Oncology **30**: 2039-2045.

12. Bergers, G, and Hanahan, D (2008). Modes of resistance to anti-angiogenic therapy. *Nature reviews Cancer* **8**: 592-603.

13. Ricci-Vitiani, L, Pallini, R, Biffoni, M, Todaro, M, Invernici, G, Cenci, T*, et al.* (2010). Tumour vascularization via endothelial differentiation of glioblastoma stem-like cells. *Nature* **468**: 824-828.

14. Wang, R, Chadalavada, K, Wilshire, J, Kowalik, U, Hovinga, KE, Geber, A*, et al.* (2010). Glioblastoma stem-like cells give rise to tumour endothelium. *Nature* **468**: 829-833.

15. Paez-Ribes, M, Allen, E, Hudock, J, Takeda, T, Okuyama, H, Vinals, F*, et al.* (2009). Antiangiogenic therapy elicits malignant progression of tumors to increased local invasion and distant metastasis. *Cancer cell* **15**: 220-231.

16. Ebos, JM, Lee, CR, Cruz-Munoz, W, Bjarnason, GA, Christensen, JG, and Kerbel, RS (2009). Accelerated metastasis after short-term treatment with a potent inhibitor of tumor angiogenesis. *Cancer cell* **15**: 232-239.

17. Siemann, DW (2011). The unique characteristics of tumor vasculature and preclinical evidence for its selective disruption by Tumor-Vascular Disrupting Agents. *Cancer treatment reviews* **37**: 63-74.

18. Dark, GG, Hill, SA, Prise, VE, Tozer, GM, Pettit, GR, and Chaplin, DJ (1997). Combretastatin A-4, an agent that displays potent and selective toxicity toward tumor vasculature. *Cancer research* **57**: 1829-1834.

19. Hollebecque, A, Massard, C, and Soria, JC (2012). Vascular disrupting agents: a delicate balance between efficacy and side effects. *Current opinion in oncology* **24**: 305-315.

20. Rewcastle, GW, Atwell, GJ, Li, ZA, Baguley, BC, and Denny, WA (1991). Potential antitumor agents. 61. Structure-activity relationships for in vivo colon 38 activity among disubstituted 9-oxo-9H-xanthene-4-acetic acids. *Journal of medicinal chemistry* **34**: 217-222.

21. Shaked, Y, Ciarrocchi, A, Franco, M, Lee, CR, Man, S, Cheung, AM*, et al.* (2006). Therapy-induced acute recruitment of circulating endothelial progenitor cells to tumors. *Science* **313**: 1785-1787.

22. Wei, YQ, Wang, QR, Zhao, X, Yang, L, Tian, L, Lu, Y*, et al.* (2000). Immunotherapy of tumors with xenogeneic endothelial cells as a vaccine. *Nature medicine* **6**: 1160-1166.

23. Facciponte, JG, Ugel, S, De Sanctis, F, Li, C, Wang, L, Nair, G*, et al.* (2014). Tumor endothelial marker 1-specific DNA vaccination targets tumor vasculature. *The Journal of clinical investigation* **124**: 1497-1511.

24. Kalos, M, Levine, BL, Porter, DL, Katz, S, Grupp, SA, Bagg, A*, et al.* (2011). T cells with chimeric antigen receptors have potent antitumor effects and can establish memory in patients with advanced leukemia. *Science translational medicine* **3**: 95ra73.

25. Beatty, GL, Haas, AR, Maus, MV, Torigian, DA, Soulen, MC, Plesa, G*, et al.* (2014). Mesothelin-specific Chimeric Antigen Receptor mRNA-Engineered T cells Induce Anti-Tumor Activity in Solid Malignancies. *Cancer immunology research* **2**: 112-120.

26. Rosenberg, SA, Yang, JC, Sherry, RM, Kammula, US, Hughes, MS, Phan, GQ*, et al.* (2011). Durable complete responses in heavily pretreated patients with metastatic melanoma using T-cell transfer immunotherapy. *Clinical cancer research : an official journal of the American Association for Cancer Research* **17**: 4550-4557.

27. Govers, C, Sebestyen, Z, Coccoris, M, Willemsen, RA, and Debets, R (2010). T cell receptor gene therapy: strategies for optimizing transgenic TCR pairing. *Trends Mol Med* **16**: 77-87.

28. Bander, NH, Milowsky, MI, Nanus, DM, Kostakoglu, L, Vallabhajosula, S, and Goldsmith, SJ (2005). Phase I trial of 177lutetium-labeled J591, a monoclonal antibody to prostate-specific membrane antigen, in patients with androgen-independent prostate cancer. *Journal of clinical oncology : official journal of the American Society of Clinical Oncology* **23**: 4591-4601.

29. Bubenik, J (2003). Tumour MHC class I downregulation and immunotherapy (Review). *Oncology reports* **10**: 2005-2008.

30. Kershaw, MH, Westwood, JA, Parker, LL, Wang, G, Eshhar, Z, Mavroukakis, SA*, et al.* (2006). A phase I study on adoptive immunotherapy using gene-modified T cells for ovarian cancer. *Clinical cancer research : an official journal of the American Association for Cancer Research* **12**: 6106-6115.

31. Park, JR, Digiusto, DL, Slovak, M, Wright, C, Naranjo, A, Wagner, J*, et al.* (2007). Adoptive transfer of chimeric antigen receptor re-directed cytolytic T

lymphocyte clones in patients with neuroblastoma. *Molecular therapy : the journal of the American Society of Gene Therapy* **15**: 825-833.

32.   Finney, HM, Lawson, AD, Bebbington, CR, and Weir, AN (1998). Chimeric receptors providing both primary and costimulatory signaling in T cells from a single gene product. *Journal of immunology* **161**: 2791-2797.

33.   Imai, C, Mihara, K, Andreansky, M, Nicholson, IC, Pui, CH, Geiger, TL, *et al.* (2004). Chimeric receptors with 4-1BB signaling capacity provoke potent cytotoxicity against acute lymphoblastic leukemia. *Leukemia* **18**: 676-684.

34.   Carpenito, C, Milone, MC, Hassan, R, Simonet, JC, Lakhal, M, Suhoski, MM, *et al.* (2009). Control of large, established tumor xenografts with genetically retargeted human T cells containing CD28 and CD137 domains. *Proceedings of the National Academy of Sciences of the United States of America* **106**: 3360-3365.

35.   Zhong, XS, Matsushita, M, Plotkin, J, Riviere, I, and Sadelain, M (2010). Chimeric antigen receptors combining 4-1BB and CD28 signaling domains augment PI3kinase/AKT/Bcl-XL activation and CD8+ T cell-mediated tumor eradication. *Molecular therapy : the journal of the American Society of Gene Therapy* **18**: 413-420.

36.   Porter, DL, Levine, BL, Kalos, M, Bagg, A, and June, CH (2011). Chimeric antigen receptor-modified T cells in chronic lymphoid leukemia. *The New England journal of medicine* **365**: 725-733.

37.   Chinnasamy, D, Yu, Z, Theoret, MR, Zhao, Y, Shrimali, RK, Morgan, RA, *et al.* (2010). Gene therapy using genetically modified lymphocytes targeting VEGFR-2 inhibits the growth of vascularized syngenic tumors in mice. *The Journal of clinical investigation* **120**: 3953-3968.

38.   Niederman, TM, Ghogawala, Z, Carter, BS, Tompkins, HS, Russell, MM, and Mulligan, RC (2002). Antitumor activity of cytotoxic T lymphocytes engineered to target vascular endothelial growth factor receptors. *Proceedings of the National Academy of Sciences of the United States of America* **99**: 7009-7014.

39.   Buckanovich, RJ, Sasaroli, D, O'Brien-Jenkins, A, Botbyl, J, Hammond, R, Katsaros, D, *et al.* (2007). Tumor vascular proteins as biomarkers in ovarian cancer. *Journal of clinical oncology : official journal of the American Society of Clinical Oncology* **25**: 852-861.

40.   St Croix, B, Rago, C, Velculescu, V, Traverso, G, Romans, KE, Montgomery, E, *et al.* (2000). Genes expressed in human tumor endothelium. *Science* **289**: 1197-1202.

41. Smith, NR, Baker, D, James, NH, Ratcliffe, K, Jenkins, M, Ashton, SE, *et al.* (2010). Vascular endothelial growth factor receptors VEGFR-2 and VEGFR-3 are localized primarily to the vasculature in human primary solid cancers. *Clinical cancer research : an official journal of the American Association for Cancer Research* **16**: 3548-3561.

42. Witmer, AN, Dai, J, Weich, HA, Vrensen, GF, and Schlingemann, RO (2002). Expression of vascular endothelial growth factor receptors 1, 2, and 3 in quiescent endothelia. *The journal of histochemistry and cytochemistry : official journal of the Histochemistry Society* **50**: 767-777.

43. Davies, G, Cunnick, GH, Mansel, RE, Mason, MD, and Jiang, WG (2004). Levels of expression of endothelial markers specific to tumour-associated endothelial cells and their correlation with prognosis in patients with breast cancer. *Clinical & experimental metastasis* **21**: 31-37.

44. Rouleau, C, Curiel, M, Weber, W, Smale, R, Kurtzberg, L, Mascarello, J, *et al.* (2008). Endosialin protein expression and therapeutic target potential in human solid tumors: sarcoma versus carcinoma. *Clinical cancer research : an official journal of the American Association for Cancer Research* **14**: 7223-7236.

45. Opavsky, R, Haviernik, P, Jurkovicova, D, Garin, MT, Copeland, NG, Gilbert, DJ, *et al.* (2001). Molecular characterization of the mouse Tem1/endosialin gene regulated by cell density in vitro and expressed in normal tissues in vivo. *The Journal of biological chemistry* **276**: 38795-38807.

46. Dolznig, H, Schweifer, N, Puri, C, Kraut, N, Rettig, WJ, Kerjaschki, D, *et al.* (2005). Characterization of cancer stroma markers: in silico analysis of an mRNA expression database for fibroblast activation protein and endosialin. *Cancer immunity* **5**: 10.

47. Nanda, A, Karim, B, Peng, Z, Liu, G, Qiu, W, Gan, C, *et al.* (2006). Tumor endothelial marker 1 (Tem1) functions in the growth and progression of abdominal tumors. *Proceedings of the National Academy of Sciences of the United States of America* **103**: 3351-3356.

48. Liu, H, Moy, P, Kim, S, Xia, Y, Rajasekaran, A, Navarro, V, *et al.* (1997). Monoclonal antibodies to the extracellular domain of prostate-specific membrane antigen also react with tumor vascular endothelium. *Cancer research* **57**: 3629-3634.

49. Chang, SS, O'Keefe, DS, Bacich, DJ, Reuter, VE, Heston, WD, and Gaudin, PB (1999). Prostate-specific membrane antigen is produced in tumor-associated neovasculature. *Clinical cancer research : an official journal of the American Association for Cancer Research* **5**: 2674-2681.

50. Chang, SS, Reuter, VE, Heston, WD, Bander, NH, Grauer, LS, and Gaudin, PB (1999). Five different anti-prostate-specific membrane antigen (PSMA) antibodies confirm PSMA expression in tumor-associated neovasculature. *Cancer research* **59**: 3192-3198.

51. Denmeade, SR, Mhaka, AM, Rosen, DM, Brennen, WN, Dalrymple, S, Dach, I*, et al.* (2012). Engineering a prostate-specific membrane antigen-activated tumor endothelial cell prodrug for cancer therapy. *Science translational medicine* **4**: 140ra186.

52. Mhawech-Fauceglia, P, Zhang, S, Terracciano, L, Sauter, G, Chadhuri, A, Herrmann, FR*, et al.* (2007). Prostate-specific membrane antigen (PSMA) protein expression in normal and neoplastic tissues and its sensitivity and specificity in prostate adenocarcinoma: an immunohistochemical study using mutiple tumour tissue microarray technique. *Histopathology* **50**: 472-483.

53. Bander, NH, Trabulsi, EJ, Kostakoglu, L, Yao, D, Vallabhajosula, S, Smith-Jones, P*, et al.* (2003). Targeting metastatic prostate cancer with radiolabeled monoclonal antibody J591 to the extracellular domain of prostate specific membrane antigen. *The Journal of urology* **170**: 1717-1721.

54. Christian, S, Ahorn, H, Koehler, A, Eisenhaber, F, Rodi, HP, Garin-Chesa, P*, et al.* (2001). Molecular cloning and characterization of endosialin, a C-type lectin-like cell surface receptor of tumor endothelium. *The Journal of biological chemistry* **276**: 7408-7414.

55. Rettig, WJ, Garin-Chesa, P, Healey, JH, Su, SL, Jaffe, EA, and Old, LJ (1992). Identification of endosialin, a cell surface glycoprotein of vascular endothelial cells in human cancer. *Proceedings of the National Academy of Sciences of the United States of America* **89**: 10832-10836.

56. Carson-Walter, EB, Watkins, DN, Nanda, A, Vogelstein, B, Kinzler, KW, and St Croix, B (2001). Cell surface tumor endothelial markers are conserved in mice and humans. *Cancer research* **61**: 6649-6655.

57. Zhao, A, Nunez-Cruz, S, Li, C, Coukos, G, Siegel, DL, and Scholler, N (2011). Rapid isolation of high-affinity human antibodies against the tumor vascular marker Endosialin/TEM1, using a paired yeast-display/secretory scFv library platform. *Journal of immunological methods* **363**: 221-232.

58. Dull, T, Zufferey, R, Kelly, M, Mandel, RJ, Nguyen, M, Trono, D*, et al.* (1998). A third-generation lentivirus vector with a conditional packaging system. *Journal of virology* **72**: 8463-8471.

59.   Lanitis, E, Poussin, M, Hagemann, IS, Coukos, G, Sandaltzopoulos, R, Scholler, N*, et al.* (2012). Redirected antitumor activity of primary human lymphocytes transduced with a fully human anti-mesothelin chimeric receptor. *Molecular therapy : the journal of the American Society of Gene Therapy* **20**: 633-643.

60.   Guest, RD, Hawkins, RE, Kirillova, N, Cheadle, EJ, Arnold, J, O'Neill, A*, et al.* (2005). The role of extracellular spacer regions in the optimal design of chimeric immune receptors: evaluation of four different scFvs and antigens. *Journal of immunotherapy* **28**: 203-211.

61.   Urbanska, K, Lanitis, E, Poussin, M, Lynn, RC, Gavin, BP, Kelderman, S*, et al.* (2012). A universal strategy for adoptive immunotherapy of cancer through use of a novel T-cell antigen receptor. *Cancer research* **72**: 1844-1852.

62.   Cao, KY, Mao, XP, Wang, DH, Xu, L, Yuan, GQ, Dai, SQ*, et al.* (2007). High expression of PSM-E correlated with tumor grade in prostate cancer: a new alternatively spliced variant of prostate-specific membrane antigen. *The Prostate* **67**: 1791-1800.

63.   Schmittgen, TD, Teske, S, Vessella, RL, True, LD, and Zakrajsek, BA (2003). Expression of prostate specific membrane antigen and three alternatively spliced variants of PSMA in prostate cancer patients. *International journal of cancer Journal international du cancer* **107**: 323-329.

64.   Su, SL, Huang, IP, Fair, WR, Powell, CT, and Heston, WD (1995). Alternatively spliced variants of prostate-specific membrane antigen RNA: ratio of expression as a potential measurement of progression. *Cancer research* **55**: 1441-1443.

65.   Yao, V, Berkman, CE, Choi, JK, O'Keefe, DS, and Bacich, DJ (2010). Expression of prostate-specific membrane antigen (PSMA), increases cell folate uptake and proliferation and suggests a novel role for PSMA in the uptake of the non-polyglutamated folate, folic acid. *The Prostate* **70**: 305-316.

66.   Carter, RE, Feldman, AR, and Coyle, JT (1996). Prostate-specific membrane antigen is a hydrolase with substrate and pharmacologic characteristics of a neuropeptidase. *Proceedings of the National Academy of Sciences of the United States of America* **93**: 749-753.

67.   Conway, RE, Petrovic, N, Li, Z, Heston, W, Wu, D, and Shapiro, LH (2006). Prostate-specific membrane antigen regulates angiogenesis by modulating integrin signal transduction. *Molecular and cellular biology* **26**: 5310-5324.

68.   Colombatti, M, Grasso, S, Porzia, A, Fracasso, G, Scupoli, MT, Cingarlini, S*, et al.* (2009). The prostate specific membrane antigen regulates the expression of IL-

6 and CCL5 in prostate tumour cells by activating the MAPK pathways. *PloS one* **4**: e4608.

69.   Song, DG, Ye, Q, Carpenito, C, Poussin, M, Wang, LP, Ji, C*, et al.* (2011). In vivo persistence, tumor localization, and antitumor activity of CAR-engineered T cells is enhanced by costimulatory signaling through CD137 (4-1BB). *Cancer research* **71**: 4617-4627.

70.   Ades, EW, Candal, FJ, Swerlick, RA, George, VG, Summers, S, Bosse, DC*, et al.* (1992). HMEC-1: establishment of an immortalized human microvascular endothelial cell line. *The Journal of investigative dermatology* **99**: 683-690.

71.   Kalli, KR, Oberg, AL, Keeney, GL, Christianson, TJ, Low, PS, Knutson, KL*, et al.* (2008). Folate receptor alpha as a tumor target in epithelial ovarian cancer. *Gynecologic oncology* **108**: 619-626.

72.   Markert, S, Lassmann, S, Gabriel, B, Klar, M, Werner, M, Gitsch, G*, et al.* (2008). Alpha-folate receptor expression in epithelial ovarian carcinoma and non-neoplastic ovarian tissue. *Anticancer research* **28**: 3567-3572.

73.   O'Shannessy, DJ, Somers, EB, Smale, R, and Fu, YS (2013). Expression of folate receptor-alpha (FRA) in gynecologic malignancies and its relationship to the tumor type. *International journal of gynecological pathology : official journal of the International Society of Gynecological Pathologists* **32**: 258-268.

74.   Arbiser, JL, Moses, MA, Fernandez, CA, Ghiso, N, Cao, Y, Klauber, N*, et al.* (1997). Oncogenic H-ras stimulates tumor angiogenesis by two distinct pathways. *Proceedings of the National Academy of Sciences of the United States of America* **94**: 861-866.

75.   Garlanda, C, Parravicini, C, Sironi, M, De Rossi, M, Wainstok de Calmanovici, R, Carozzi, F*, et al.* (1994). Progressive growth in immunodeficient mice and host cell recruitment by mouse endothelial cells transformed by polyoma middle-sized T antigen: implications for the pathogenesis of opportunistic vascular tumors. *Proceedings of the National Academy of Sciences of the United States of America* **91**: 7291-7295.

76.   Thorpe, PE (2004). Vascular targeting agents as cancer therapeutics. *Clinical cancer research : an official journal of the American Association for Cancer Research* **10**: 415-427.

77.   Zhang, L, Yang, N, Garcia, JR, Mohamed, A, Benencia, F, Rubin, SC*, et al.* (2002). Generation of a syngeneic mouse model to study the effects of vascular endothelial growth factor in ovarian carcinoma. *The American journal of pathology* **161**: 2295-2309.

78. Lutz, AM, Bachawal, SV, Drescher, CW, Pysz, MA, Willmann, JK, and Gambhir, SS (2014). Ultrasound molecular imaging in a human CD276 expression-modulated murine ovarian cancer model. *Clinical cancer research : an official journal of the American Association for Cancer Research* **20**: 1313-1322.

79. Chacko, AM, Li, C, Nayak, M, Mikitsh, JL, Hu, J, Hou, C*, et al.* (2014). Development of 124I immuno-PET targeting tumor vascular TEM1/endosialin. *Journal of nuclear medicine : official publication, Society of Nuclear Medicine* **55**: 500-507.

80. Li, C, Chacko, AM, Hu, J, Hasegawa, K, Swails, J, Grasso, L*, et al.* (2014). Antibody-based tumor vascular theranostics targeting endosialin/TEM1 in a new mouse tumor vascular model. *Cancer biology & therapy* **15**: 443-451.

81. Moreno Garcia, V, Basu, B, Molife, LR, and Kaye, SB (2012). Combining antiangiogenics to overcome resistance: rationale and clinical experience. *Clinical cancer research : an official journal of the American Association for Cancer Research* **18**: 3750-3761.

82. Christiansen, JJ, Rajasekaran, SA, Inge, L, Cheng, L, Anilkumar, G, Bander, NH*, et al.* (2005). N-glycosylation and microtubule integrity are involved in apical targeting of prostate-specific membrane antigen: implications for immunotherapy. *Molecular cancer therapeutics* **4**: 704-714.

83. Devlin, AM, Ling, EH, Peerson, JM, Fernando, S, Clarke, R, Smith, AD*, et al.* (2000). Glutamate carboxypeptidase II: a polymorphism associated with lower levels of serum folate and hyperhomocysteinemia. *Hum Mol Genet* **9**: 2837-2844.

84. Williams, T, and Kole, R (2006). Analysis of prostate-specific membrane antigen splice variants in LNCap cells. *Oligonucleotides* **16**: 186-195.

85. Horsman, MR, and Siemann, DW (2006). Pathophysiologic effects of vascular-targeting agents and the implications for combination with conventional therapies. *Cancer research* **66**: 11520-11539.

86. Brentjens, RJ, Davila, ML, Riviere, I, Park, J, Wang, X, Cowell, LG*, et al.* (2013). CD19-targeted T cells rapidly induce molecular remissions in adults with chemotherapy-refractory acute lymphoblastic leukemia. *Science translational medicine* **5**: 177ra138.

87. Gilham, DE, Debets, R, Pule, M, Hawkins, RE, and Abken, H (2012). CAR-T cells and solid tumors: tuning T cells to challenge an inveterate foe. *Trends in molecular medicine* **18**: 377-384.

88. Li, C, Wang, J, Hu, J, Feng, Y, Hasegawa, K, Peng, X, *et al.* (2014). Development, optimization, and validation of novel anti-TEM1/CD248 affinity agent for optical imaging in cancer. *Oncotarget*.

89. Motz, GT, and Coukos, G (2013). Deciphering and reversing tumor immune suppression. *Immunity* **39**: 61-73.

90. Kinoshita, Y, Kuratsukuri, K, Landas, S, Imaida, K, Rovito, PM, Jr., Wang, CY, *et al.* (2006). Expression of prostate-specific membrane antigen in normal and malignant human tissues. *World journal of surgery* **30**: 628-636.

91. Silver, DA, Pellicer, I, Fair, WR, Heston, WD, and Cordon-Cardo, C (1997). Prostate-specific membrane antigen expression in normal and malignant human tissues. *Clinical cancer research : an official journal of the American Association for Cancer Research* **3**: 81-85.

92. Milowsky, MI, Nanus, DM, Kostakoglu, L, Sheehan, CE, Vallabhajosula, S, Goldsmith, SJ, *et al.* (2007). Vascular targeted therapy with anti-prostate-specific membrane antigen monoclonal antibody J591 in advanced solid tumors. *Journal of clinical oncology : official journal of the American Society of Clinical Oncology* **25**: 540-547.

93. Barrett, DM, Liu, X, Jiang, S, June, CH, Grupp, SA, and Zhao, Y (2013). Regimen-specific effects of RNA-modified chimeric antigen receptor T cells in mice with advanced leukemia. *Human gene therapy* **24**: 717-727.

94. Casucci, M, and Bondanza, A (2011). Suicide gene therapy to increase the safety of chimeric antigen receptor-redirected T lymphocytes. *Journal of Cancer* **2**: 378-382.

95. Frank, O, Rudolph, C, Heberlein, C, von Neuhoff, N, Schrock, E, Schambach, A, *et al.* (2004). Tumor cells escape suicide gene therapy by genetic and epigenetic instability. *Blood* **104**: 3543-3549.

96. Di Stasi, A, Tey, SK, Dotti, G, Fujita, Y, Kennedy-Nasser, A, Martinez, C, *et al.* (2011). Inducible apoptosis as a safety switch for adoptive cell therapy. *The New England journal of medicine* **365**: 1673-1683.

97. Budde, LE, Berger, C, Lin, Y, Wang, J, Lin, X, Frayo, SE, *et al.* (2013). Combining a CD20 chimeric antigen receptor and an inducible caspase 9 suicide switch to improve the efficacy and safety of T cell adoptive immunotherapy for lymphoma. *PloS one* **8**: e82742.

98.   Sasaroli, D, Gimotty, PA, Pathak, HB, Hammond, R, Kougioumtzidou, E, Katsaros, D, *et al.* (2011). Novel surface targets and serum biomarkers from the ovarian cancer vasculature. *Cancer biology & therapy* **12**: 169-180.

99.   Siemann, DW, and Shi, W (2008). Dual targeting of tumor vasculature: combining Avastin and vascular disrupting agents (CA4P or OXi4503). *Anticancer research* **28**: 2027-2031.

100.   Chinnasamy, D, Tran, E, Yu, Z, Morgan, RA, Restifo, NP, and Rosenberg, SA (2013). Simultaneous targeting of tumor antigens and the tumor vasculature using T lymphocyte transfer synergize to induce regression of established tumors in mice. *Cancer research* **73**: 3371-3380.

101.   Barrett, DM, Singh, N, Porter, DL, Grupp, SA, and June, CH (2014). Chimeric antigen receptor therapy for cancer. *Annual review of medicine* **65**: 333-347.

102.   Pameijer, CR, Navanjo, A, Meechoovet, B, Wagner, JR, Aguilar, B, Wright, CL, *et al.* (2007). Conversion of a tumor-binding peptide identified by phage display to a functional chimeric T cell antigen receptor. *Cancer gene therapy* **14**: 91-97.

103.   Ghosh, A, and Heston, WD (2004). Tumor target prostate specific membrane antigen (PSMA) and its regulation in prostate cancer. *Journal of cellular biochemistry* **91**: 528-539.

104.   Davis, MI, Bennett, MJ, Thomas, LM, and Bjorkman, PJ (2005). Crystal structure of prostate-specific membrane antigen, a tumor marker and peptidase. *Proceedings of the National Academy of Sciences of the United States of America* **102**: 5981-5986.

105.   Schulke, N, Varlamova, OA, Donovan, GP, Ma, D, Gardner, JP, Morrissey, DM, *et al.* (2003). The homodimer of prostate-specific membrane antigen is a functional target for cancer therapy. *Proceedings of the National Academy of Sciences of the United States of America* **100**: 12590-12595.

CHAPTER 7: TABLES AND FIGURES

Tumor-VDAs	Anti-angiogenic agents
Administered acutely	Administered chronically
Disrupt the established tumor vasculature	Inhibit neovascularization
Cause vessel occlusion and inhibition of blood flow	Induce vascular normalization with initial improved tumor blood flow
Cause extensive tumor necrosis	Prevent or limit tumor growth
Particularly active against large tumor masses, causing extensive central necrosis	Particularly active in peripheral tumor locations where nascent vessels are more predominant

Table 1: Key differences between anti-angiogenic therapy and vascular disruption therapy. (Used with permission)[17]

Tumor Type	Wernicke et al[1] Number (%)	Abdel-Hadi et al[2] Number (%)	Samplaski et al[3] Number (%)	Haffner et al[4] Number (%)	Haffner et al[5] Number (%)	Denmeade et al[6] Number (%)	Silver et al[7] Number (%)	Chang et al[8] Number (%)
Bladder Cancer			8/167 (5%)			40/94 (43%)	68/92 (54%)	
Breast Cancer	68/92 (74%)					34/44 (75%)		5/6 (83%)
Colorectal Carcinoma		75/100 (75%)			110/130 (85%)		3/29 (16%)	5/5 (100%)
Gastric Cancer					79/119 (66%)			
Hepatocellular Cancer						39/41 (95%)		
Melanoma						25/44 (57%)		5/5 (100%)
Non-small cell lung carcinoma								5/5 (100%)
Oral Cancer				72/96 (75%)				
Ovarian Cancer						25/34 (75%)		
Pancreatic ductal carcinoma								4/4 (100%)
Renal Cancer						44/46 (95%)	8/17 (47%)	11/11 (100%)

1. Wernicke, AG, Varma, S, Greenwood, EA, Christos, PJ, Chao, KS, Liu, H, *et al.* (2014). Prostate-specific membrane antigen expression in tumor-associated vasculature of breast cancers. *APMIS : acta pathologica, microbiologica, et immunologica Scandinavica* **122**: 482-489.

2. Abdel-Hadi, M, Ismail, Y, and Younis, L (2014). Prostate-specific membrane antigen (PSMA) immunoexpression in the neovasculature of colorectal carcinoma in Egyptian patients. *Pathology, research and practice*.

3. Samplaski, MK, Heston, W, Elson, P, Magi-Galluzzi, C, and Hansel, DE (2011). Folate hydrolase (prostate-specific membrane [corrected] antigen) 1 expression in bladder cancer subtypes and associated tumor neovasculature. *Modern pathology : an official journal of the United States and Canadian Academy of Pathology, Inc* **24**: 1521-1529.

4. Haffner, MC, Kronberger, IE, Ross, JS, Sheehan, CE, Zitt, M, Muhlmann, G, *et al.* (2009). Prostate-specific membrane antigen expression in the neovasculature of gastric and colorectal cancers. *Human pathology* **40**: 1754-1761.

5. Haffner, MC, Laimer, J, Chaux, A, Schafer, G, Obrist, P, Brunner, A, *et al.* (2012). High expression of prostate-specific membrane antigen in the tumor-associated neo-vasculature is associated with worse prognosis in squamous cell carcinoma of the oral cavity. *Modern pathology : an official journal of the United States and Canadian Academy of Pathology, Inc* **25**: 1079-1085.

6. Denmeade, SR, Mhaka, AM, Rosen, DM, Brennen, WN, Dalrymple, S, Dach, I, *et al.* (2012). Engineering a prostate-specific membrane antigen-activated tumor endothelial cell prodrug for cancer therapy. *Science translational medicine* **4**: 140ra186.

7. Silver, DA, Pellicer, I, Fair, WR, Heston, WD, and Cordon-Cardo, C (1997). Prostate-specific membrane antigen expression in normal and malignant human tissues. *Clinical cancer research : an official journal of the American Association for Cancer Research* **3**: 81-85.

8. Chang, SS, Reuter, VE, Heston, WD, Bander, NH, Grauer, LS, and Gaudin, PB (1999). Five different anti-prostate-specific membrane antigen (PSMA) antibodies confirm PSMA expression in tumor-associated neovasculature. *Cancer research* **59**: 3192-3198.

Table 2: PSMA expression on the tumor vasculature, a summary of selected studies.

scFv	Affinity
scFv78	2 nM
scFv131	1 µM
scFv132	280 nM
scFv133	480 nM
scFv137	4.8 µM

Table 3: Affinity of the anti-TEM1 scFvs. The comparative affinity of the anti-TEM1 scFvs, as determined by ELISA.[57]

Tumor Type	Less than 50% tumor vessels expressing PSMA	Percentage
Bladder Cancer	NA	10-100%[1]
Breast Cancer	26/48	54%[2]
Colorectal Carcinoma	52/75, 52/130	69%[3], 40%[4]
Gastric Cancer	56/79	71%[4]
Oral Cancer	48/72	67%[5]

1 Samplaski, MK, Heston, W, Elson, P, Magi-Galluzzi, C, and Hansel, DE (2011). Folate hydrolase (prostate-specific membrane [corrected] antigen) 1 expression in bladder cancer subtypes and associated tumor neovasculature. *Modern pathology : an official journal of the United States and Canadian Academy of Pathology, Inc* **24**: 1521-1529.

2 Wernicke, AG, Varma, S, Greenwood, EA, Christos, PJ, Chao, KS, Liu, H*, et al.* (2014). Prostate-specific membrane antigen expression in tumor-associated vasculature of breast cancers. *APMIS : acta pathologica, microbiologica, et immunologica Scandinavica* **122**: 482-489.

3 Abdel-Hadi, M, Ismail, Y, and Younis, L (2014). Prostate-specific membrane antigen (PSMA) immunoexpression in the neovasculature of colorectal carcinoma in Egyptian patients. *Pathology, research and practice*.

4 Haffner, MC, Kronberger, IE, Ross, JS, Sheehan, CE, Zitt, M, Muhlmann, G*, et al.* (2009). Prostate-specific membrane antigen expression in the neovasculature of gastric and colorectal cancers. *Human pathology* **40**: 1754-1761.

5 Haffner, MC, Laimer, J, Chaux, A, Schafer, G, Obrist, P, Brunner, A*, et al.* (2012). High expression of prostate-specific membrane antigen in the tumor-associated neo-vasculature is associated with worse prognosis in squamous cell carcinoma of the oral cavity. *Modern pathology : an official journal of the United States and Canadian Academy of Pathology, Inc* **25**: 1079-1085.

Table 4: PSMA expression is heterogeneously expressed on blood vessels within the tumor.

Tissue	Antibody				
	7E11*	J591*	HPA010593**	CAB001451**	3E6
Adrenal Gland	0/5	0/5	0/3	0/2	0/1
Bladder	0/5	0/5	0/2	0/3	0/1
Brain	0/3	0/3	?	?	0/2
Breast	8/8	8/8	0/2	3/3	0/1 †Ducts
Colon	1/12	1/12	0/2	0/3	NA
Heart	NA	NA	0/3	0/3	0/1
Kidney tubules	5/5	5/5	3/3	3/3	1/1
Liver	0/5	0/5	0/3	3/3	3/3
Lung	0/5	0/5	0/3	0/3	0/1 †Lung Macrophages
Ovary	0/5	0/5	0/3	0/3	0/1
Pancreas	0/7	0/7	0/3	0/3	0/2
Prostate	28/28	28/28	3/3	3/3	1/1
Skeletal Muscle	7/7	0/7	0/3	0/2	NA
Skin	0/5	0/5	3/3	0/2	0/1
Small Intestine	11/11	11/11	3/3	3/3	1/1
Spleen	NA	NA	0/3	0/3	1/1
Stomach	0/6	0/6	0/3	0/3	0/1
Thyroid	0/5	0/5	0/3	0/3	NA

Positive
Negative

*Flash Frozen Tissues (Chang, S.S., Reuter, V.E., Heston, W.D.W., Bander, N.H., Grauer, L.S. & Gaudin, P.B. Five Different Anti-Prostate-specific Membrane Antigen (PSMA) Antibodies Confirm PSMA Expression in Tumor-associated Neovasculature. Cancer Research, *59*, 3192-3198 1999.)

** Parrafin embeded TMA (www.proteinatlas.org, results for FOLH1)

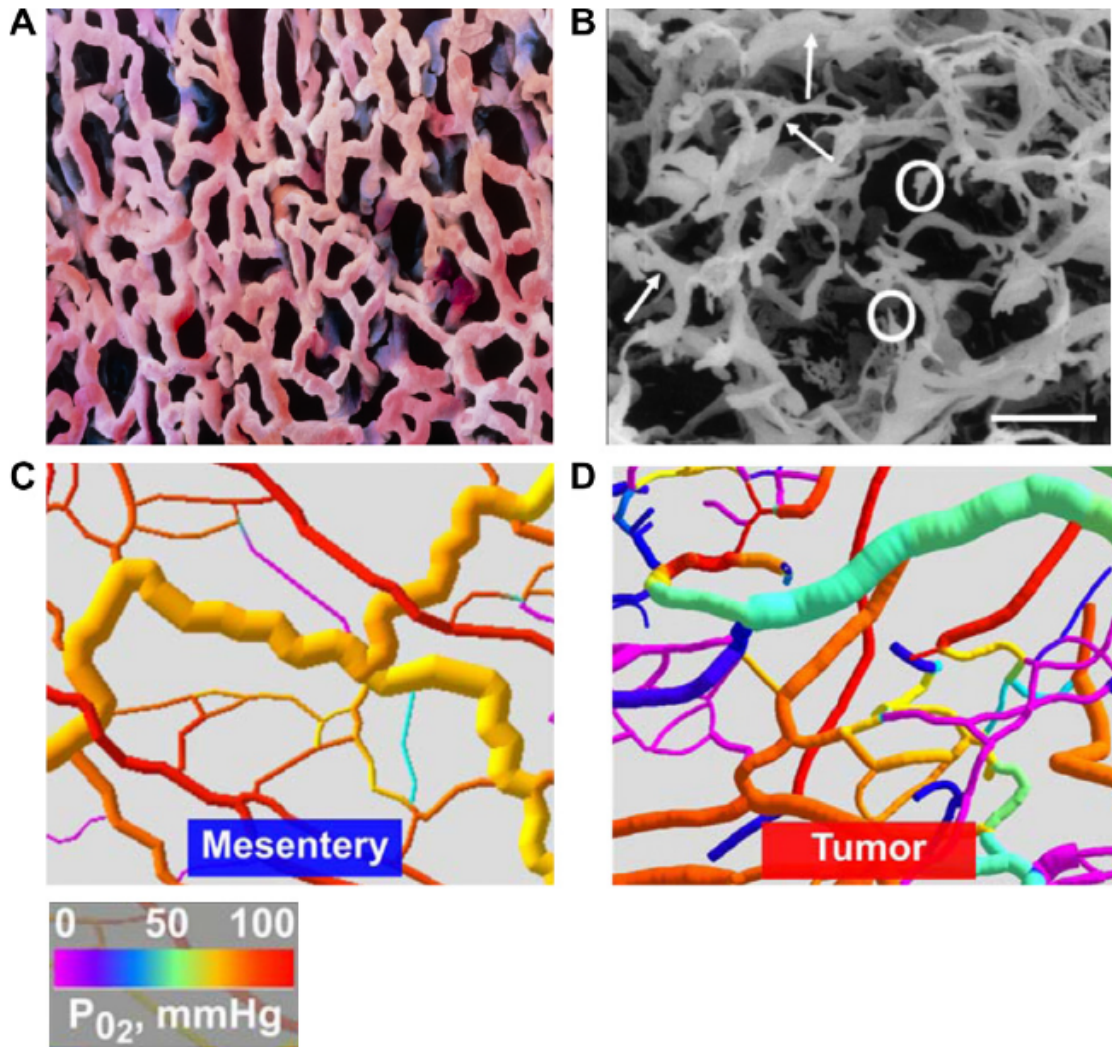**Table 5: PSMA expression in normal tissues as indicated by immunohistochemistry.**

Figure 1: A Comparison of the normal vasculature with the tumor vasculature. (**a**) An image of normal vessels within the lung exhibiting regular spacing and organized structure. Obtained using a scanning electron microscope (SEM). (**b**) A SEM image of a sigmoidal adenocarcinoma in which the irregular and torturous phenotype of the tumor vasculature can be observed, as well as abnormal bulges (arrows) and blind ends (circles). Scale bar = 100 μm. (**c,d**) Oxygenation in normal and tumor vascular networks as visualized by computer software. (Used with permission)[17]
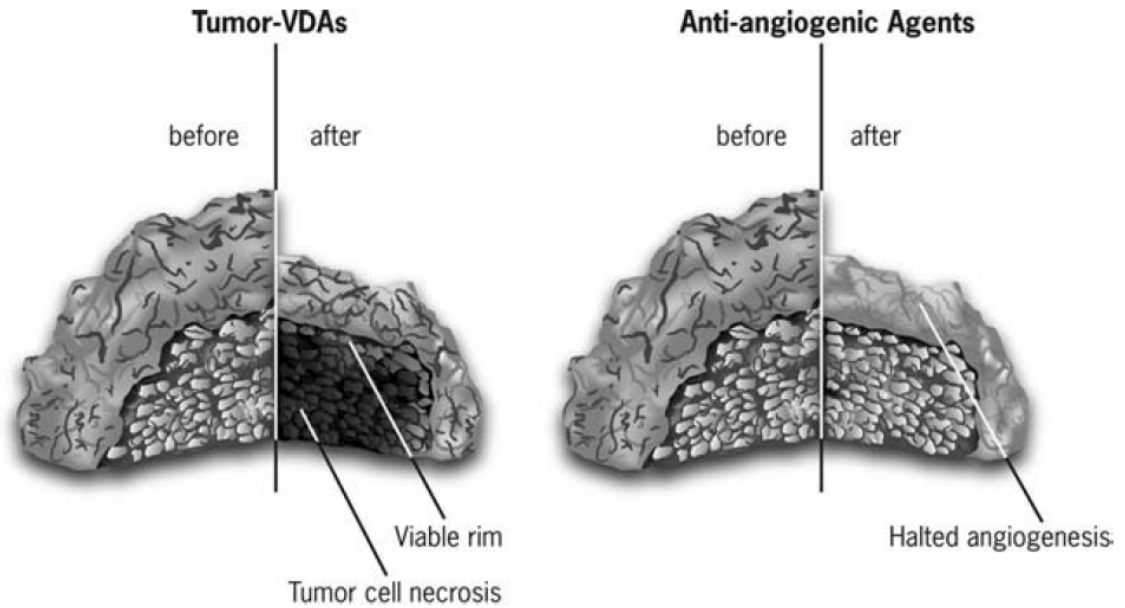
Figure 2: Comparison of anti-angiogenic therapy with vascular disruption therapy. Destruction of the tumor vasculature using vascular disruption agents results in necrosis of the central tumor mass. Tumor cells survive at the periphery of the neoplasm, as they can obtain oxygen and nutrient exchange through adjacent tissues. In contrast, anti-angiogenic therapy aims to halt the recruitment of new tumor blood vessels, thereby slowing tumor growth. (Used with permission)[7]
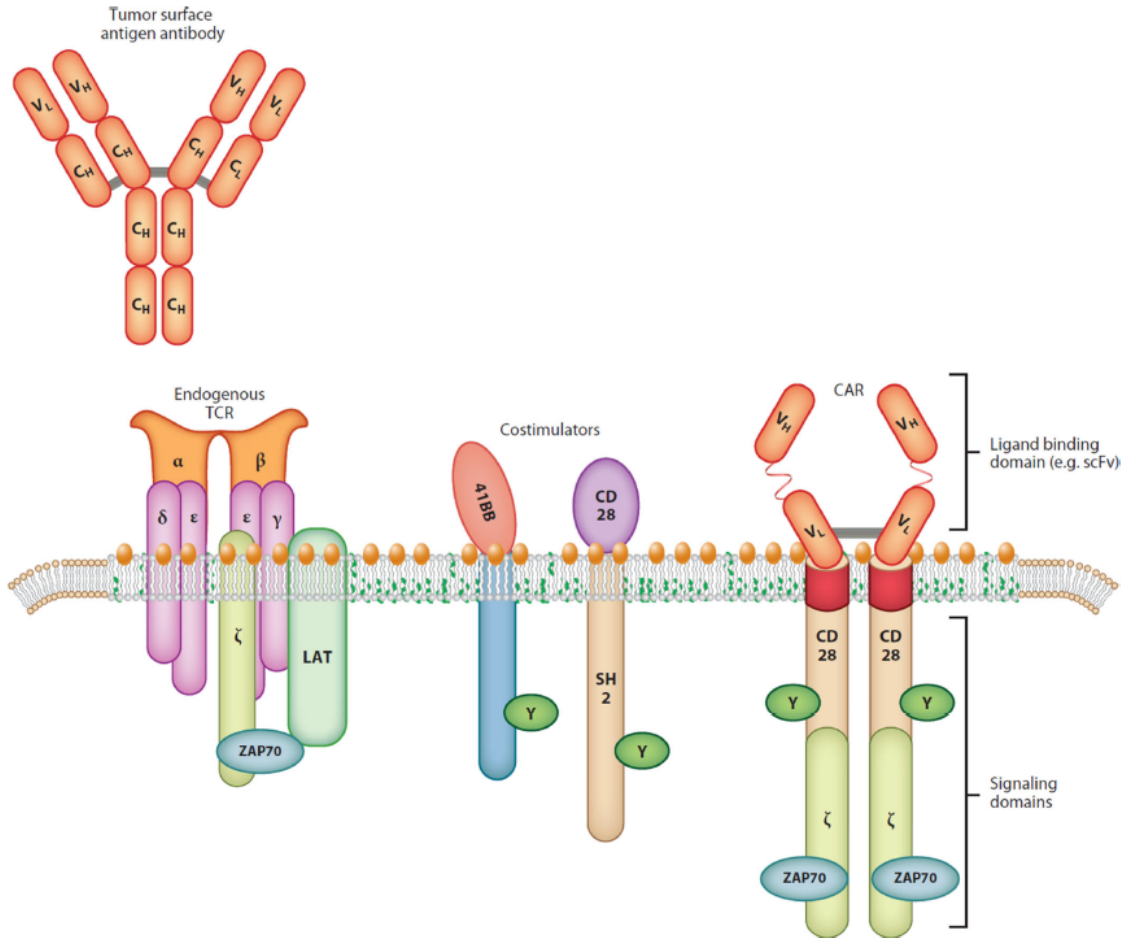
Figure 3: A schematic representation of a chimeric antigen receptor. CARs are generated by fusing an antigen-binding domain (most often a scFv) to the intracellular signaling domains of TCR, frequently CD3ζ. Co-stimulatory domains may also be utilized, and may include the signaling domains from CD28 or CD137/4-1BB. (Used with permission)[101]
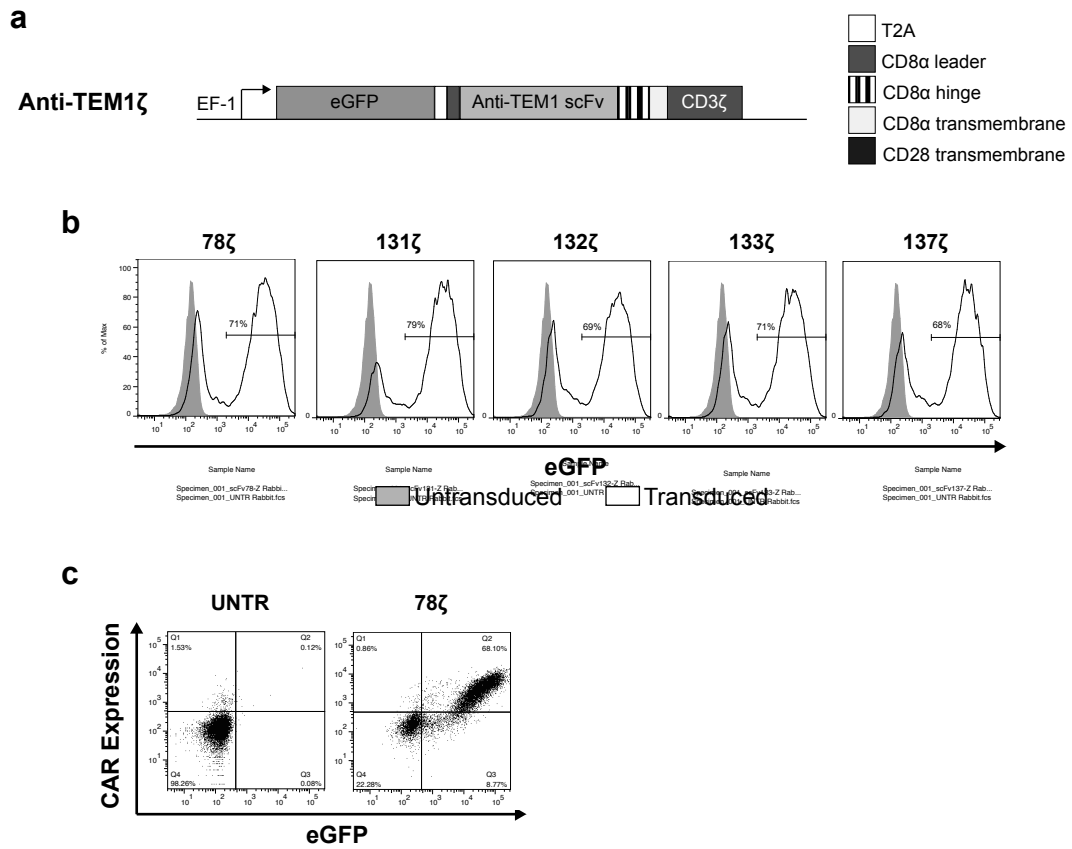
Figure 4: Design of a CAR against TEM1. (**a**) Schematic representation of the anti-TEM1 CARs. scFv78, 131, 132, 133, or 137 was cloned downstream of the EF-1 promoter and an eGFP reporter, which is separated from the scFv by a 2A cleavage sequence. All CARs contain the CD3ζ signaling domain. (**b**) Representative CAR expression on primary human T cells for all five anti-TEM1 CARs. Six days after transduction, eGFP signal was measured using a flow cytometer. (**c**) CAR surface detection correlates with eGFP. Primary human T cells were transduced with lentivirus containing the scFv78ζ CAR. T cells were stained for CAR expression 6 days after transduction using a biotinylated goat anti-mouse F(ab')$_2$ fragment followed by streptavidin-APC secondary.
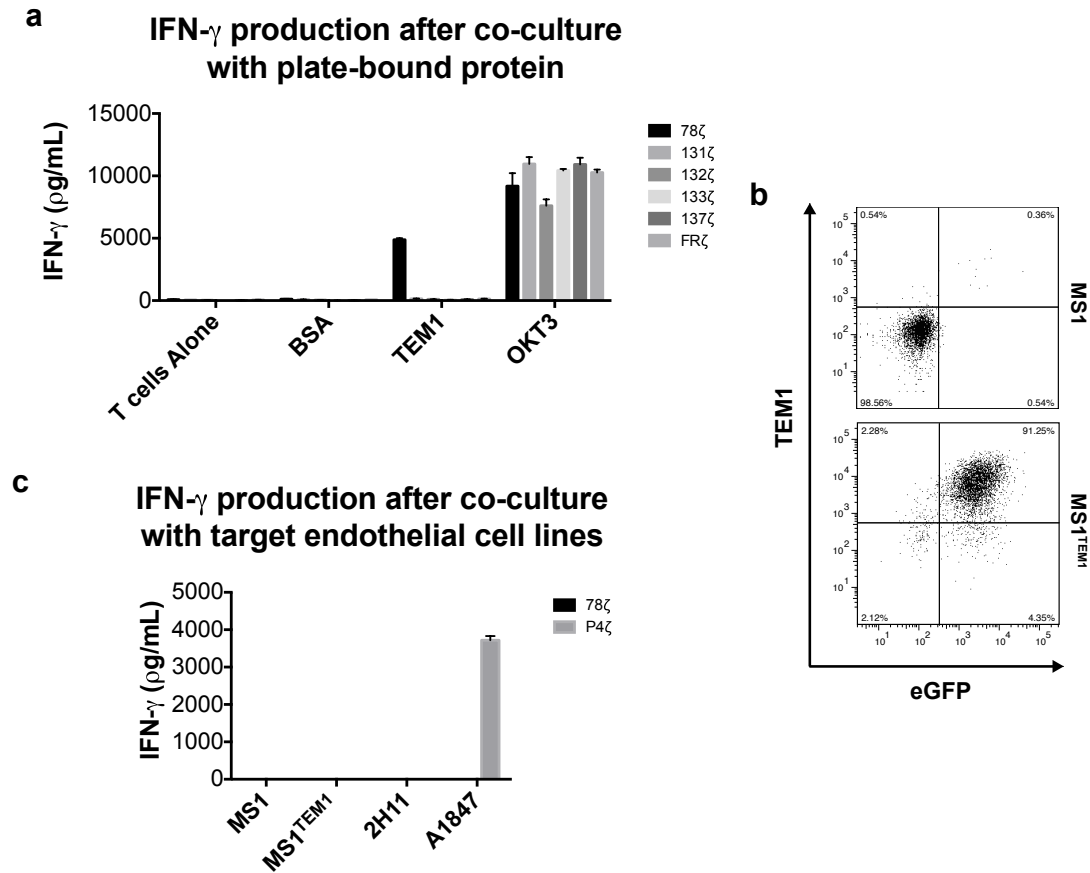
Figure 5: 78ζ CAR-bearing T cells recognize plate-bound immobilized TEM1 protein, but not TEM1 on the surface of target cell lines. (**a**) IFN-γ production by T cells harboring anti-TEM1 CARs in response to recombinant TEM1 protein. CAR T cells were co-cultured overnight in wells previously coated with BSA, recombinant TEM1 protein, or the anti-CD3 antibody OKT3. IFN-γ ELISAs were performed on the collected supernatants. Representative experiment from a 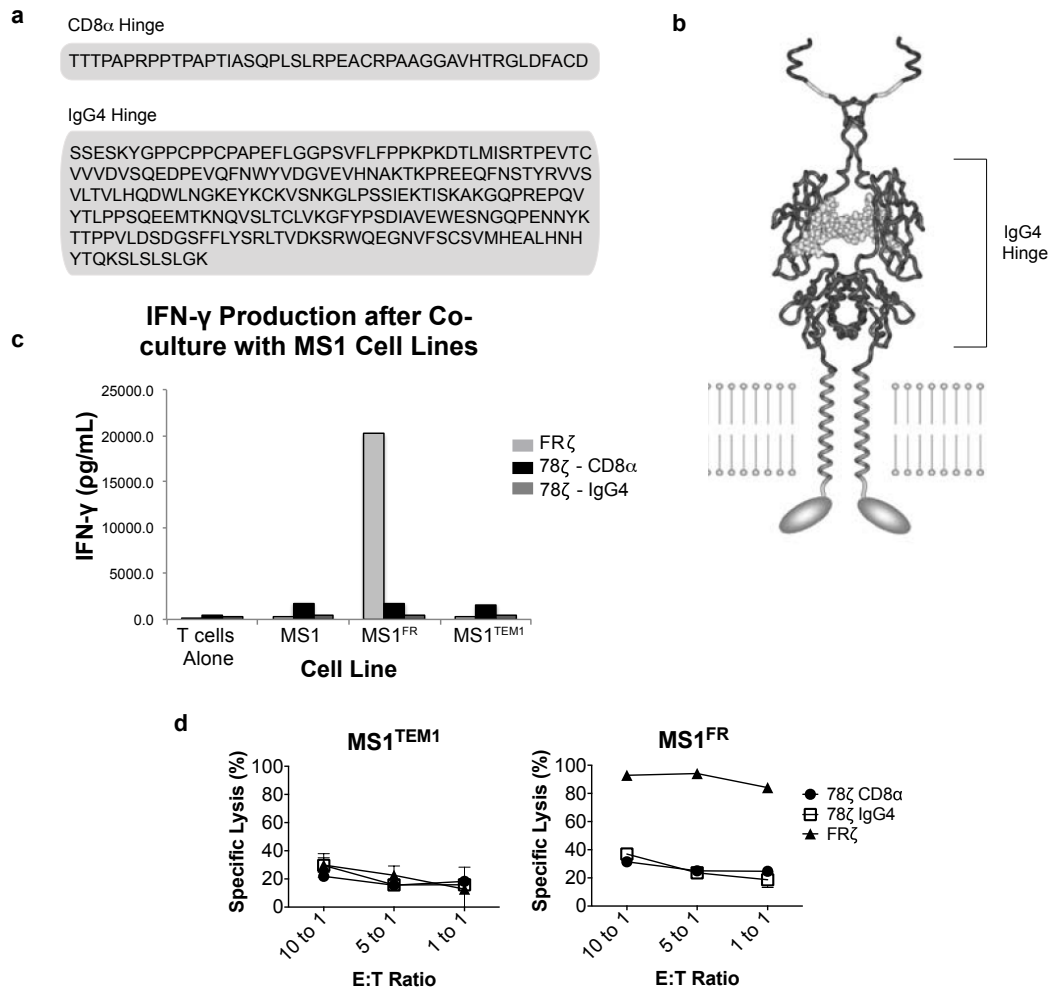single donor shown. Data are means ±SD from duplicate wells. (**b**) Detection of TEM1 on the surface of the MS1 or MS1^TEM1-transduced mouse endothelial cell lines. TEM1 was detected using soluble scFv78 followed by APC-conjugated anti-V5 antibody. (**c**) IFN-γ production by 78ζ CAR T cells following co-culture with target cell lines. Overnight co-cultures were performed with T cells and target cells at an E:T ratio of 5:1. The human ovarian cancer cell line, A1847, was used as a positive control for the P4ζ control CAR, as this line expresses mesothelin but not TEM1. IFN-γ ELISAs were performed on the collected supernatants. Representative experiment from a single donor shown. Data are means ±SD from duplicate wells.

a

CD8α Hinge

TTTPAPRPPTPAPTIASQPLSLRPEACRPAAGGAVHTRGLDFACD

IgG4 Hinge

SSESKYGPPCPPCPAPEFLGGPSVFLFPPKPKDTLMISRTPEVTC
VVVDVSQEDPEVQFNWYVDGVEVHNAKTKPREEQFNSTYRVVS
VLTVLHQDWLNGKEYKCKVSNKGLPSSIEKTISKAKGQPREPQV
YTLPPSQEEMTKNQVSLTCLVKGFYPSDIAVEWESNGQPENNYK
TTPPVLDSDGSFFLYSRLTVDKSRWQEGNVFSCSVMHEALHNH
YTQKSLSLSLGK

b

IgG4 Hinge

c

IFN-γ Production after Co-culture with MS1 Cell Lines

IFN-γ (pg/mL)

FRζ
78ζ - CD8α
78ζ - IgG4

Cell Line: T cells Alone, MS1, MS1^{FR}, MS1^{TEM1}

d

MS1^{TEM1}

MS1^{FR}

Specific Lysis (%)

78ζ CD8α
78ζ IgG4
FRζ

E:T Ratio: 10 to 1, 5 to 1, 1 to 1

Figure 6: Hinge extension does not improve the ability of the scFv78 CAR to recognize TEM1 on the cell surface. (a) Comparison of the amino acid sequence for the CD8α and IgG4 hinge domains. **(b)** Schematic representation of the IgG4 hinge domain. (Used with permission)[102] **(c)** IFN-γ production of CAR T cells containing either the CD8α or IgG4 hinge domain, after co-culture with MS1 endothelial targets. Overnight co-cultures were performed with T cells and target cells at an E:T ratio of 5:1. IFN-γ ELISAs were performed on the collected supernatants. Data are means ±SD from duplicate wells. **(d)** Specific lysis of endothelial cell lines after overnight co-culture with T cells containing either the CD8α or IgG4 hinge domain. Data are means ±SD from duplicate wells.
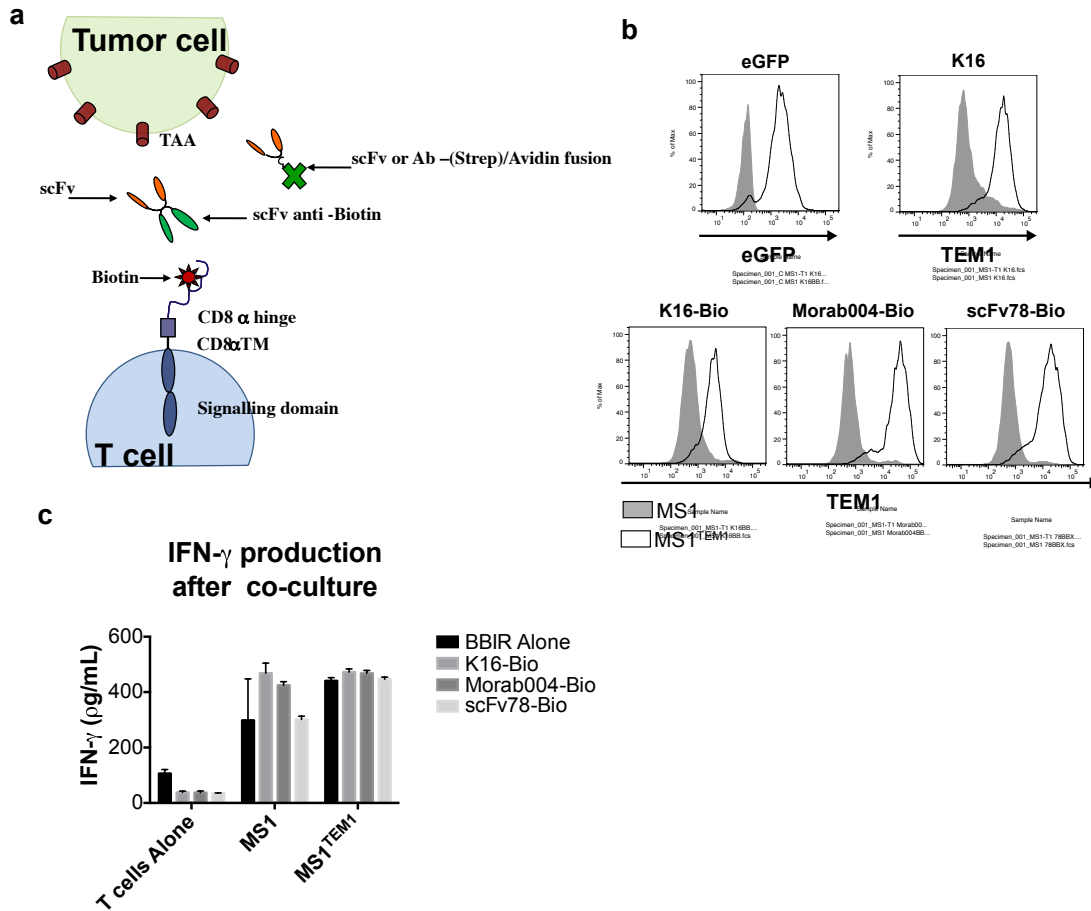
Figure 7: BBIR T cells fail to recognize TEM1 when expressed on the cell surface.
(**a**) A schematic diagram of a BBIR T cell. Briefy, T cells are transduced with a streptavidin-based BBIR that confers specificity to the T cells for biotionylated substrates. Biotinylated antibodies are used to stain the surface of target tumor cells, which will then be recognized by the BBIR T cells. (Used with permission – K. Urbanska) (**b**) Biotinylation of three antibodies against TEM1 and their ability to stain TEM1-positive endothelial targets. MS1 or MS1^TEM1 cells were stained with the listed antibodies before being split for (b) staining verification by flow cytometry or (c) co-culture with BBIR T cells. Cells stained for flow cytometry were washed and stained with a streptavidin-APC secondary before analysis by flow cytometry. (**c**) IFN-γ production by BBIR T cells after co-culture with labeled endothelial targets. Overnight co-cultures were performed with T cells and target cells at an E:T ratio of 5:1. IFN-γ ELISAs were performed on the collected supernatants. Representative experiment from a single donor shown. Data are means ±SD from duplicate wells.
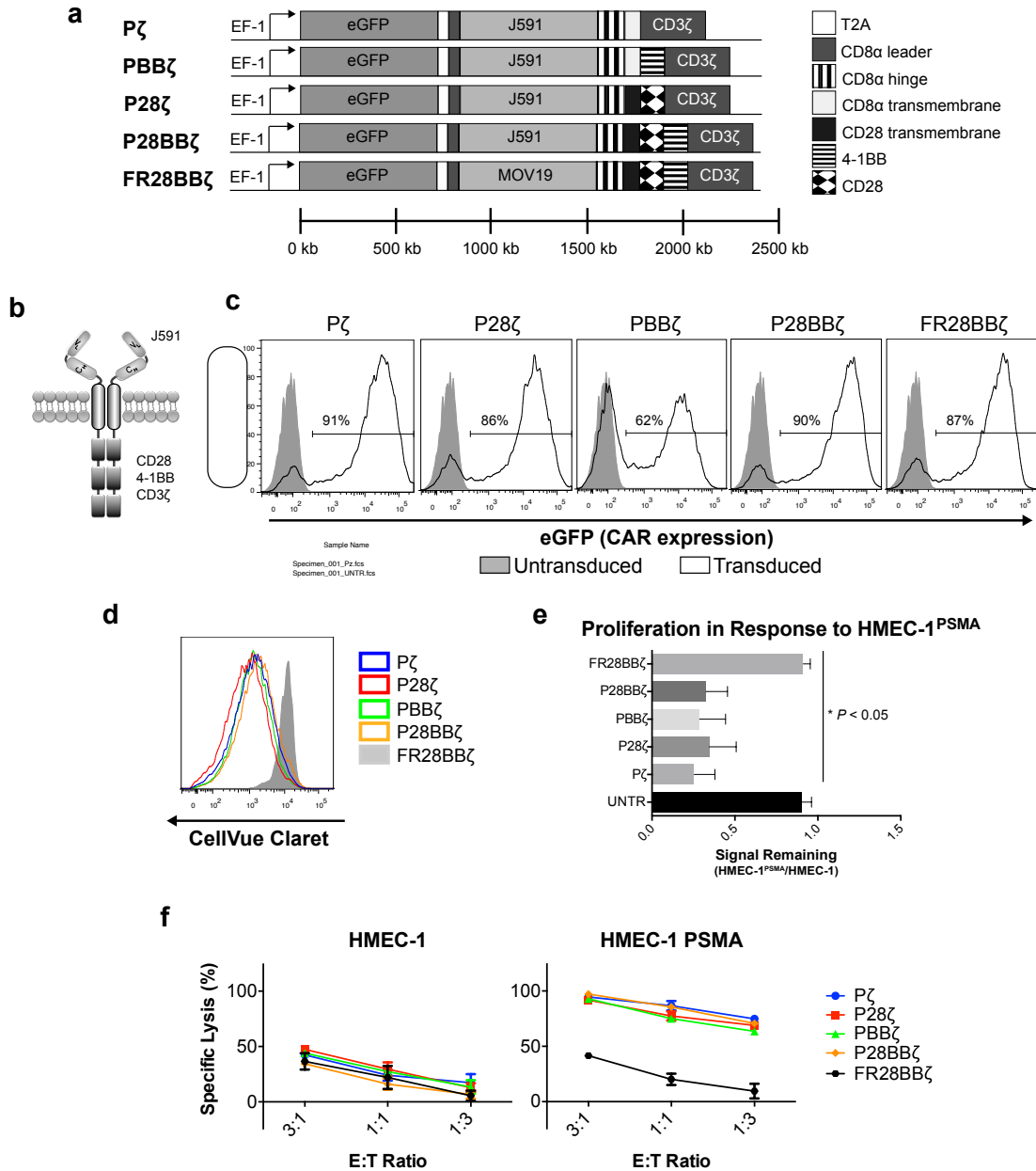
Figure 8: Design and characterization of an anti-PSMA CAR. (**a**) Lentiviral cassette design for the J591-based CAR constructs: Pζ, P28ζ, PBBζ, P28BBζ and the FR28BBζ specificity control. (**b**) Schematic representation of the P28BBζ CAR. (**c**) Representative transduction efficiencies, as measured by eGFP reporter, for the CAR constructs in primary human T cells. Closed histograms depict untransduced cells; open histograms depict transduced T cells. (**d**) Overlay of histograms comparing the proliferative capacity of the T cells groups 5 days after co-culture with HMEC-1[PSMA]. (**e**) Quantitative comparison of proliferation between CAR constructs harboring the different signaling domains. The geometric mean fluorescence intensity of Cellvue®

87

Claret staining was measured for the CAR-positive T cells after 5 days in co-culture with either HMEC-1 or HMEC-1^{PSMA} (E:T = 2:1). To normalize across multiple donors, the MFI of CellVue® staining on CAR$^+$ T cells after co-culture with HMEC-1^{PSMA} was divided by the MFI of the CAR$^+$ T cells after co-culture with the HMEC-1. *$P < 0.05$; data are means ±SEM from three independent donors. (**f**) Cytolytic activity of the various T cells after 18 h co-culture with HMEC-1 or HMEC-1^{PSMA}. Lysis was measured via luciferase assay (specific lysis = 100 − (luciferase signal treated / luciferase signal untreated × 100)). Data are means ±SD from triplicate cultures.
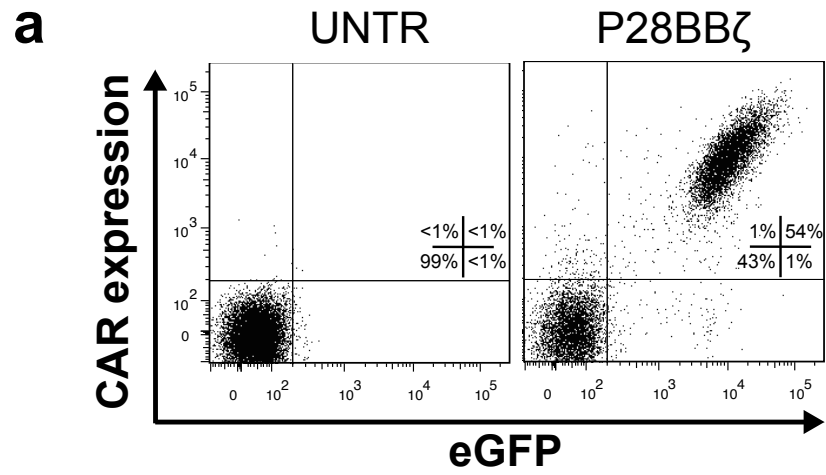
Figure 9: Anti-PSMA CAR surface expression correlates with eGFP reporter expression. (**a**) Surface staining of untransduced and P28BBζ T cells using an APC-conjugated goat anti-mouse F(ab')$_2$ fragment.
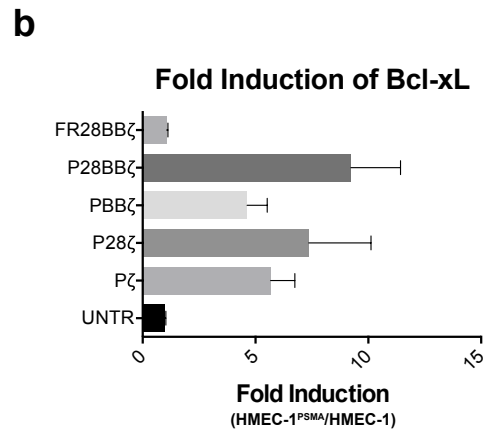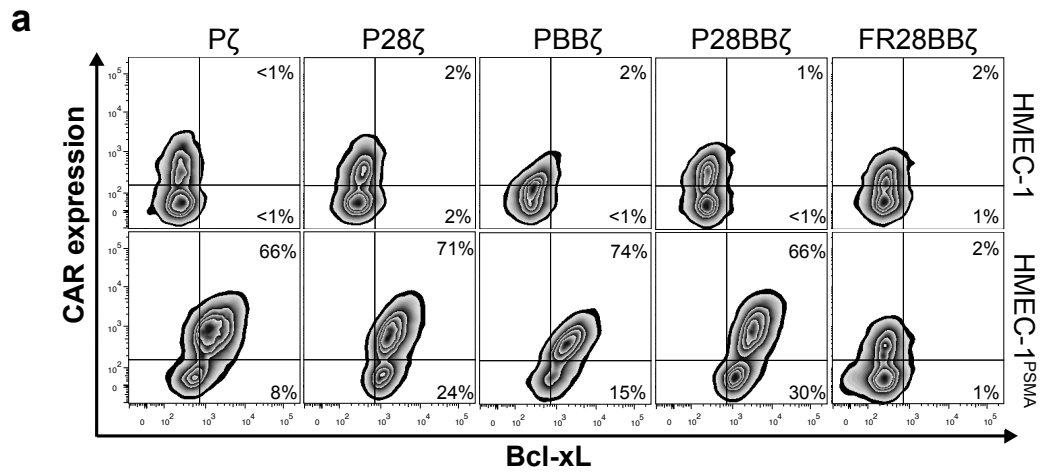
Figure 10: Bcl-xL induction in response to CAR T cell activation. (**a**) Expression of Bcl-xL in T cells five days after co-culture with HMEC-1 or HMEC-1^{PSMA} endothelial targets (E:T = 2:1). Representative donor shown. (**b**) Quantification of Bcl-xL induction in T cells bearing the various CAR constructs. T cells were stained for Bcl-xL five days after co-culture with HMEC-1 or HMEC-1^{PSMA}, and the geometric mean fluorescence intensity was measured for the CAR-positive cells. Results reported as fold induction of HMEC-1^{PSMA}/HMEC-1. Data are means ±SEM from four independent donors.
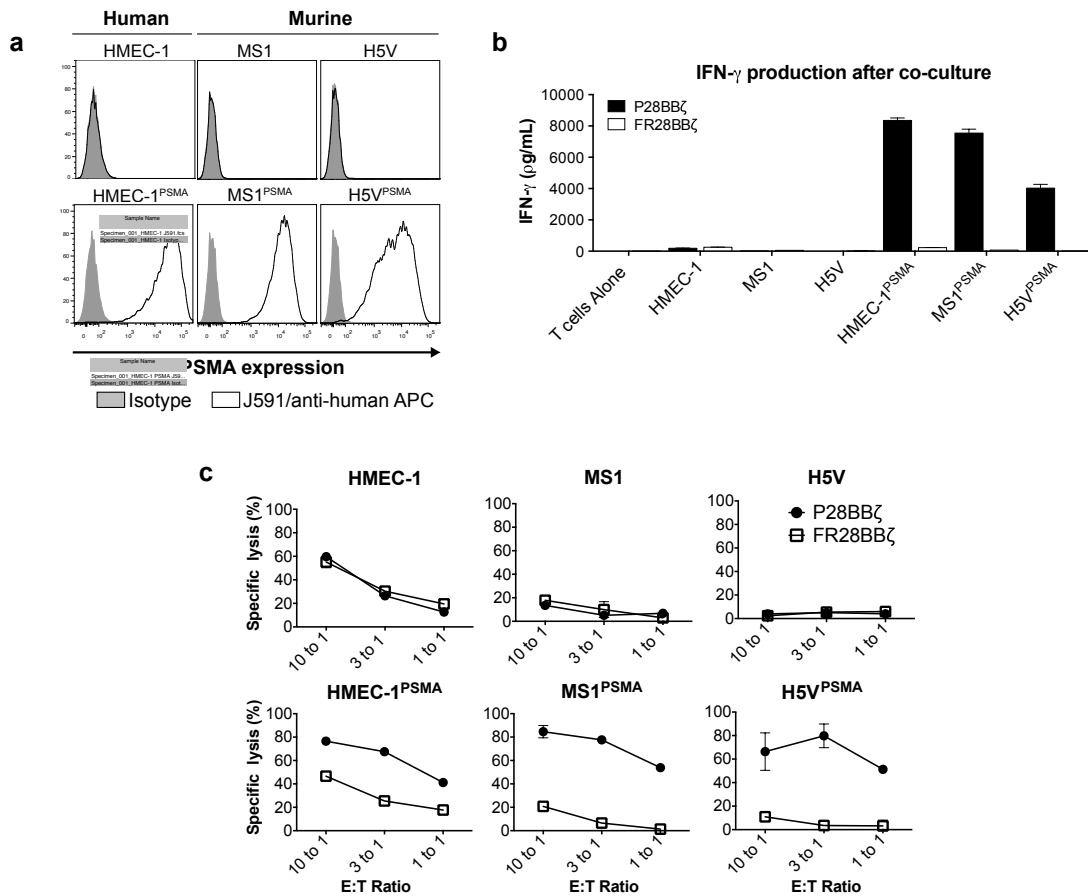
Figure 11: P28BBζ T cells recognize and eliminate PSMA-positive endothelial cells *in vitro*. (**a**) Human PSMA expression on native (top row) and engineered (bottom row) endothelial cell lines. PSMA was detected by humanized J591 Ab (open histogram) and compared with human IgG control (closed histogram). (**b**) IFN-γ production by P28BBζ T cells after co-culture with endothelial targets (E:T = 3:1). Culture supernatants were collected at 18 h and IFN-γ was measured by ELISA. Representative donor shown; data are means ±SD of triplicate cultures. (**c**) Cytolytic activity of P28BBζ T cells after 18 h co-culture with endothelial cell targets. Cell lysis measured by chromium release. Representative donor shown; data are means ±SD of triplicate cultures.

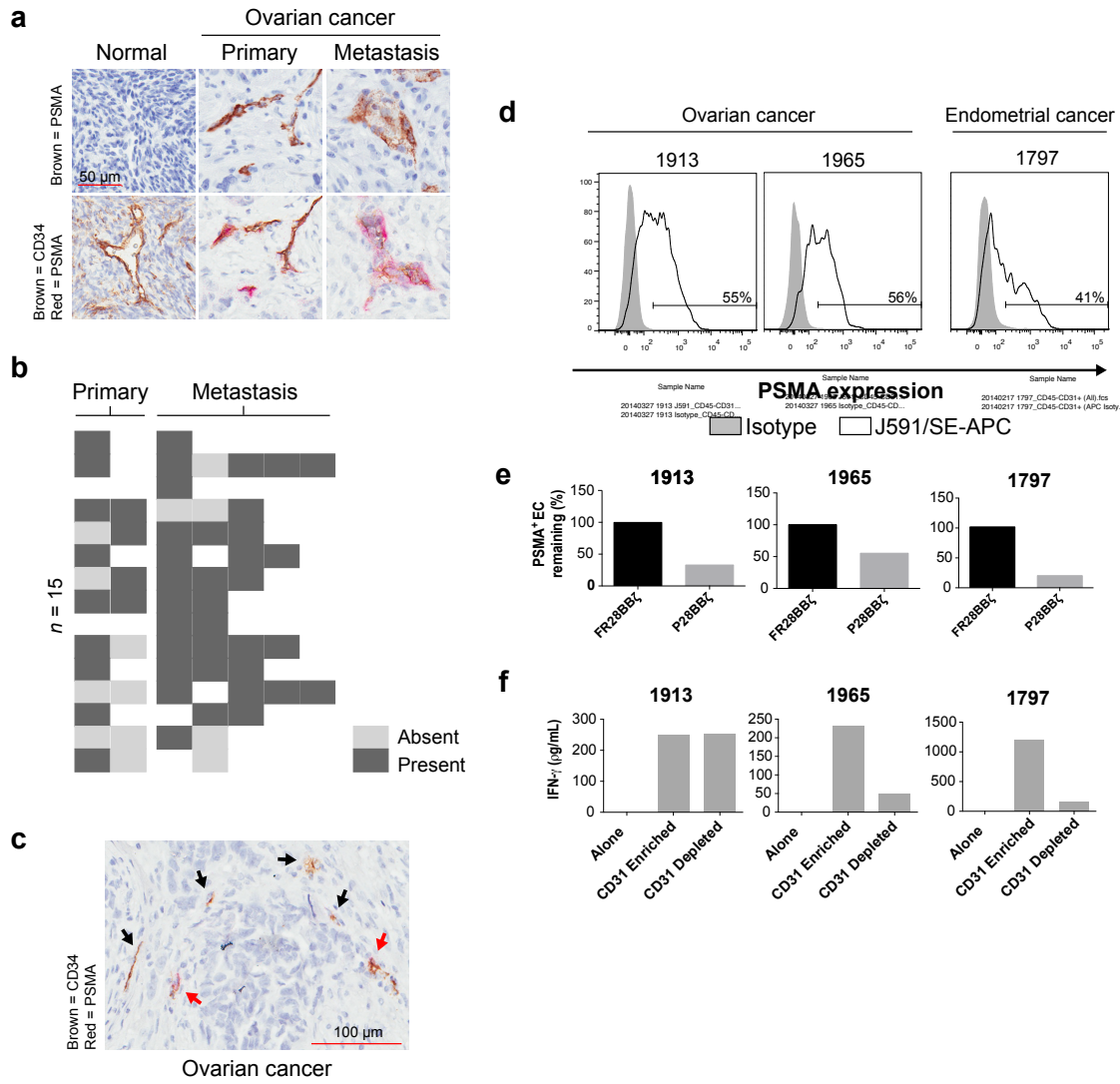**Figure 12: PSMA is expressed on the vasculature of primary and metastatic cancer.** (**a**) Representative staining for PSMA on primary and metastatic ovarian tumors. Top row: PSMA staining alone (brown). Bottom row: Dual staining for PSMA (red) and the endothelium (CD34, brown). Original magnification, 200×; scale bar, 50 μm. (**b**) A heat map showing the presence or absence of PSMA on the vasculature of tumors taken from subjects with resected ovarian cancer ($n = 15$). (**c**) Representative tumor core staining for both PSMA (red) and CD34 (brown). Black arrows indicate CD34$^+$ vessels that are negative for PSMA expression, whereas the red arrows indicate dual-positive (CD34$^+$PSMA$^+$) vessels. (**d**) Level of PSMA expression on tumor endothelial cells (CD45$^-$CD31$^+$) from three subjects with gynecological cancer. Tumor endothelial cells were collected by CD45 depletion followed by CD31 enrichment. PSMA was detected by humanized J591 Ab (open histogram) and compared with human IgG control (closed

histogram). (**e**) The percentage of PSMA-positive CD45$^-$CD31$^+$ endothelial cells remaining after overnight co-culture with CAR T cells (E:T = 1:1). Percentage = treated / untreated × 100. (**f**) IFN-γ production by P28BBζ T cells after co-culture with CD31 enriched or depleted targets (E:T = 1:1). Culture supernatants were collected at 18 h and IFN-γ was measured by ELISA.
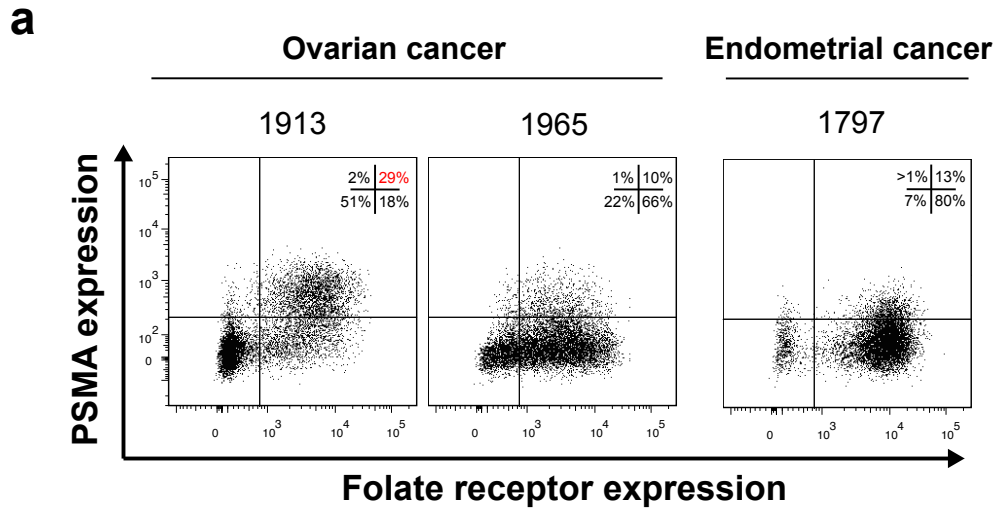
Figure 13: PSMA expression on tumor cells. (**a**) PSMA and folate receptor expression on CD45 and CD31 depleted tumor digests from three women with gynecological cancer (patient #1913, 1965, and 1797). Cell suspensions were stained for CD45, CD31, PSMA and folate receptor. Dot plots show PSMA and folate receptor expression on the CD45⁻ CD31⁻ gated populations. PSMA expression was detected by humanized J591 Ab; folate receptor was detected using a commercially available Ab.
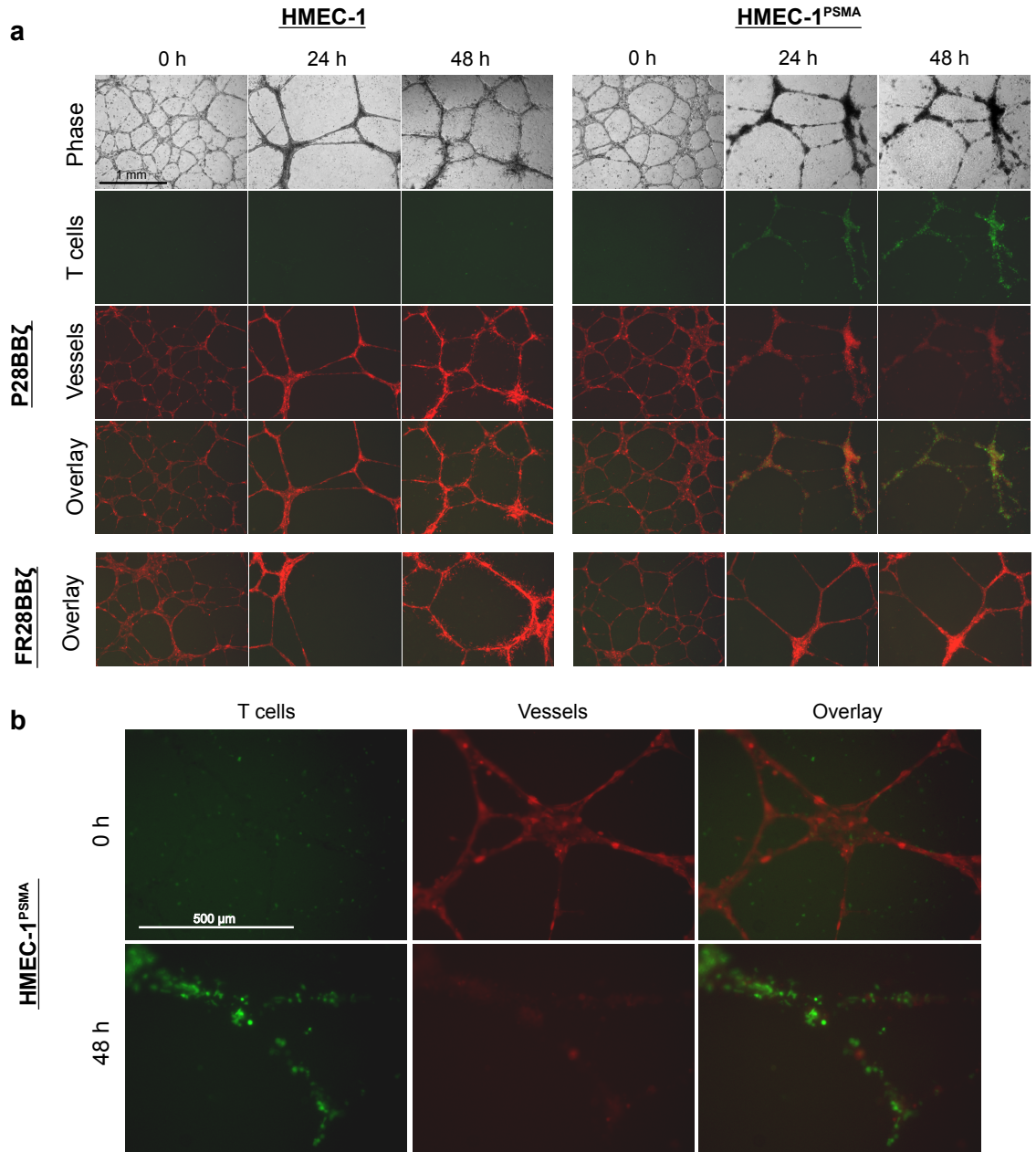
Figure 14: P28BBζ CAR T cells target human tumor vasculature expressing PSMA
***in vitro*.** (**a**) Antigen-specific destruction of HMEC-1^{PSMA} microvessels after 48 h co-culture with P28BBζ T cells. HMEC-1 or HMEC-1^{PSMA} endothelial cells (red) were seeded atop a Matrigel basement membrane and allowed to form microvessels for 8 h prior to co-culture with CAR-bearing T cells (green)(E:T = 3:1). Images were taken at 0, 24, and 48 h. Original magnification, 40×; scale bar, 1 mm. (**b**) Immunofluorescence images of the HMEC-1^{PSMA} endothelial cells at initiation (0 h) and termination (48 h) of co-culture with the P28BBζ T cells. Original magnification, 100×; scale bar, 500 μm.
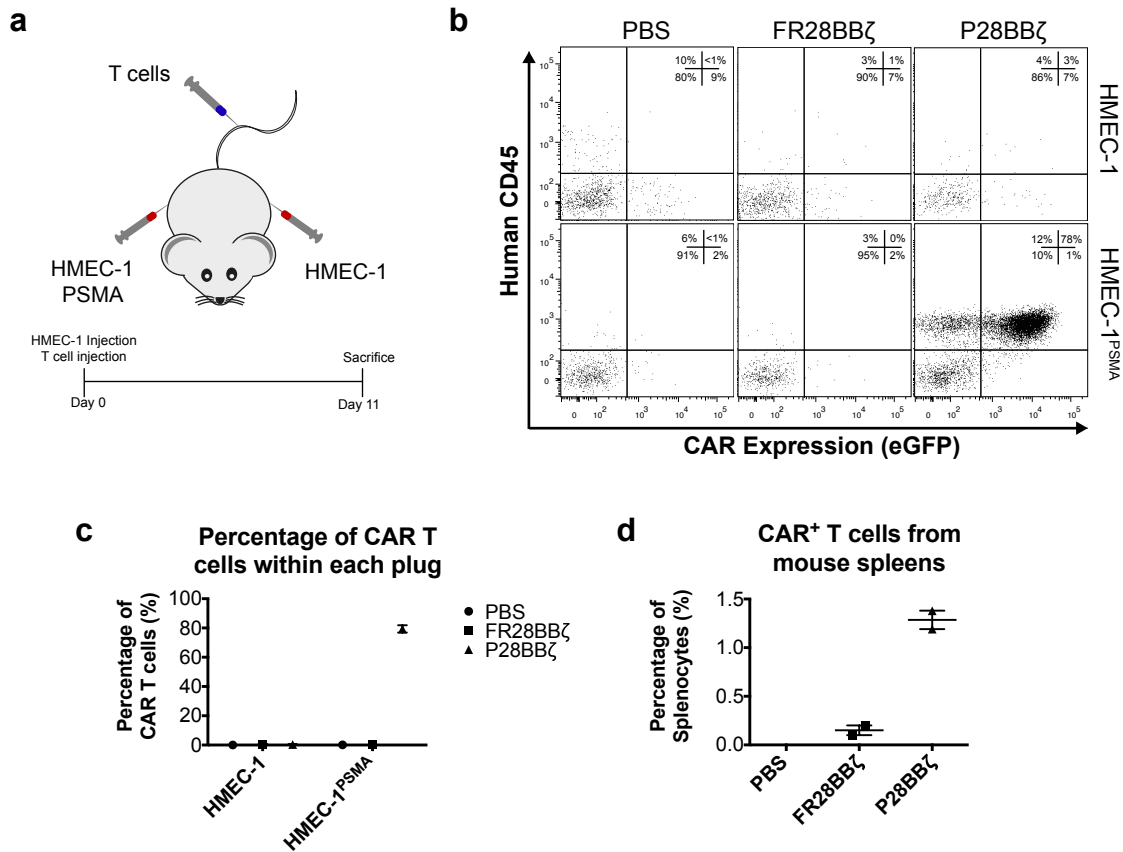
95

Figure 15: P28BBζ CAR T cells target human tumor vasculature expressing PSMA *in vivo.* (**a**) Experimental design for the HMEC-1 pilot study. Mice were injected s.c. on each flank with 1.0×10^6 HMEC-1 (left flank) and 1.0×10^6 HMEC-1^{PSMA} (right flank) endothelial cells. T cells were administered concurrently via i.v. injection. Treated mice received 5.0×10^6 CAR-positive T cells. (**b**) Representative dot plots from treated or control mice showing human CD45 and CAR (eGFP) expression. Matrigel plugs were retrieved upon sacrifice (11 d) and were digested with dispase and DNase to yield a single cell suspension. Cells were subsequently stained for human CD45 and analyzed for eGFP expression using a flow cytometer. (**c**) CAR T cells as a percentage of the cells isolated from the Matrigel plugs. $n = 2$ mice in the FR28BBζ and P28BBζ; $n = 1$ mouse in the untreated (PBS) group. Data are means ±SEM. (**d**) CAR T cells as a percentage of total splenocytes. Spleens were isolated from mice upon sacrifice, mechanically disrupted, and analyzed for the presence of CAR T cells (eGFP). $n = 2$ mice in the FR28BBζ and P28BBζ; $n = 1$ mouse in the untreated (PBS) group. Data are means ±SEM.
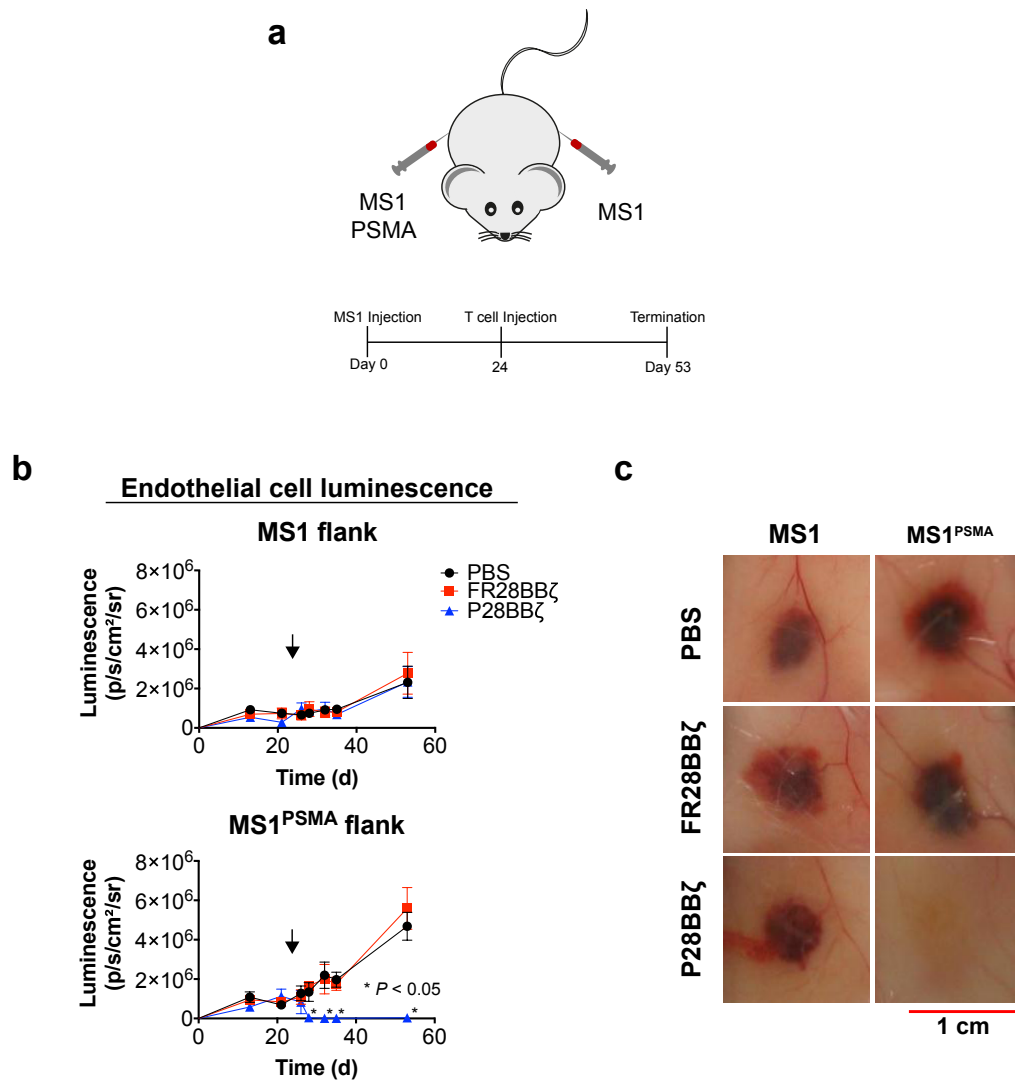
Figure 16: P28BBζ CAR T cells eliminate PSMA$^+$ hemangiomas. (**a**) Tumor injection schematic and experimental design for the MS1 hemangioma study. Mice were injected s.c. on each flank with 1.0×10^7 MS1 (left flank) and 1.0×10^7 MS1^{PSMA} (right flank) endothelial cells. Hemangiomas were allowed to develop for 24 days prior to i.v. injection of T cells. (**b**) Tumor progression, as measured by luciferase luminescence, in mice receiving PBS, FR28BBζ, or P28BBζ T cells. Mice were given a single injection of 5.0×10^6 CAR-positive T cells (arrows) 24 days after inoculation with tumor. $n = 5$ mice per group; data are means ±SEM. *$P < 0.05$, as determined by two-tailed Student's t test, for the P28BBζ treated group when compared to the FR28BBζ control group at the indicated time points. (**c**) Representative hemangiomas at the time of sacrifice (day 53).
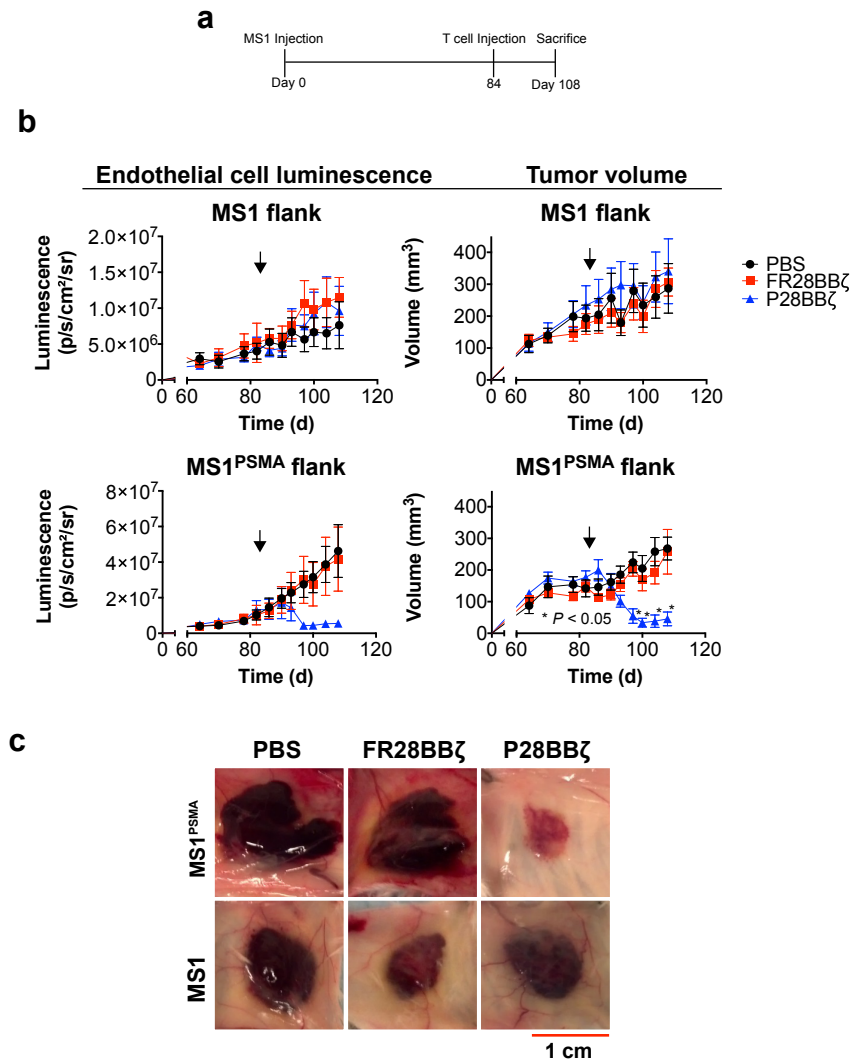
97

Figure 17: P28BBζ T cell mediated regression of large PSMA$^+$ hemangiomas. (**a**) Experimental design for the MS1 hemangioma study. Mice were injected s.c. on each flank with 1.5×10^7 MS1 (left flank) and 1.5×10^7 MS1^{PSMA} (right flank) endothelial cells. The MS1 and MS1^{PSMA} endothelial cells were engineered to express firefly luciferase. Large palpable hemangiomas were allowed to form prior to i.v. injection of T cells. (**b**) Tumor progression, as measured by luciferase luminescence, in mice receiving PBS, FR28BBζ, or P28BBζ T cells. Mice were given a single injection of 1.0×10^7 CAR-positive T cells (arrows) 84 days after inoculation with tumor. Hemangioma progression was monitored longitudinally via luciferase luminescence (left column) and caliper measurement (volume, right column). $n = 5$ mice per group; data are means ±SEM. *$P < 0.05$, as determined by two-tailed Student's t test, for the P28BBζ treated group when compared to the FR28BBζ control group at the indicated time points. (**c**) Representative hemangiomas at the time of sacrifice (day 106).
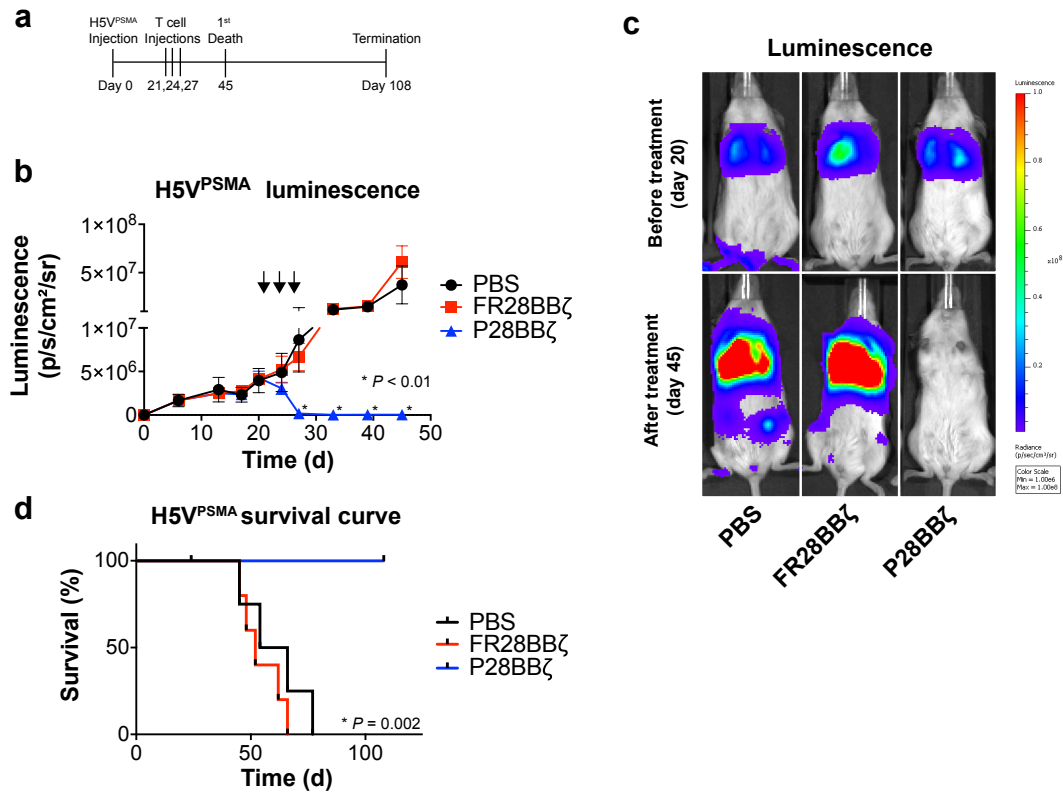
98

Figure 18: P28BBζ CAR T cells eliminate PSMA⁺ hemangiosarcomas. (**a**) Experimental design for the H5V hemangiosarcoma tumor study. Mice were injected i.v. with 5.0×10^5 H5V^{PSMA} endothelial cells. Lung tumors were allowed to engraft for 3 weeks prior to administration of T cells. (**b**) Tumor progression, as measured by luciferase luminescence, in mice receiving PBS, FR28BBζ, or P28BBζ T cells. Mice were given three injections of 5.0×10^6 CAR-positive T cells beginning 21 days after tumor inoculation (arrows). $n = 5$ mice per group; data are means ±SEM. *$P < 0.05$, as determined by two-tailed Student's t test, for the P28BBζ treated group when compared to the FR28BBζ control group at the indicated time points. (**c**) Survival curve for mice with H5V^{PSMA} tumors. P28BBζ treated mice were sacrificed on day 108. $P = 0.002$, as determined by log-ranked (Mantel-Cox) test. $n = 5$ mice per group. (**d**) Tumor luminescence in representative mice before (day 20) and after T cell treatment (day 45).
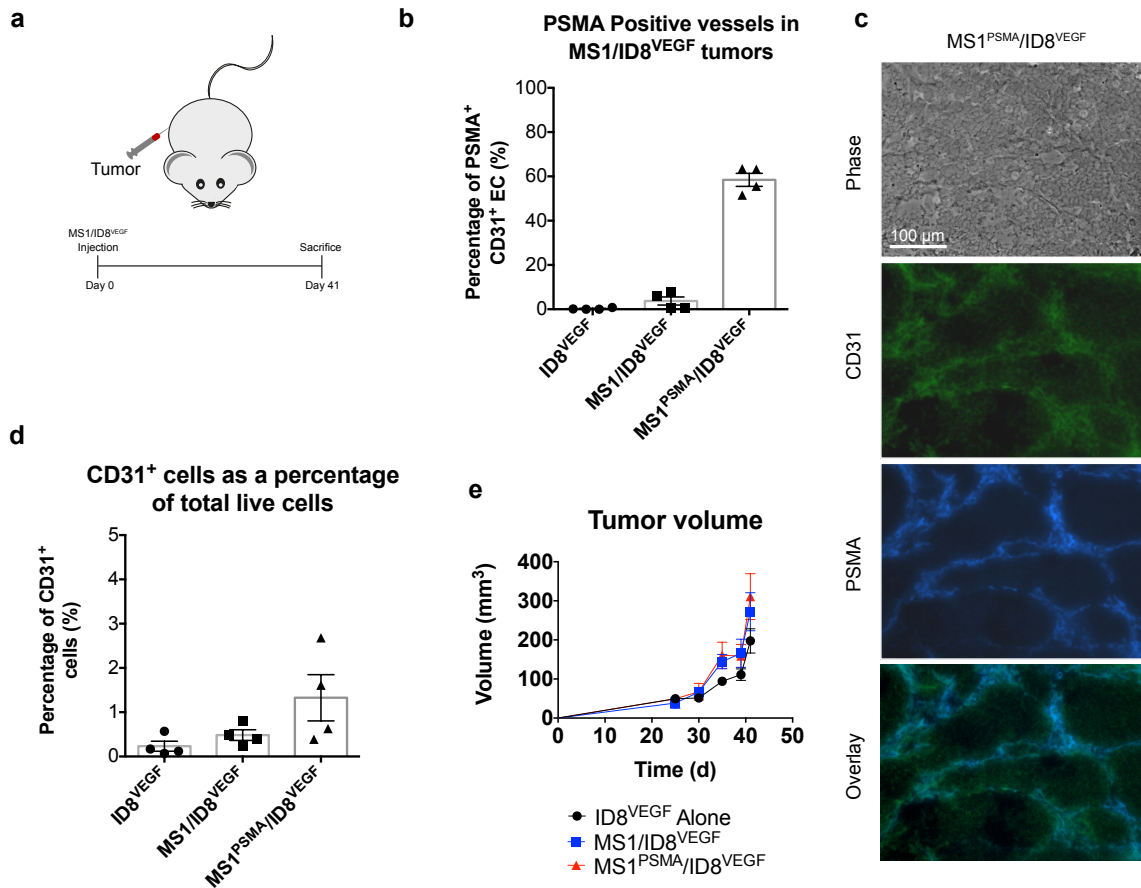
Figure 19: The MS1/ID8^{VEGF} tumor model closely mimics normal tumor physiology. (**a**) Tumor injection schematic and experimental design for the MS1/ID8^{VEGF} characterization study. Mice were given a single s.c. injection of 1.0×10^6 ID8^{VEGF} tumor cells either alone or with 1.5×10^7 MS1 or 1.5×10^7 MS1^{PSMA} endothelial cells and monitored for 41 days. (**b**) The percentage of MS1^{PSMA} derived endothelial cells (CD31$^+$) in ID8 tumors at time of sacrifice. PSMA was detected by humanized J591 Ab. *$P < 0.0001$, as determined by two-tailed Student's t test. $n = 4$ mice per group; data are means ±SEM. (**c**) Representative staining for CD31 (green) and PSMA (blue) from an MS1^{PSMA}/ID8^{VEGF} tumor (d 41). Original magnification, 200×; scale bar, 100 μm. (**d**) The portion of CD31$^+$ endothelial cells present in tumor digests reported as a percentage of the total number of live cells collected. $n = 4$ mice per group; data are means ±SEM. (**e**) Tumor progression in mice harboring ID8^{VEGF}, MS1/ID8^{VEGF}, or MS1^{PSMA}/ID8^{VEGF} tumors. Tumor volumes were calculated via caliper measurement. $n = 4$ mice per group; data are means ±SEM.

b

Correlation of luminesence with radiant efficiency: MS1

(scatter plot)
- Mouse 1 (blue circle)
- Mouse 2 (red square)
- Mouse 3 (green triangle)
- Mouse 4 (orange inverted triangle)

Y-axis: Average Radiant Efficiency (p/s/cm²/sr) / (µW/cm²)
X-axis: Luminescence (p/s/cm²/sr)

c

Mouse	1	2	3	4
Pearson correlation (*r*)	0.7944	0.4971	0.8968	0.9179
Two-tailed significance (*P*)	0.0328	0.2564	0.0062	0.0035
Number (n)	7	7	7	7

d

Correlation of Luminesence with radiant efficiency: MS1PSMA

(scatter plot)
- Mouse 1 (blue circle)
- Mouse 2 (red square)
- Mouse 3 (green triangle)
- Mouse 4 (orange inverted triangle)

Y-axis: Average Radiant Efficiency (p/s/cm²/sr) / (µW/cm²)
X-axis: Luminescence (p/s/cm²/sr)

e

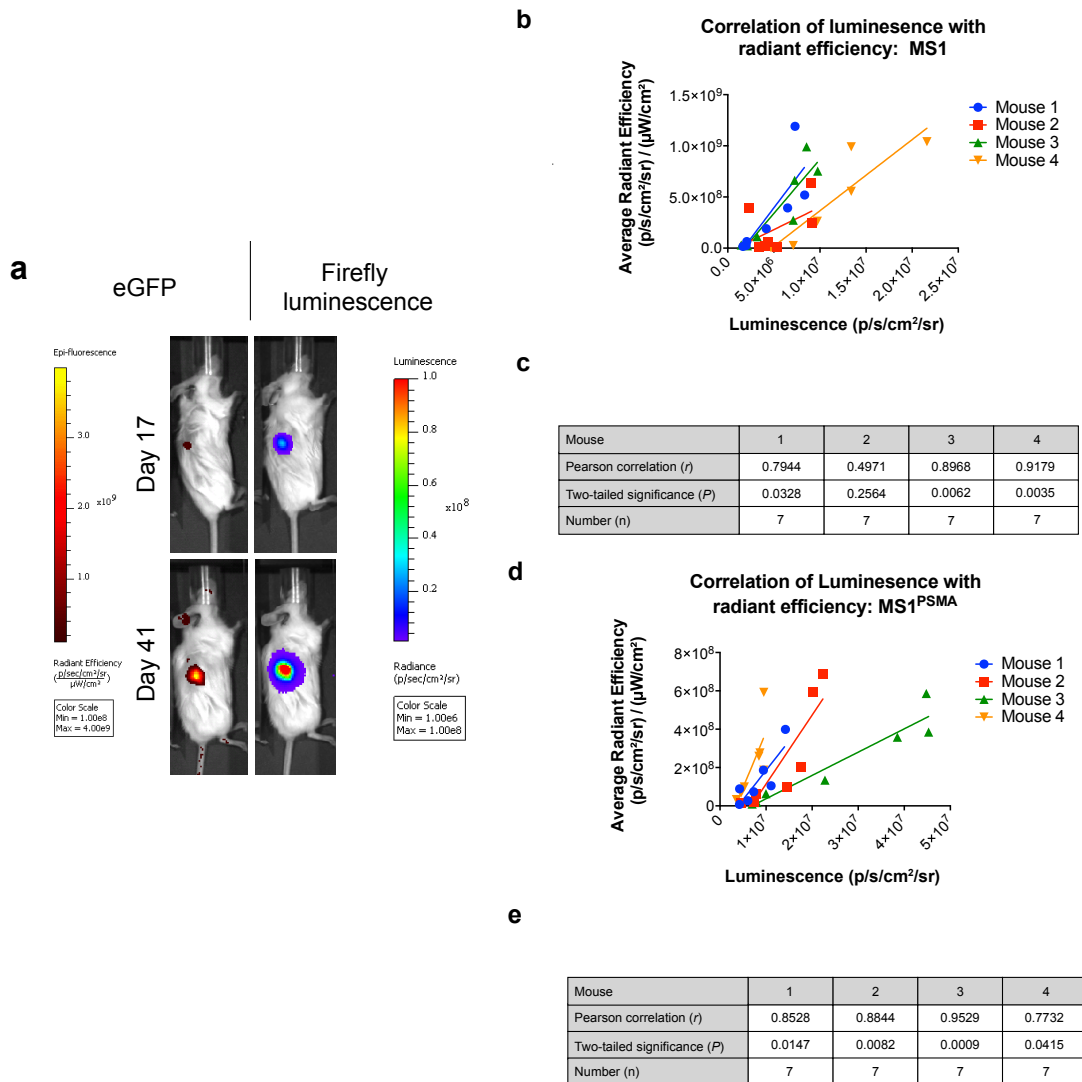| Mouse	1	2	3	4
Pearson correlation (*r*)	0.8528	0.8844	0.9529	0.7732
Two-tailed significance (*P*)	0.0147	0.0082	0.0009	0.0415
Number (n)	7	7	7	7

Figure 20: The contribution of endothelial cells to tumor cells remains constant during tumor development. (**a**) Representative images taken from the same mouse on day 17 and 41 showing eGFP radiance and firefly luminescence. (**b,d**) Correlation of endothelial cell signal (firefly luciferase, luminescence) with tumor signal (eGFP, radiant efficiency). Linear regression analysis was performed and the slope of best fit is shown (solid lines) for individual mice with either MS1/ID8^{VEGF} (f) or MS1^{PSMA}/ID8^{VEGF} (g) tumors. (**c,e**) Statistical analysis describing the correlation of luminescence and radiant efficiency in mice with MS1/ID8^{VEGF} (h) and MS1^{PSMA}/ID8^{VEGF} (i) tumors. Measurements were taken at time points between 17–41 days after inoculation with tumor and the luciferase and radiant efficiency measurements were plotted against one another (*n* = 7). Pearson correlation coefficients were calculated for each mouse (*r*). Significance evaluated by two-tailed test (*P*).
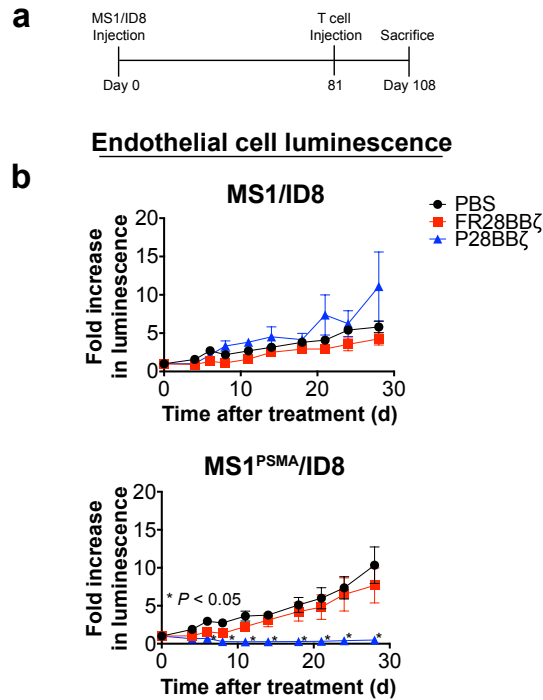
101

Figure 21: CAR T cells ablate PSMA$^+$ vasculature in MS1/ID8 solid tumors. (**a**) Experimental design for the MS1/ID8 tumor study. $6.7×10^5$ ID8 tumor cells were mixed with either $1.0×10^7$ MS1 (left flank) or $1.0×10^7$ MS1^{PSMA} (right flank) endothelial cells and injected s.c. on the opposite flanks of each mouse. Tumors were allowed to engraft for 81 days before T cell administration. (**b**) The persistence of the MS1 and MS1^{PSMA} endothelial cells after treatment with PBS, FR28BBζ, or P28BBζ T cells. Mice were given a single injection of $1.0×10^7$ CAR-positive T cells 81 days after inoculation with tumor. The presence (or absence) of the MS1 and MS1^{PSMA} endothelial cells was monitored via luciferase luminescence and is reported as fold change over the values taken immediately prior to T cell administration on day 81. $n = 5$ mice per group; data are means ±SEM. *$P < 0.05$, as determined by two-tailed Student's t test, for the P28BBζ treated group when compared to the FR28BBζ control group at the indicated time points.
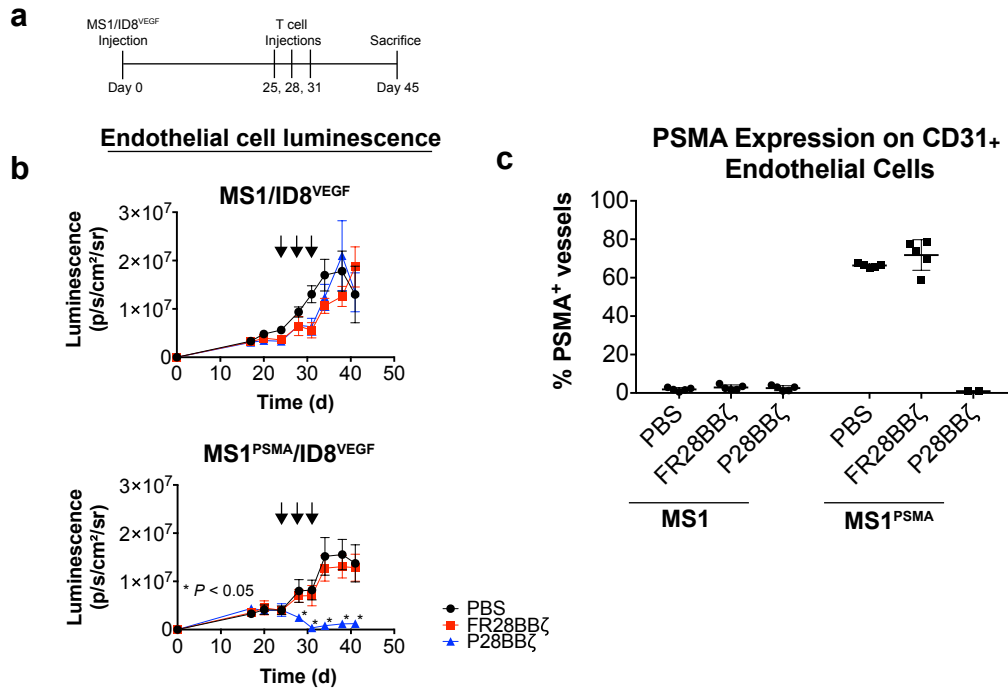
Figure 22: CAR T cells ablate PSMA$^+$ vasculature in MS1/ID8^{VEGF} solid tumors. (a) Experimental design for the MS1/ID8^{VEGF} tumor study. 6.7×10^5 ID8^{VEGF} tumor cells were mixed with either 1.0×10^7 MS1 (left flank) or 1.0×10^7 MS1^{PSMA} (right flank) endothelial cells and injected s.c. on the opposite flanks of each mouse. Tumors were allowed to engraft for 25 days before treatment with CAR T cells. **(b)** The persistence of the MS1 and MS1^{PSMA} endothelial cells after treatment with PBS, FR28BBζ, or P28BBζ T cells. Mice were given three injections of 5.0×10^6 CAR-positive T cells beginning 25 days after tumor inoculation (arrows). The presence (or absence) of the MS1 and MS1^{PSMA} endothelial cells was monitored via luciferase luminescence. $n = 5$ mice per group; data are means ±SEM. *$P < 0.05$, as determined by two-tailed Student's t test, for the P28BBζ treated group when compared to the FR28BBζ control group at the indicated time points. **(c)** The percentage of PSMA positive tumor endothelial cells (CD45$^-$ CD31$^+$) remaining after T cell administration to mice harboring MS1/ID8^{VEGF} and MS1^{PSMA}/ID8^{VEGF} tumors. PSMA was detected by humanized J591 Ab. $n = 5$ mice in the PBS and FR28BBζ groups; $n = 2$ mice in P28BBζ group. Data are means ±SEM.
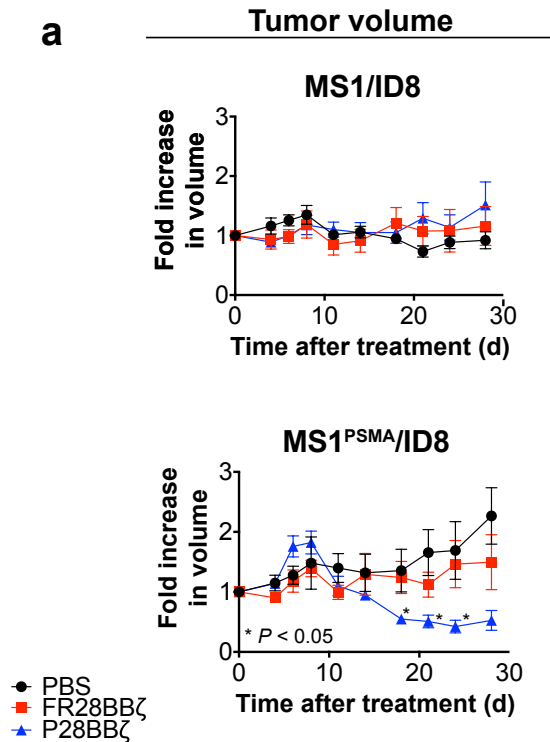
a

Tumor volume

MS1/ID8

MS1^{PSMA}/ID8

* $P < 0.05$

- PBS
- FR28BBζ
- P28BBζ

Figure 23: Anti-vascular CAR T cells cause tumor regression of MS1/ID8 solid tumors. (**a**) Tumor progression in the MS1/ID8 and MS1^{PSMA}/ID8 tumors (Figure 21a) after treatment with PBS, FR28BBζ, or P28BBζ T cells. Mice were given a single injection of 1.0×10^7 CAR-positive T cells 81 days after inoculation with tumor. Tumor volumes were calculated via caliper measurement and are reported as fold change over values taken immediately prior to T cell administration on day 81. $n = 5$ mice per group; data are means ±SEM. *$P < 0.05$, as determined by two-tailed Student's t test, for the P28BBζ treated group when compared to the FR28BBζ control group at the indicated time points.
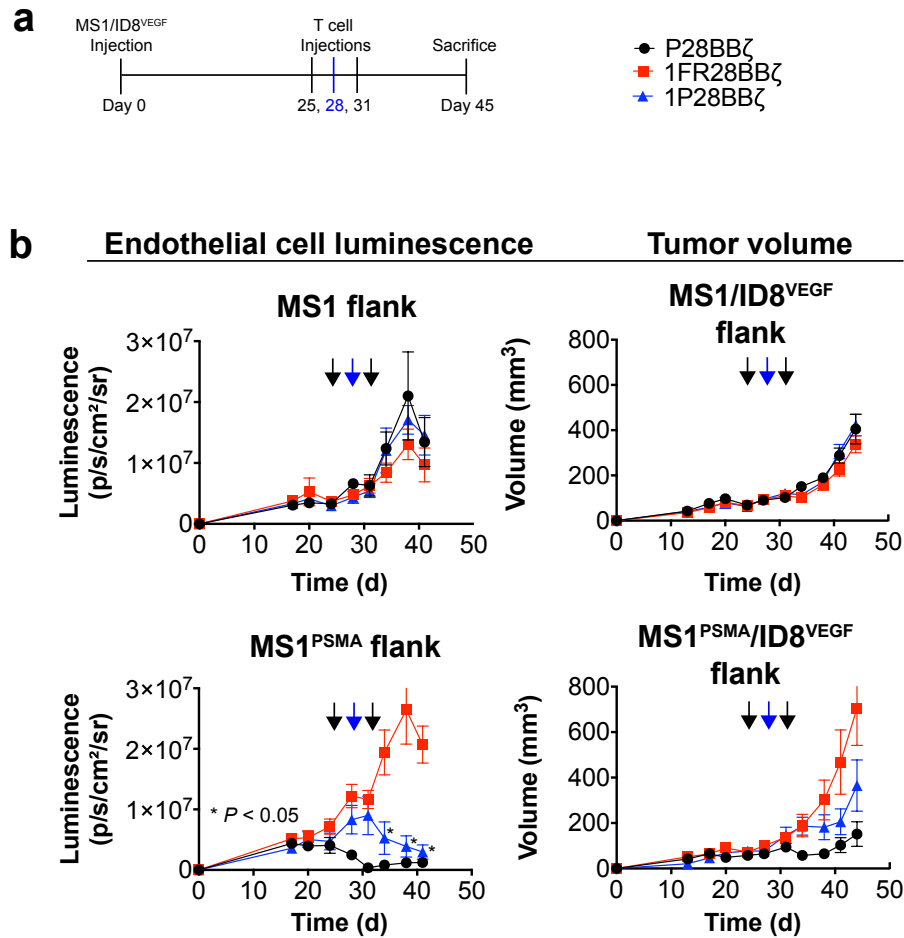
Figure 24: Comparison of single vs. multiple injections of P28BBζ T cells. (**a**) Experimental design for the comparative dosing study. 6.7×10^5 ID8^{VEGF} tumor cells were mixed with either 1.0×10^7 MS1 (left flank) or 1.0×10^7 MS1^{PSMA} (right flank) endothelial cells and injected s.c. on opposite flanks of the same mice. Mice received either a single dose of 1.0×10^7 CAR-positive T cells (1FR28BBζ and 1P28BBζ, blue arrows) or a series of three injections of 5.0×10^7 CAR-positive T cells (P28BBζ, black arrows). Experiment was run concurrently with Figure 22a. Luminescence values for the P28BBζ group are identical to those shown in Figure 22b. (**b**) Tumor progression in mice receiving P28BBζ, 1FR28BBζ, or 1P28BBζ T cells. The presence (or absence) of endothelial cells was monitored via luciferase luminescence (left column). Tumor volumes (right column) were calculated via caliper measurement. $n = 5$ mice in the P28BBζ and 1P28BBζ groups; $n = 4$ mice in 1FR28BBζ group. Data are means ±SEM. *$P < 0.05$, as determined by two-tailed Student's t test, for the 1P28BBζ treated group when compared to the 1FR28BBζ control group at the indicated time points.
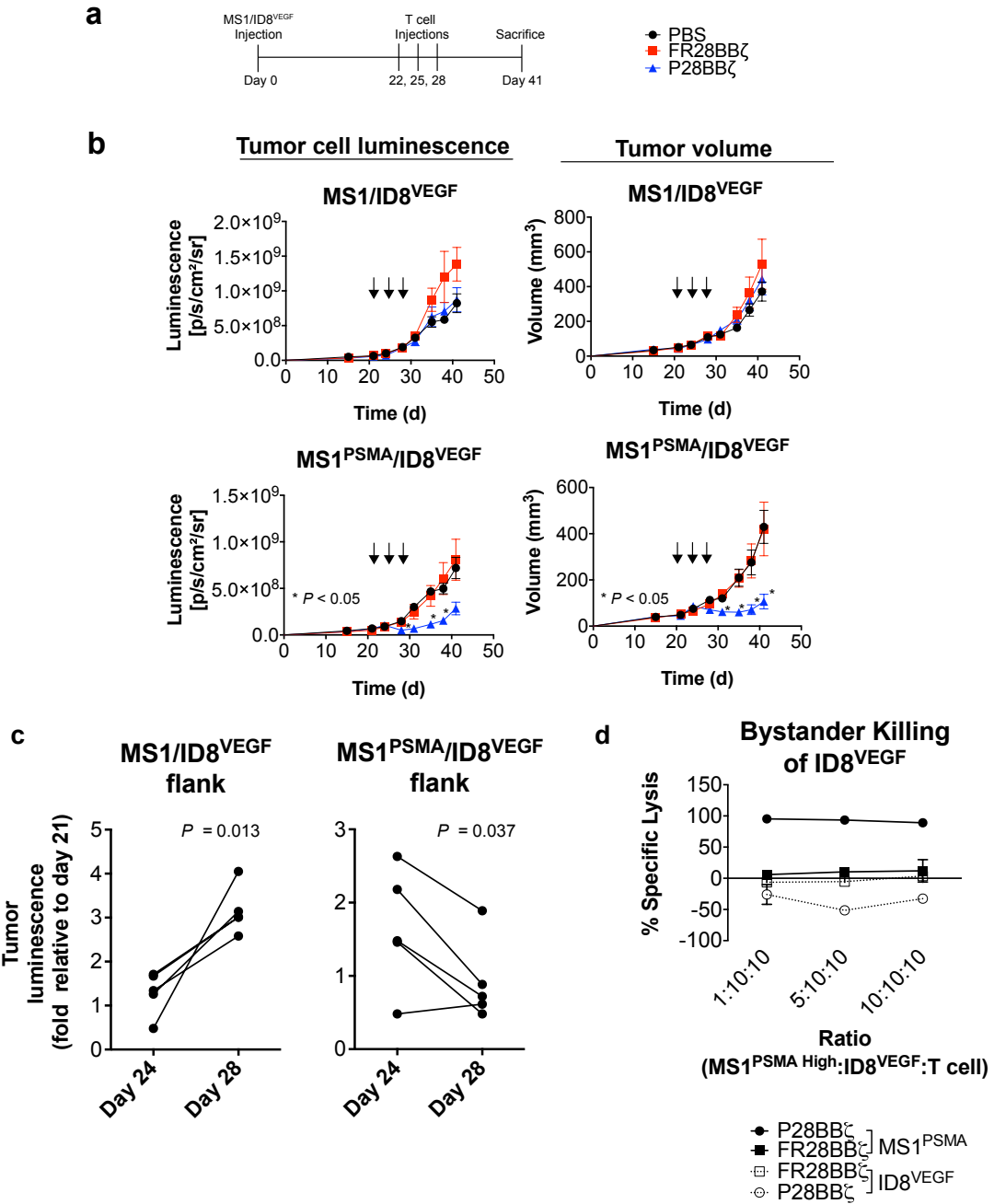
Figure 25: CAR T cells induce secondary loss of tumor cells and regression of solid tumors. (**a**) Experimental design for the MS1/ID8^{VEGF} tumor study. 6.7×10^5 ID8^{VEGF} tumor cells were mixed with either 1.0×10^7 MS1 (left flank) or 1.0×10^7 MS1^{PSMA} (right flank) endothelial cells and injected s.c. on opposite flanks of the same mice. Tumors were allowed to engraft for 22 days before T cell administration. (**b**) Tumor progression in mice receiving PBS, FR28BBζ, or P28BBζ T cells. Mice were given three injections

106

of $5.0×10^6$ CAR-positive T cells beginning 22 days after tumor inoculation (arrows). The impact of T cell administration on the ID8^{VEGF} tumor cells was measured via luciferase luminescence (left column) and tumor volumes were calculated using caliper measurements (right column). $n = 5$ mice per group; data are means ±SEM. *$P < 0.05$, as determined by two-tailed Student's t test, for the P28BBζ treated group when compared to the FR28BBζ control group at the indicated time points. (**c**) The fold change in ID8^{VEGF} tumor cell luminescence from the MS1/ID8$^{VEGF \ and}$ MS1^{PSMA}/ID8^{VEGF} tumors in mice receiving P28BBζ T cells. Luminescence measurements were normalized to those made prior to treatment (day 21). P values were determined by two-tailed Student's t test and reflect the significance of changes between day 24 and day 28. $n = 5$. (**d**) P28BBζ T cells do not elicit bystander killing of ID8^{VEGF} when cultured in the presence of MS1^{PSMA}. MS1^{PSMA} cells were titrated into wells with ID8^{VEGF} tumor cells and T cells at the described ratios and were cultured for 18 h. Lysis was measured via luciferase assay (specific lysis = 100 − (luciferase signal treated / luciferase signal untreated × 100)). Data are means ±SD from triplicate cultures.
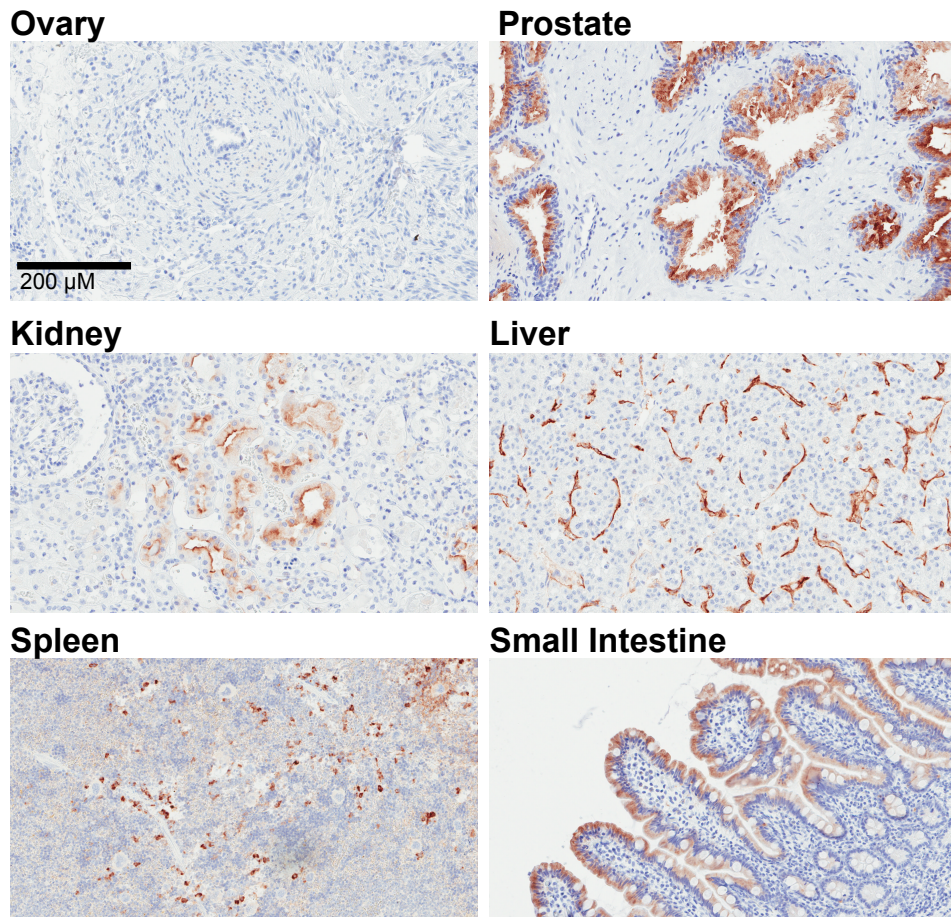
Figure 26: PSMA expression in normal tissues. Representative staining, using the 3E6 antibody, for PSMA on normal tissues. PSMA staining alone (brown). Original magnification, 200×; scale bar, 200 μm.
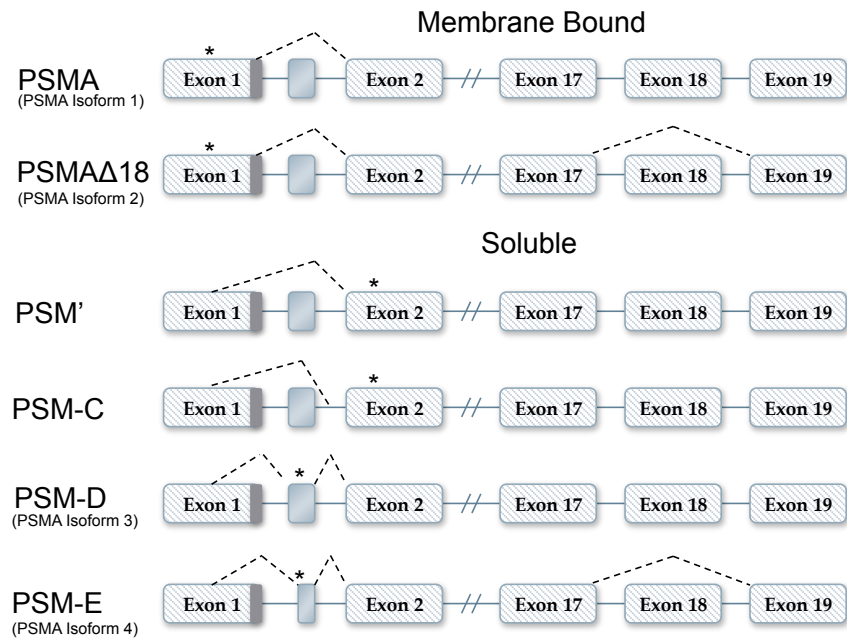
a

Figure 27: PSMA exists as multiple isoforms. In the normal prostate, PSMA is expressed predominantly as PSM'. Although the PSM' isoform retains its catalytic domain, it is unclear whether it functions as a hydrolase within the cytosol.[103] In prostate cancer, as well as on the neovasculature of solid tumors, full length PSMA isoform 1 is highly expressed. The exclusion of exon 18 from PSMA isoform 2 is expected leave the enzyme catalytically inactive, as this exon contains the dimerization domain required for catalytic function of the protein.[104,105] The functional relevance of this isoform, as well as the remaining variants, has yet to be determined.

a

IFN-γ production after co-culture
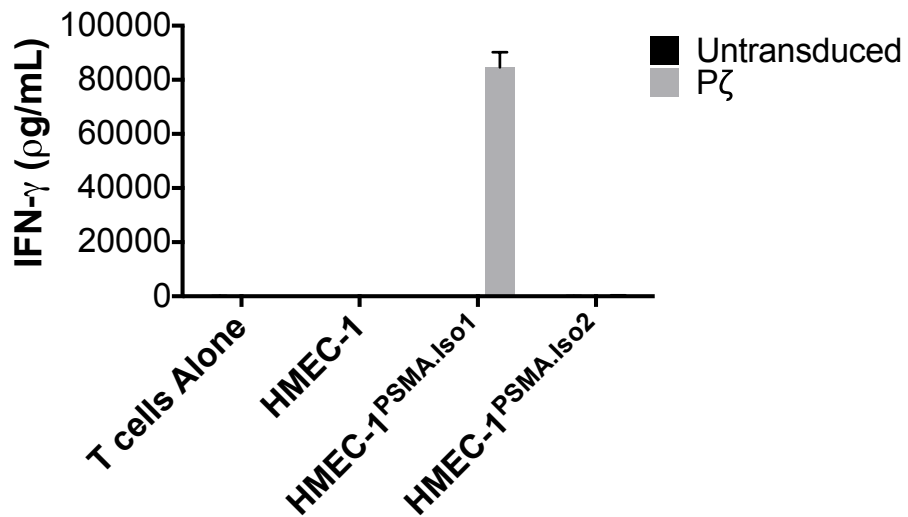
Legend: Untransduced, Pζ

Figure 28: J591-based CAR T cells exclusively recognize PSMA isoform 1. IFN-γ production by Pζ T cells after co-culture with endothelial targets (E:T = 5:1). Culture supernatants were collected at 18 h and IFN-γ was measured by ELISA. Representative donor shown; data are means ±SD of triplicate cultures.
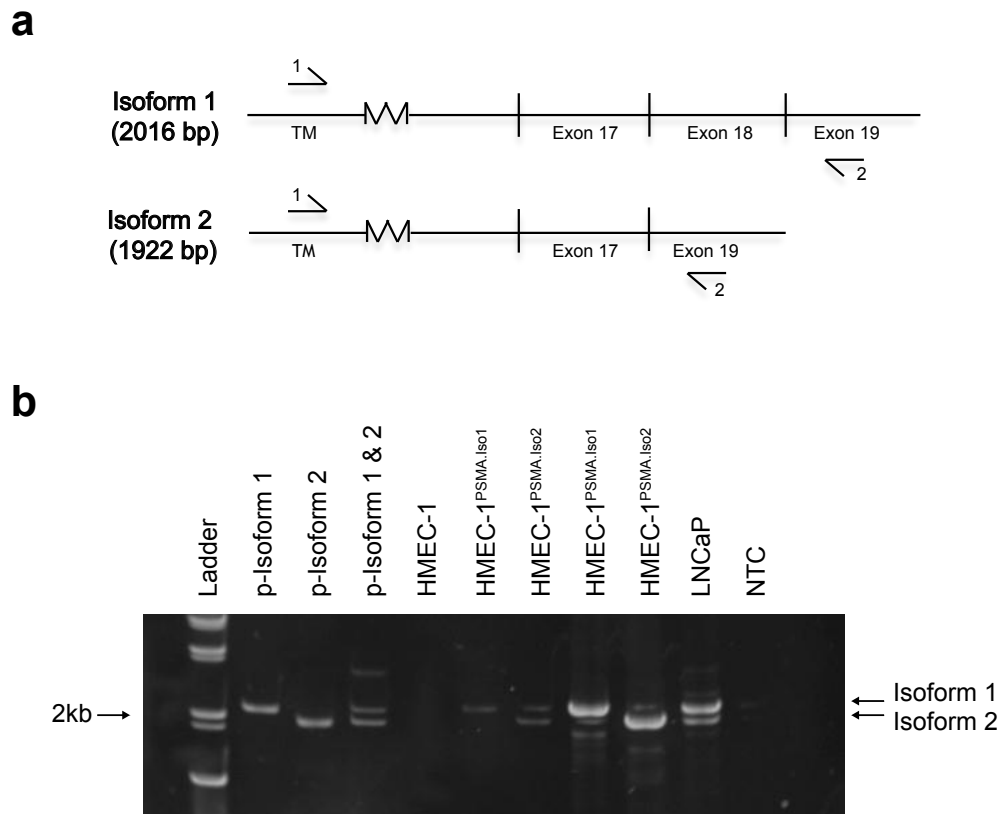
Figure 29: Validation of PCR primers used to distinguish PSMA isoform 1 and 2. (**a**) Schematic representation of PCR primers designed to distinguish PSMA isoform 1 from PSMA isoform 2. The forward primer (1) was designed to sit within the shared transmembrane domain between the two isoforms, thereby excluding the cytosolic variants of the protein. The reverse primer (2) recognizes a sequence on exon 19, which is shared between the two isoforms. PCR products of 2016 bp and 1922 bp are expected for PSMA isoforms 1 and 2, respectively. (**b**) RT-PCR analysis for PSMA isoforms 1 and 2 performed on cDNA samples collected from endothelial cells engineered to express PSMA (HMEC-1) or a prostate cancer cell line control, LNCaP. Plasmids containing PSMA isoform 1 and/or 2 were also amplified as controls.
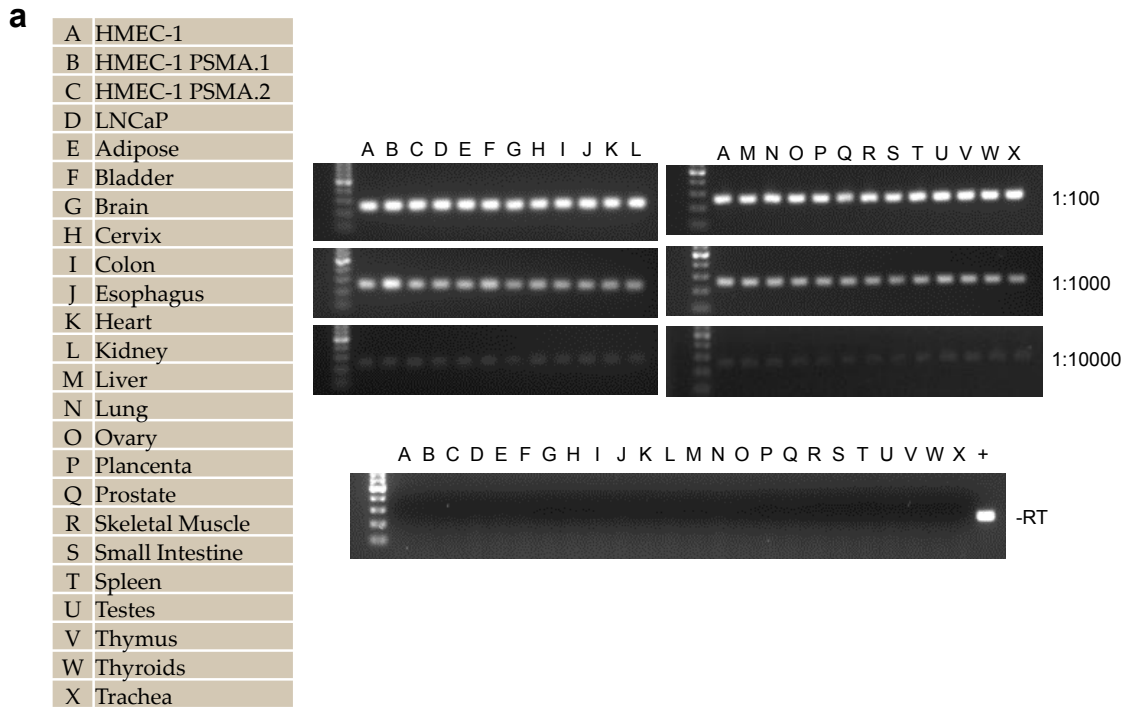
a

A	HMEC-1
B	HMEC-1 PSMA.1
C	HMEC-1 PSMA.2
D	LNCaP
E	Adipose
F	Bladder
G	Brain
H	Cervix
I	Colon
J	Esophagus
K	Heart
L	Kidney
M	Liver
N	Lung
O	Ovary
P	Plancenta
Q	Prostate
R	Skeletal Muscle
S	Small Intestine
T	Spleen
U	Testes
V	Thymus
W	Thyroids
X	Trachea

Figure 30: 18s internal loading controls for cDNA created from normal tissues. **(a)** PCR was performed on cDNA collected from cell lines and normal tissues using primers specific for the 18s ribosomal RNA. Dilutions were made from the resulting product and gel electrophoresis was conducted to confirm similar concentrations of starting material were used across all samples. The cDNA was then used for PSMA isoform analysis (**Figure 31**).
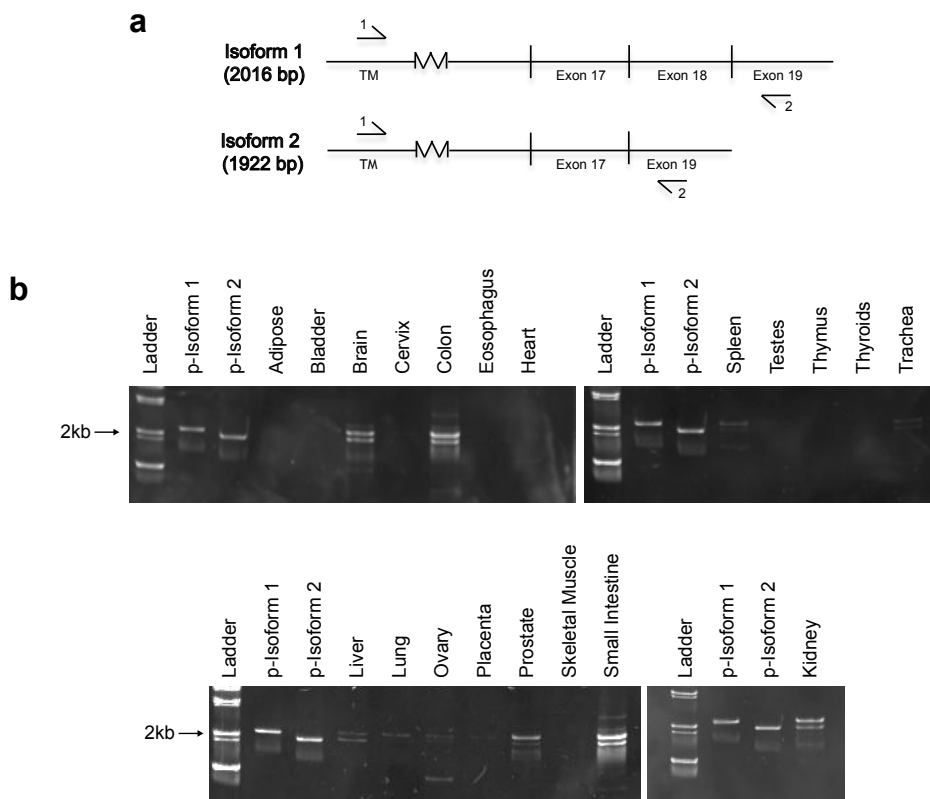
Figure 31: RT-PCR analysis of the membrane-bound PSMA isoforms from normal tissues. (**a**) Schematic representation of PCR primers designed to distinguish PSMA isoform 1 from PSMA isoform 2. (**b**) Polyacrylamide gel electrophoresis of PCR products generated from a panel of normal tissues. Plasmid DNA containing PSMA isoform 1 and/or 2 were also amplified, and serve as controls.

113